学位論文

Control of Molecular Rotational Motions toward the Construction of Highly Functionalized Molecular Machines

（高度に機能化された分子機械の構築に向けた分子回転運動の制御）

平成２９年１２月博士（理学）申請

東京大学大学院理学系研究科

化学専攻

山田　諒

Abstract

1. Introduction

Rotary motion transmission, especially by gear coupling, is indispensable to the construction of macroscopic machines, which can be used for adjustment of the direction and torque of the rotation as well as of integration or division of the power. Synthetic molecules with a similar structure would show promise as an important element of highly sophisticated molecular machines.

Several examples have been previously reported on motion transmission based on the mechanical meshing of gear-shaped molecules. However, most of them are two-gear systems and there is no report that demonstrates mechanical transmission through more than three engaging gears, because, with an increase in the number of gears, it becomes more difficult to design, synthesize, and analyze the motion of gear systems.

2-1. Construction of a sextuple triptycene gearing system

A gear molecule **1**, in which six triptycenes are circularly attached to a central benzene ring through an ethynyl linker, was designed and synthesized (Figure 1). The key reaction to construct such a crowded structure was a trimerization reaction of bis-substituted alkynes to generate a hexakis-substituted benzene in the final step.

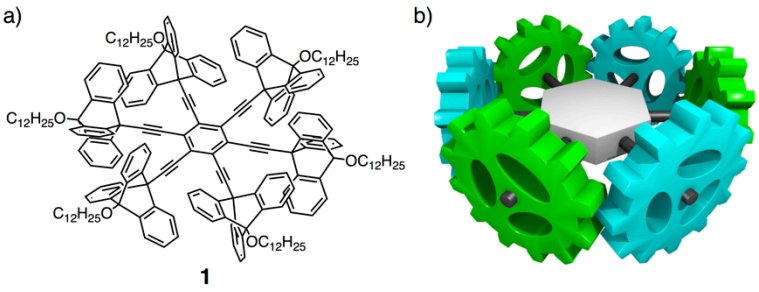

Figure 1. a) Chemical structure of the gear molecule **1**. b) Schematic representation of the gear molecule **1**.

Its tightly geared structure was determined both in solution and in the solid state by NMR spectroscopy and single-crystal X-ray analysis, respectively. Rotational speeds of the triptycene gears in solution were evaluated by variable temperature-(VT-)NMR spectroscopy. The activation enthalpy and entropy were estimated to be +12.4 kcal·mol^{-1} and +3.17 cal·K^{-1}·mol^{-1}, respectively, determined by the Eyring plots.

2-2. Metal-mediated control of the gearing system

By mixing the gear molecule **1** with [RuCp*(NCMe)$_3$]PF$_6$, a 1:1 complex [**1**·RuCp*]PF$_6$ was obtained in 55% yield (Figure 2). The complex was well characterized by a wide variety of NMR measurements, ESI-MS spectrometry, and elemental analysis. The NMR spectrum became more complicated after complexation, indicating the RuCp* complex was attached to one of the surrounding triptycene phenylene rings. At 320 K, the RuCp*-bound triptycene showed distinctive signals, and the other five triptycenes showed coalescence for each triptycene moiety. This means the other five triptycenes can rotate at this temperature regardless of the presence of the bulky RuCp*. If all the rotational motions are completely restricted in the whole molecule, all the eighteen benzene rings should provide distinctive signals.

The dynamic behaviors of [**1**·RuCp*]PF_6 were investigated by VT-NMR spectroscopy in detail. The rotation rate of the RuCp*-bound triptycene was assumed to be zero (k'_1 = 0, table in Figure 3) in the range of measured temperatures. For the other five triptycenes, the rate constant k' of each triptycene was estimated as shown in the table of Figure 3. With increasing the distance from the Ru center (from k'_2 to k'_6), the values increase. This result suggests that the gears are not completely meshed with each other but a "gear slippage" takes place to some extent.

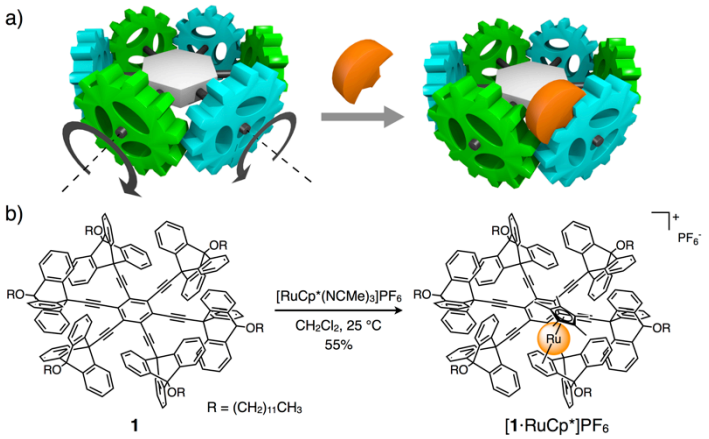

Figure 2. a) Schematic representation of the effect of a bulky "stopper" on the gear system. b) Synthetic scheme of complexation between [RuCp*(NCMe)$_3$]PF_6 and **1**.

Notably, the rotational speed calculated from k'_4, that for unadjacent triptycene to the Ru-attached position, is smaller than that of a metal-free gearing system **1**. This indicates that, although it is incomplete due to the gear slippage, the rotational motion is definitely transmitted through the gearing process.

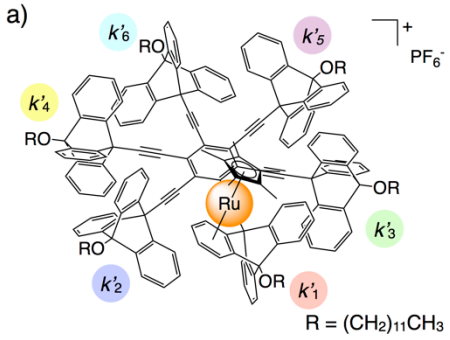

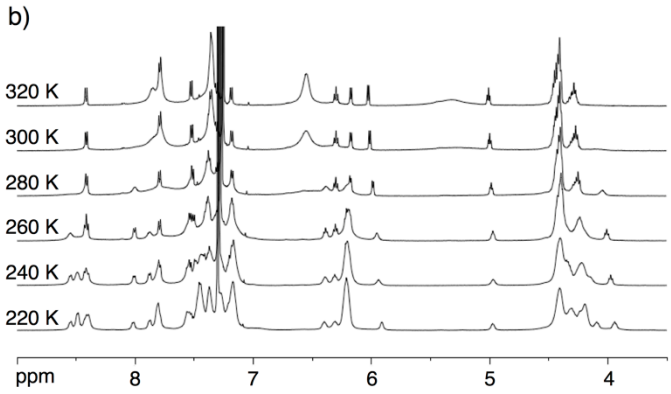

c)

	k'_1	k'_2	k'_3	k'_4	k'_5	k'_6	k' of **1**
320 K	0	5.0×10^2	2.0×10^3	1.0×10^4	1.5×10^4	1.5×10^4	5.0×10^4
300 K	0	1.0×10^2	8.0×10^2	4.0×10^3	7.0×10^3	7.0×10^3	1.4×10^4
280 K	0	20	1.5×10^2	5.0×10^2	1.0×10^3	1.0×10^3	3.0×10^3
260 K	0	5.0	20	50	1.2×10^2	1.2×10^2	5.0×10^2
240 K	0	5.0	10	25	25	25	55
220 K	0	10	10	10	10	10	5.0

Figure 3. a) Structure of [**1**·RuCp*]PF_6. b) VT-^{1}H NMR spectra of [**1**·RuCp*]PF_6 ($CDCl_3$, 500 MHz). c) Table of the estimated rate constants (k') for the rotational motion of triptycenes at each temperature.

3. Conclusion

In this study, I have established the synthesis of the circularly arranged sextuple triptycene gearing system, and evaluated its rotational motion with or without a metal-based inhibitor. Addition of a RuCp* complex has a significant influence on the whole motion of the gearing system. The result also suggests that considerable gear slippage motions occurred in spite of the tightly meshed structure. By tuning the structure, transmission efficiency would be improved. Combination with a molecular motor would provide highly functionalized molecular systems for constructing hybrid molecular machines.

Abbreviations

ATP	adenosine triphosphate
ATR	attenuated total reflection
aq.	aqueous solution
Bn	benzyl
Bu	butyl
Co.	corporation
COSY	correlation spectroscopy
Cp*	pentamethylcyclopentadienyl
d	dextro-rotatory
D	dimension
e^-	electron
eq.	equivalent
ESI	electrospray ionization
Et	ethyl
etc.	et cetera
FT	fourier transform
GPC	gel permeation chromatography
h	hour(s)
HPLC	high performance liquid chromatography
HRMS	high resolution mass spectrometry
Hz	hertz
IR	infrared spectroscopy
J	coupling constant
l	levo-rotatory
L	ligand
Ltd	limited
M	metal ions / molar [mol/L]
Me	methyl
min	minute(s)
MM	molecular mechanics
mp	melting point
MS	mass spectrometry
m/z	mass-to-charge ratio
n-	normal
NBS	*N*-bromosuccinimide
NMR	nuclear magnetic resonance
NOESY	NOE correlated spectroscopy
ORTEP	Oak ridge thermal ellipsoid plot
Ph	phenyl
ppm	parts per million
R	functional groups
rt	room temperature
sat.	saturated
STM	scanning tunneling microscope
Tf	trifluoromethanesulfonyl
TMS	trimethylsilyl
TOF	time-of-flight
Ts	*p*-toluenesulfonyl
UV	ultra violet
vis	visible
VT	variable temperature
µW	microwave

Contents

1. General Introduction

1-1. Molecular Machines

Molecules are dynamic. Molecules themselves are always moving by thermal fluctuation induced by surrounding thermal bath. Also, molecules change their structures and chemical and physical properties through chemical reactions and environment.

Chemistry concerned with "Molecular machine" focuses on such a change of the three-dimensional structures of molecules, and aims to conduct a useful work like real machines in microscale.

There are a variety of molecular machines made from proteins in nature, and they play an important role in physiological phenomena. For example, ATP synthase synthesizes ATP by using a proton concentration gradient, while rotating itself in one direction.[1] Motor proteins such as myosin or kinesin can move on the suitable surface by using chemical energy of ATP hydrolysis, supporting the activity of living organisms.[2] While these biomolecules are huge molecules whose molecular weights are over several tens of thousand, we may be able to make nano-sized and simpler architectures with similar structures and functions by synthetic chemistry. A molecule is the smallest unit we can control its size and shape, in other words, the construction of synthetic molecular machines is equivalent to the construction of the smallest machine. By making the smallest machine and evaluating its movement, development of more sophisticated nanotechnology is expected.

Nobel Prize winners in chemistry 2016, Jean-Pierre Sauvage, J. Fraser Stoddart, and Bernard L. Feringa, who are pioneers in artificial molecular machines, have inspired many chemists to drive forward this vibrant field. [3–6]

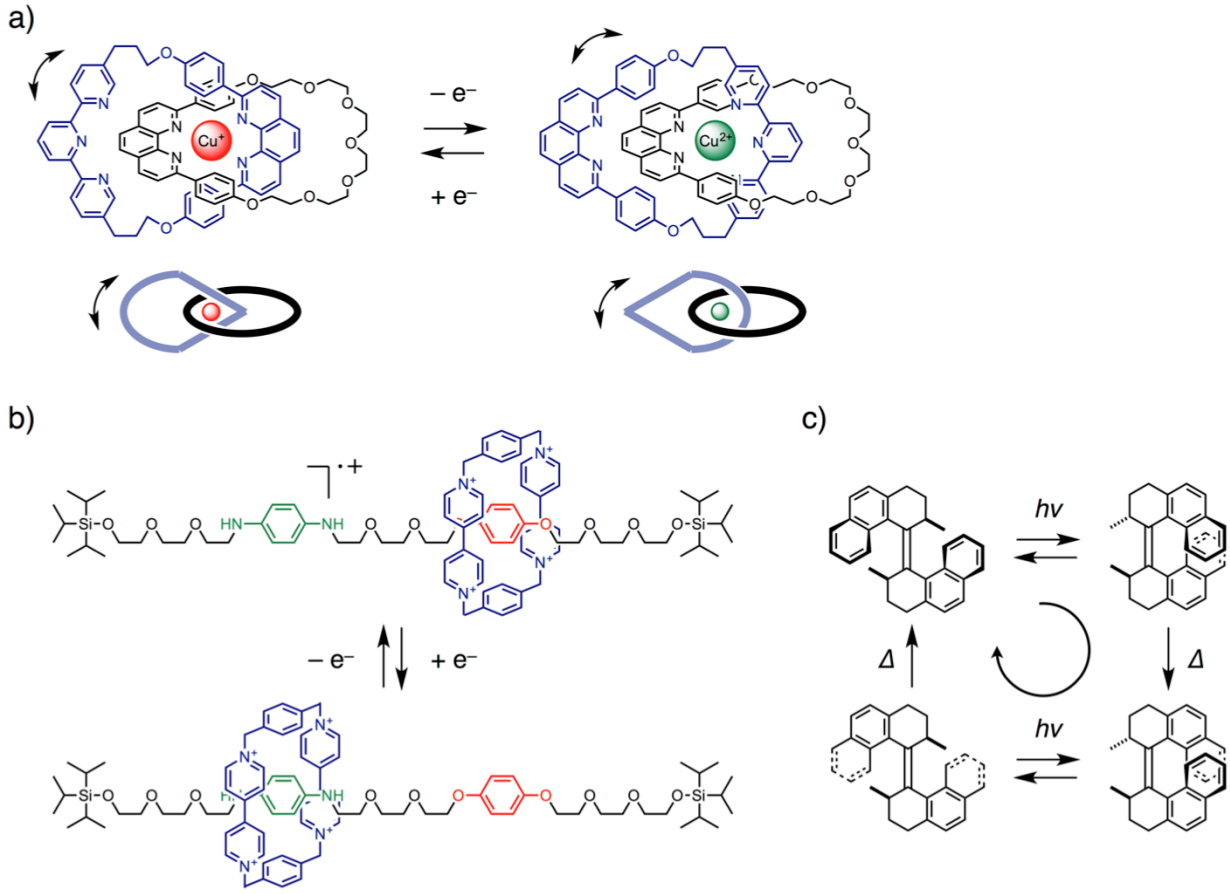

Figure 1-1-1. a) Electrochemical swinging of a [2]catenane molecule developed by Sauvage.[3b] b) Chemically and electrochemically switchable molecular shuttle using [2]rotaxanes developed by Stoddart.[4] c) Light-driven unidirectional molecular motor developed by Feringa.[5]

Sauvage and coworkers established an efficient synthesis of catenane in 1983, which was found to be an excellent motif for molecular machines.[3a] They have achieved inducement of rotational motion by combining catenane structure with redox property of copper (Figure 1-1-1-a).[3b] Stoddart group has achieved translational motion of molecule driven by external stimuli using mechanically interlocked molecules (Figure 1-1-1-b).[4] Feringa group has developed light-driven rotary molecular motors using photo- and thermal isomerization reactions (Figure 1-1-1-c).[5] Inspired by these pioneering works, a great number of sophisticated artificial molecular machines have been developed.[6]

1-2. Molecular Gearing Systems

Rotary motion transmission, especially by gear coupling, is indispensable to the construction of macroscopic machines, which can be used for adjustment of the direction and torque of the rotation as well as of integration or division of the power. Synthetic molecules with a similar structure would show promise as an important element of highly sophisticated molecular machines.[7]

Here, the definition of the term “rotational motion” in this thesis should be described first. Rotational motion is defined as a relative circular motion around a rotation axis by a certain angle, and it does not matter the direction of the motion. A partial circular motion, a pendular motion, is also included as a rotational motion in this context, however, I only deal with the system that can potentially rotate 360 degrees in this study, because I focus on the rotational motion of the molecular gears.

Correlated rotation in molecules has been studied since around the 1970s. Mislow investigated the correlated dynamics in propeller-like triarylmethane molecules[8a,8b] and they expanded the analytic method to hexaisopropylbenzene.[8c]

Using gear-shaped molecules is a common method to achieve efficient correlated motion. Triptycene has been widely used as a molecular-sized gear (Figure 1-2-1).[9] This molecule has three teeth, rigid structure, and high symmetry reflecting its [2,2,2] bicyclic structure. And as for gear-use, the bridgehead position can be chemically modified to connect with rotational axis. These structural characteristics are also utilized for construction of organic thin films with long-range structural integrity.[10] Other molecules such as pentiptycene,[11] porphyrin,[12] tetraphenyl cyclobutadiene,[13] and metal complex[14] have been also used as molecular-sized gears.

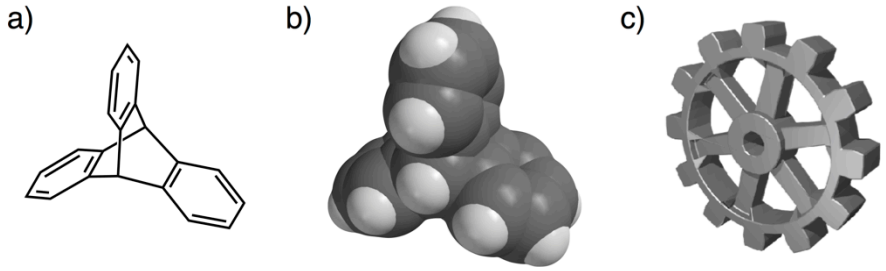

Figure 1-2-1. a) Chemical structure and b) a space filling model of triptycene molecule, which can be served as a molecular-sized gear (c).

Iwamura and Mislow independently reported the syntheses of bis-(9-triptycyl) molecules in 1980[15a,15b] and investigated triptycene gearing dynamics (Figure 1-2-2-a).[15] In these molecules, the “gear slippage” motion, in which the phase of meshing in the gear is shifted, is evaluated by introducing substituents to triptycenes, and it has been confirmed that almost no gear slippage motions occur even at high temperature.

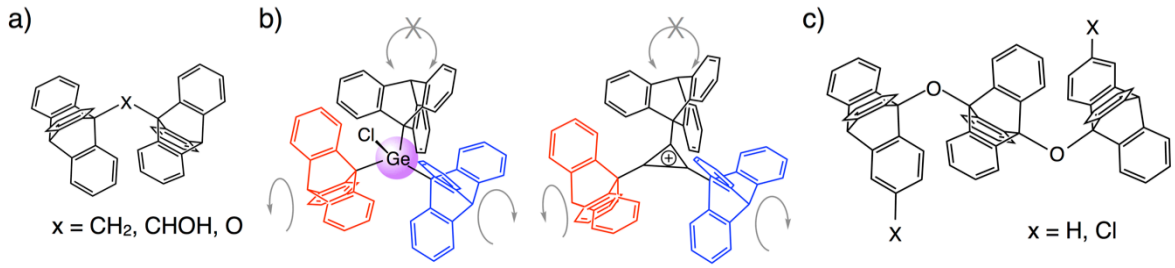

Figure 1-2-2. Molecular gearing systems developed by Iwamura and Mislow.[15–17]

They have synthesized molecules with up to three triptycenes in one molecule. Mislow constructed geared molecules in which three triptycenes were circularly arranged around germanium or cyclopropenium, and showed that its rotational motion was considerably restricted because an odd number of gears cannot rotate concertedly in a circularly arranged, closed system (Figure 1-2-2-b).[16] From this result, paradoxically, a mechanically interlocked structure was demonstrated, but the motion transmission ability as a gear was lost in these molecules.

On the other hand, Iwamura has constructed 9,10-bis(9-triptycyloxy)triptycene in which three triptycenes were crosslinked at the bridgehead positions, and evaluated its interlocking rotational motion (Figure 1-2-2-c).[17] However, from the viewpoint of motion transmission, this design is not suitable for motion transmission in a specific direction due to its structural flexibility, that is, the relative position of the triptycene gears are not fixed due to the lack of stators (Figure 1-2-3).

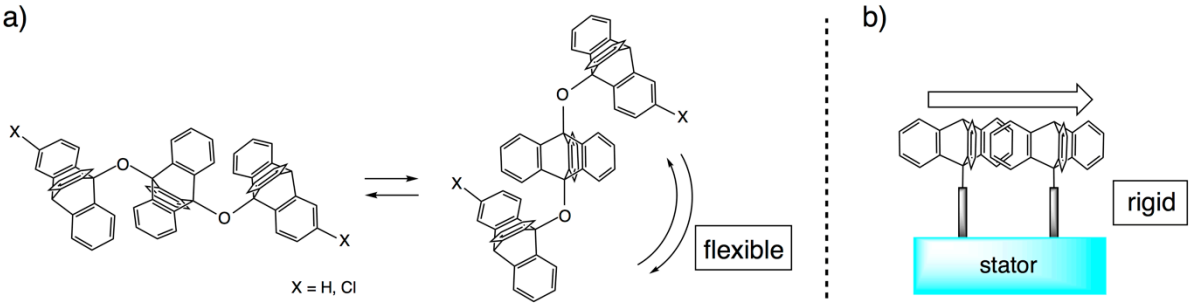

Figure 1-2-3. Structural flexibility depending on the presence of stator.

Since Iwamura and Mislow's pioneering works, molecular gearing systems have been intensively studied to evaluate the correlated motion of two adjacent gears. The design can be largely divided into three types depending on the angle of two rotational axes: i) linear (crown gears), ii) bent (bevel gears), and iii) parallel (spur gears) (Figure 1-2-4).[18]

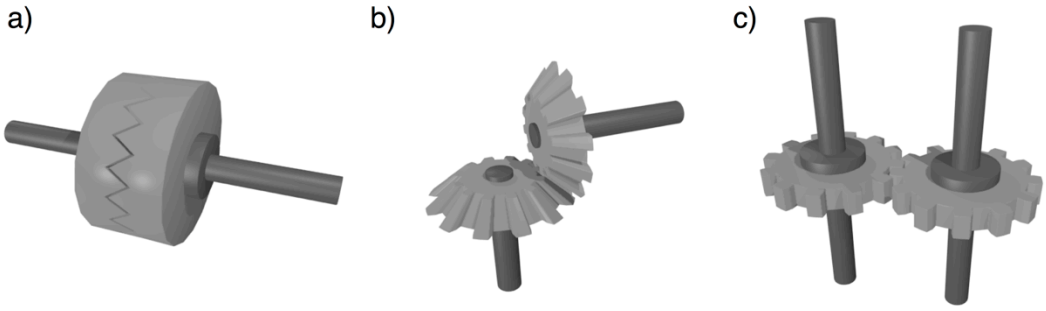

Figure 1-2-4. Several types of macroscopic gearing systems. a) Crown gears. b) Bevel gears. c) Spur gears.

As for the linear system, Vögtle group reported bis(9-triptycyl)ethynes as a first example of hindered rotation around the triple bond (Figure 1-2-5).[19] Since then, the dynamics of these systems have been extensively studied by Toyota group.[20] However, these systems exhibit not dynamic but static gearing: They could not observe dynamic gearing motions because of its structural features.

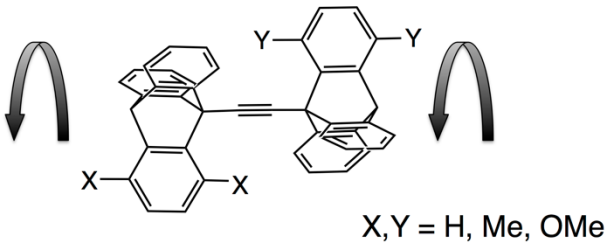

Figure 1-2-5. Linear gearing system extensively investigated by Toyota.[20] Relative motions of the gears could not be demonstrated because of its structural features. (See also Figure 1-2-4-a.)

A bevel gear system has been most studied because it is generally difficult to construct completely parallel multiple rotational axes. As for stator (scaffold or basement), various kinds of motif were investigated to examine the efficiency of gearing motion (Figure 1-2-6-b–e).[11,15,21] Changing of gearing ratio was also attempted in a few groups (Figure 1-2-6-f,g).[13,14]

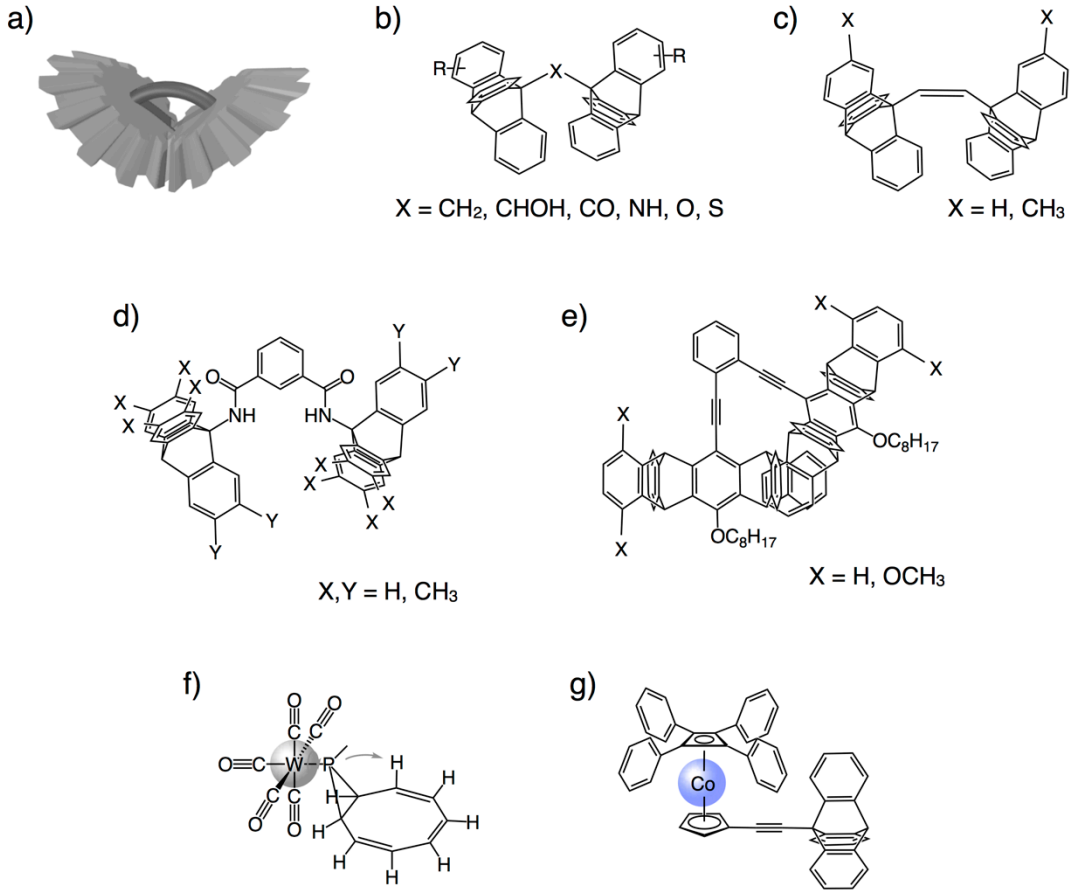

Figure 1-2-6. a) Schematic representation of the bevel gears. b)–g) Various kinds of molecular bevel gear systems.[11,15,21] Changing of gearing ratio was attempted in a few cases (f, g).[13,14]

Construction of a spur gear system was tried by using various scaffolds. Flexible systems were constructed using crown ether (Figure 1-2-7-a),[22a] and a triple gear system was also reported (Figure 1-2-7-b).[22b,22c] Toyota group synthesized a series of bis(9-triptycylethynyl) molecules as prototypes of spur gear systems (Figure 1-2-7-c).[23] Siegel and Baldridge elegantly designed molecules that are suitable for spur gear systems, and dynamic gearing of the system was elucidated (Figure 1-2-7-d).[24]

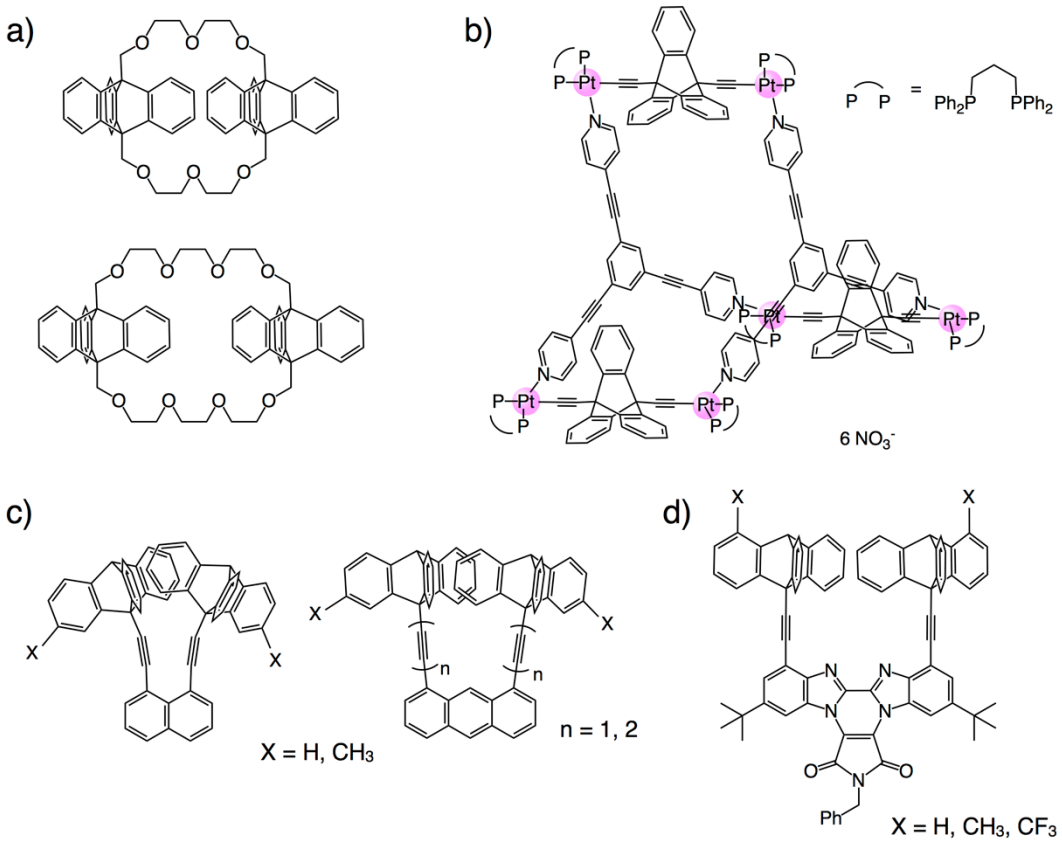

Figure 1-2-7. Various spur gear systems.[22–24]

There are a few examples of gearing systems, which can tune the bent angle between two gears. It acts as “clutch system”, in which engagement or disengagement of the gears can be regulated by external stimuli. Kira and Setaka reported a molecular clutch system based on silane-silicate interconversion driven by fluoride ion (Figure 1-2-8-a).[25] Our group also reported photo- and thermally driven clutch system using *cis-trans* isomerization reaction on a platinum complex (Figure 1-2-8-b).[26] Tuning gear meshing was also examined by applying metal-ion-responsible conformational changes of foldamer as a stator (Figure 1-2-8-c).[27]

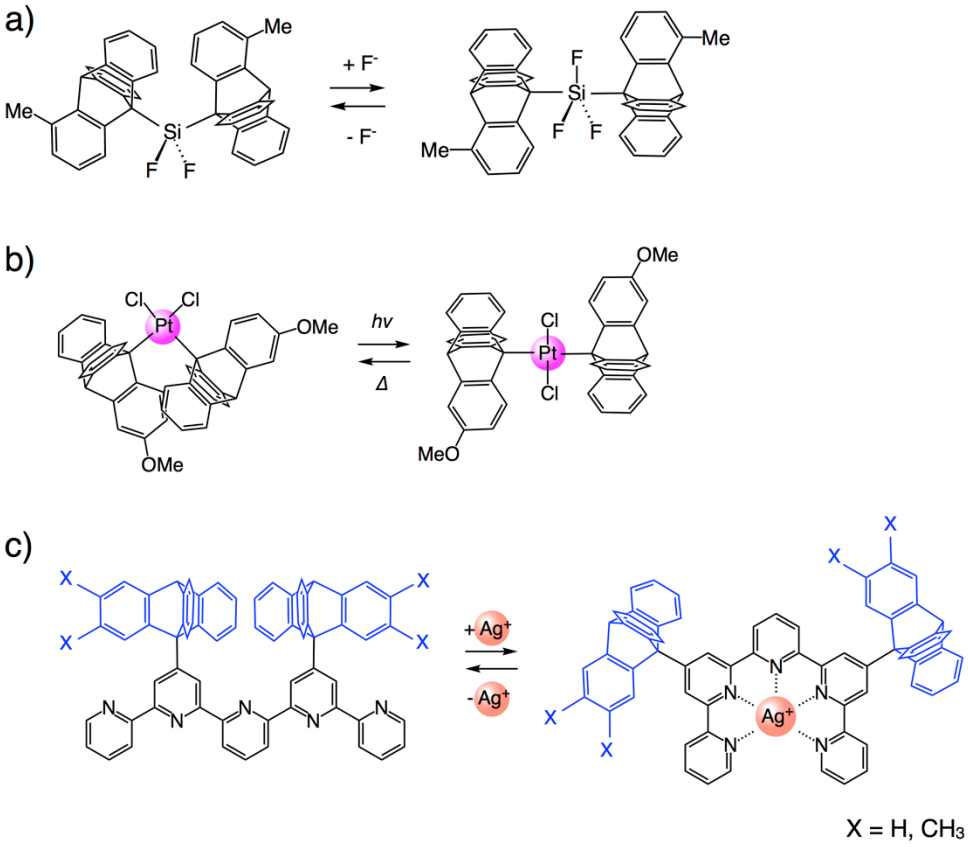

Figure 1-2-8. Molecular clutch systems.[25–27]

As described above, most studies aiming to construct molecular gearing systems are two-gear systems and there are only a limited number of examples using more than two gears. This is probably because, with an increase in the number of gears, it becomes more difficult to design, synthesize, and analyze the motion of the gear systems. To the best of my knowledge, below five examples are known as an intramolecular gearing system composed of more than two gears that can serves as a motion transmission system.[12,17, 28–30]

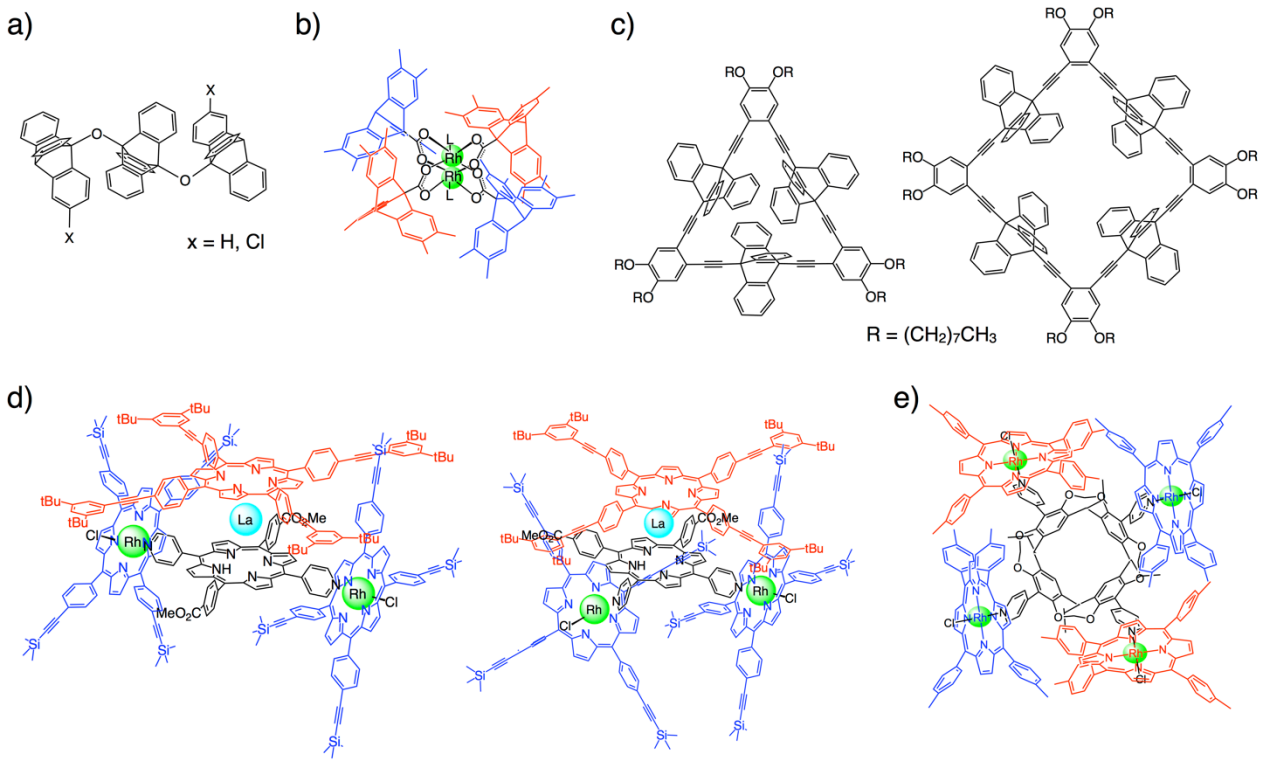

Figure 1-2-9. Molecular gearing systems composed of more than two gears.[12,17,28–30]

The first example was Iwamura's doubly geared molecule as mentioned above (Figure 1-2-9-a).[17] Our group also reported a dirhodium-centered quadruple triptycene gearing system whose rotational speed can be tuned by axial ligands (Figure 1-2-9-b).[28] Recently, Toyota group reported triple and quadruple gearing systems using macrocyclic frameworks (Figure 1-2-9-c).[29]

Porphyrin was also utilized as a molecular-sized gear in some cases. Takeuchi and Shinkai reported interlocking of up to three porphyrin rotors, in which the rotational speeds of the gears in the molecule are different from each other under basic conditions, which suggests that gear meshing can be controlled by acid-base (Figure 1-2-9-d).[12] Kobayashi also synthesized quadruple interlocking porphyrin gear systems (Figure 1-2-9-e).[30]

A gear is a motion transmission element, however, there is no report that demonstrates mechanical transmission through more than three engaging gears. As explained above, most of the studies have focused on the relationship between gears with discussion of a degree of meshing. So far, no researches have focused on a transmission of stimulus through molecular gearing.

1-3. Control of Molecular Rotational Speed

A speed of molecular motion by thermal energy can be, of course, changed depending on temperature; faster motion at higher temperatures and slower motion at lower temperatures. However, it is never “meaningful” control.

One epoch-making study is Kelly’s molecular brake system (Figure 1-3-1).[31] The conformation of coordination site attached to a bridgehead position of triptycene is fixed between teeth of the triptycene by addition of a metal ion, whereby the relative rotational motion of triptycene is restricted.

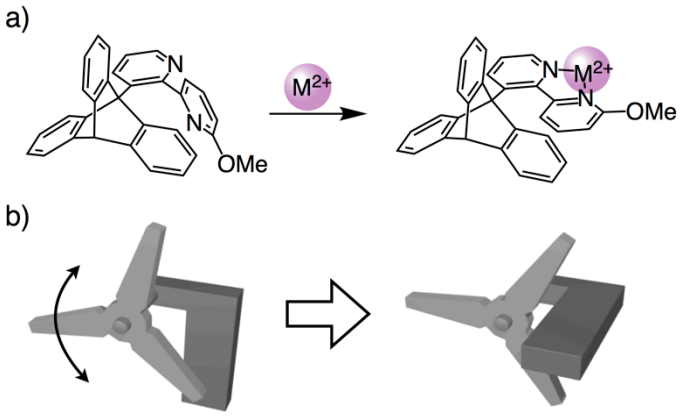

Figure 1-3-1. Molecular brake system developed by Kelly.[31] a) Reaction scheme and b) its schematic representation.

Since then, various study about the restriction of rotational motion are achieved (Figure 1-3-2). Metal-,[32,33] pH-,[33] light-,[34] redox-[35] responsible molecular brake systems have been reported.

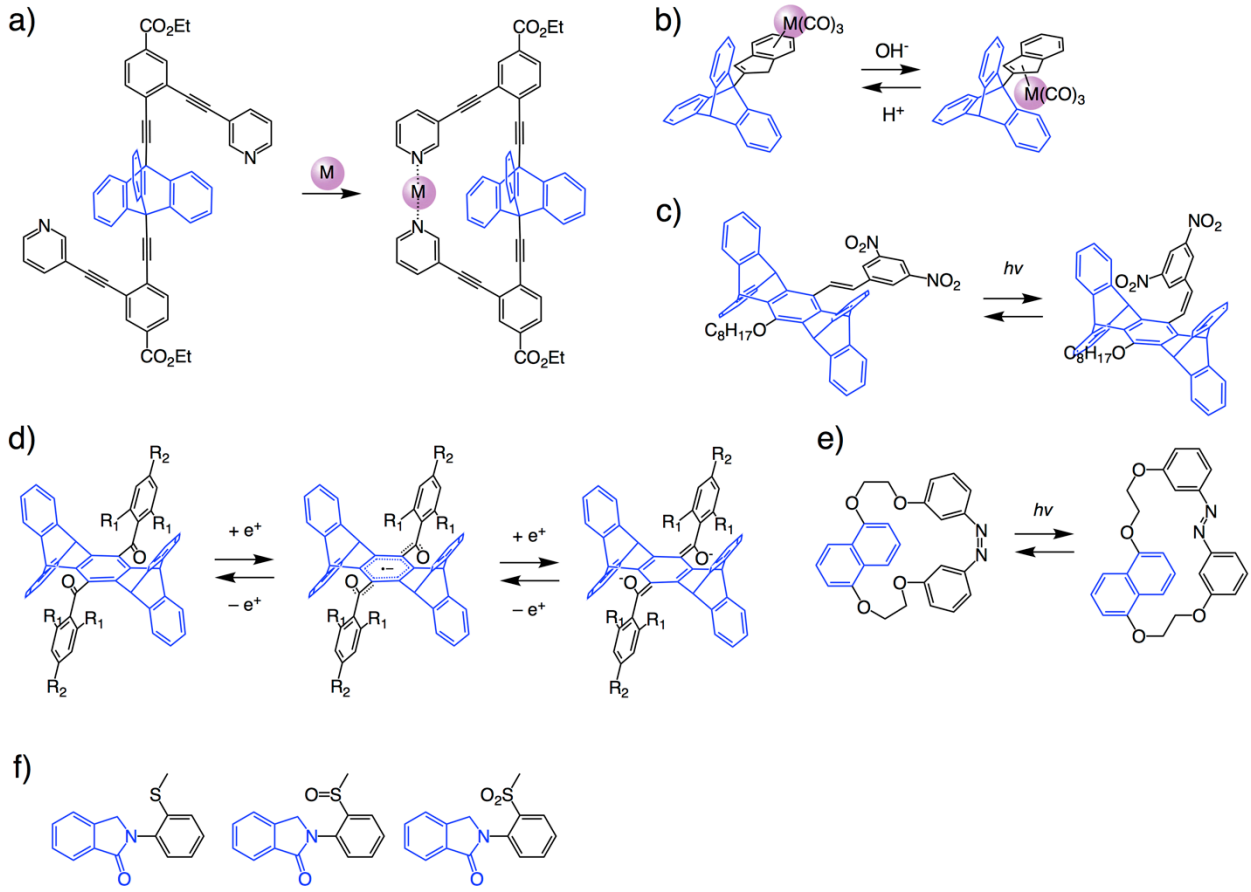

Figure 1-3-2. Some examples of molecular brake systems.[32–35]

Not only molecular brake systems, but also fine tuning of molecular rotational motion is achieved, using porphyrins,[36,37] *N*-aryl imide,[38] and other motifs[39] including acceleration of rotational motion (Figure 1-3-3).

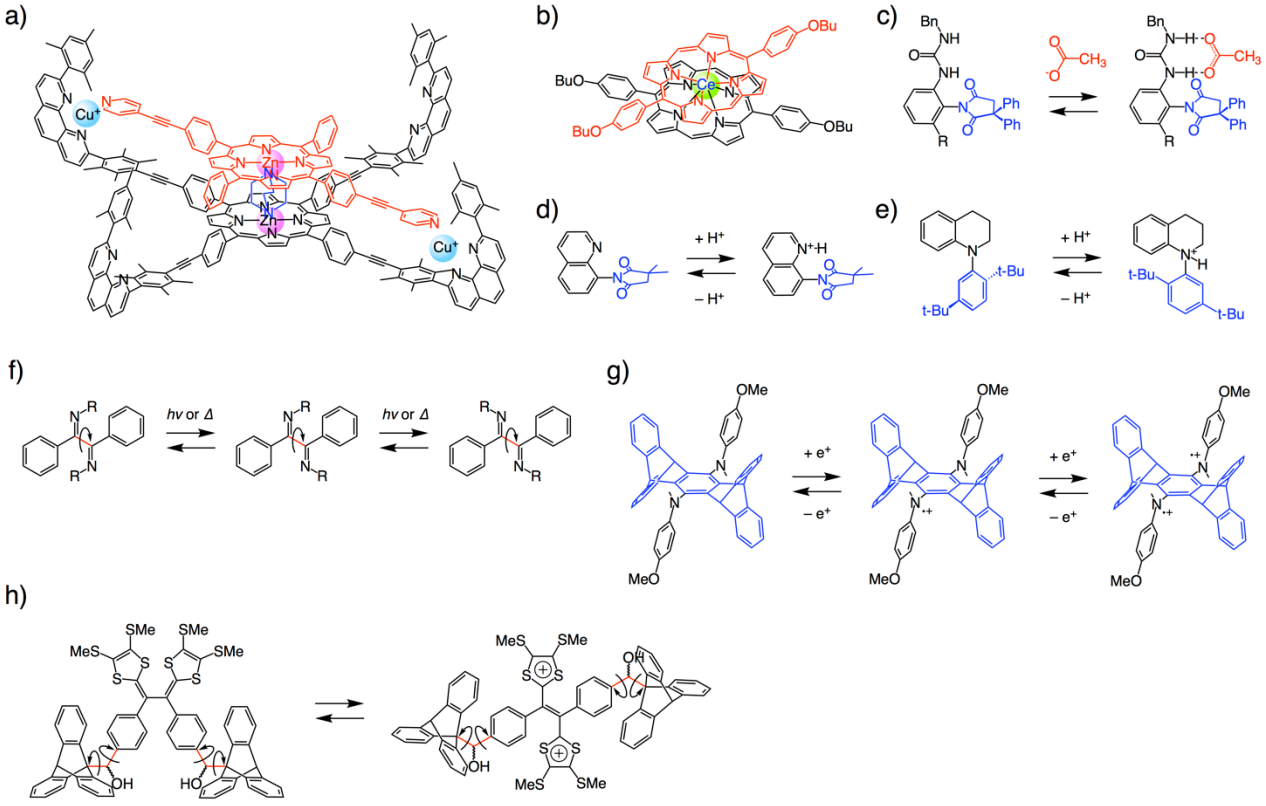

Figure 1-3-3. Some examples of molecular rotational motion regulation by external stimuli.[36–39]

As mentioned before, our dirhodium triptycene gearing system also regulate its rotational motion by changing axial ligands.[28]

1-4. Aim of This Study

Construction of controllable molecular rotational motion device is important for further development of nanotechnology. Molecular gearing systems would provide excellent structural motifs not only for motion transmission but also as a motion regulator unit. However, there are only a limited number of examples having more than two gears in one system. Moreover, there is no report that demonstrates mechanical transmission through gearing, although a gear is designed as a motion transmission element.

In this study, I designed and synthesized a circularly arranged sextuple triptycene gearing system and evaluated its structure and dynamic property. Notably, when a RuCp* (Cp* = pentamethylcyclopentadienyl) complex forms an arene complex with one triptycene phenylene ring of the gearing system, the bulky RuCp* group significantly affects the whole motion in the gearing system, that is, sterical inhibition signals would be transmitted through mechanical meshing of the molecular gears.

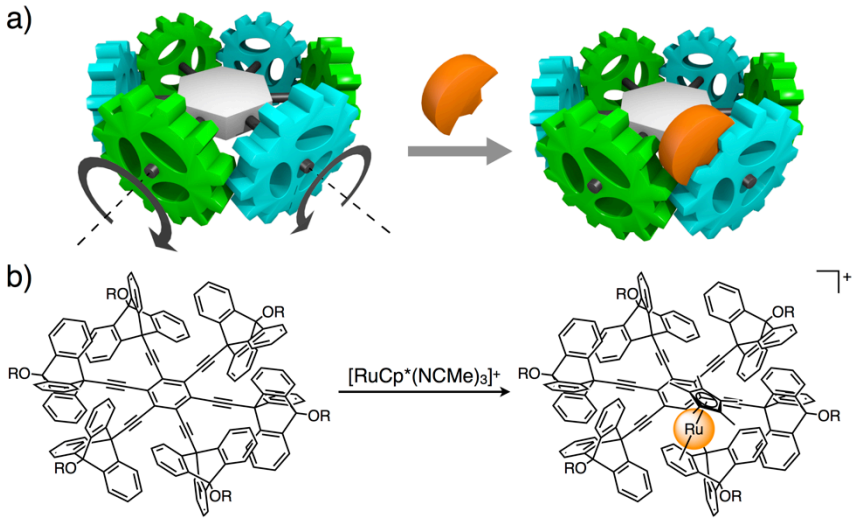

Figure 1-4-1. a) Schematic representation of the gearing system and the effect of a bulky "stopper". b) Synthetic scheme of complexation between the molecular gearing system and $[RuCp^*(NCMe)_3]^+$.

1-5. References

1. H. Noji, R. Yasuda, M. Yoshida, K. Kinosita, *Nature* **1997**, *386*, 299–302.
2. M. L. Walker, S. A. Burgess, J. R. Sellers, F. Wang, J. A. Hammer III, J. Trinick, P. J. Knight, *Nature* **2000**, *405*, 804–807.
3. (a) C. O. Dietrich-Buchecker, J. P. Sauvage, J. P. Kintzinger, *Tetrahedron Lett.* **1983**, *24*, 5095–5098. (b) A. Livoreil, C. O. Dietrich-Buchecker, J. P. Sauvage, *J. Am. Chem. Soc.* **1994**, *116*, 9399–9400.
4. R. A. Bissell, E. Córdova, A. E. Kaifer, J. F. Stoddart, *Nature* **1994**, *369*, 133–137.
5. N. Koumura, R. W. J. Zijlstra, R. A. van Delden, N. Harada, B. L. Feringa, *Nature* **1999**, *401*, 152–155.
6. (a) V. Balzani, A. Credi, F. M. Raymo, J. F. Stoddart, *Angew. Chem. Int. Ed.* **2000**, *39*, 3348–3391. (b) K. Kinbara, T. Aida, *Chem. Rev.* **2005**, *105*, 1377–1400. (c) W. R. Browne, B. L. Feringa, *Nat. Nanotechnol.* **2006**, *1*, 25–35. (d) E. R. Kay, D. A. Leigh, F. Zerbetto, *Angew. Chem. Int. Ed.* **2007**, *46*, 72–191. (e) S. Erbas-Cakmak, D. A. Leigh, C. T. McTernan, A. L. Nussbaumer, *Chem. Rev.* **2015**, *115*, 10081–10206.
7. G. S. Kottas, L. I. Clarke, D. Horinek, J. Michl, *Chem. Rev.* **2005**, *105*, 1281–1376.
8. (a) P. Finocchiaro, D. Gust, K. Mislow, *J. Am. Chem. Soc.* **1974**, *96*, 3198–3205. (b) P. Finocchiaro, D. Gust, K. Mislow, *J. Am. Chem. Soc.* **1974**, *96*, 3205–3213. (c) J. Siegel, A. Gutiérrez, W. B. Schweiser, O. Ermer, K. Mislow, *J. Am. Chem. Soc.* **1986**, *108*, 1569–1575.
9. (a) J. H. Chong, M. J. MacLachlan, *Chem. Soc. Rev.* **2009**, *38*, 3301–3305.
10. N. Seiki, Y. Shoji, T. Kajitani, F. Ishiwari, A. Kosaka, T. Hikima, M. Takata, T. Someya, T. Fukushima, *Science* **2015**, *348*, 1122–1126.
11. C.-Y. Kao, Y.-T. Hsu, H.-F. Lu, I. Chao, S.-L. Huang, Y.-C. Lin, W.-T. Sun, J.-S. Yang, *J. Org Chem.* **2011**, *76*, 5782–5792.
12. (a) S. Ogi, T. Ikeda, R. Wakabayashi, S. Shinkai, M. Takeuchi, *Chem. Eur. J.* **2010**, *16*, 8285–8290. (b) S. Ogi, T. Ikeda, R. Wakabayashi, S. Shinkai, M. Takeuchi, *Eur. J. Org. Chem.* **2011**, 1831–1836.
13. A. M. Stevens, C. J. Richards, *Tetrahedron Lett.* **1997**, *38*, 7805–7808.

14. R. E. Bulo, F. Allaart, A. W. Ehlers, F. J. J. de Kanter, M. Schakel, M. Lutz, A. L. Spek, K. Lammertsma, *J. Am. Chem. Soc.* **2006**, *128*, 12169–12173.

15. (a) Y. Kawada, H. Iwamura, *J. Org. Chem.* **1980**, *45*, 2547–2548. (b) W. D. Hounshell, C. A. Johnson, A. Guenzi, F. Cozzi, K. Mislow, *Proc. Natl. Acad. Sci. USA* **1980**, *77*, 6961–6964. (c) H. Iwamura, K. Mislow, *Acc. Chem. Res.* **1988**, *21*, 175–182. (d) F. Cozzi, A. Guenzi, C. A. Johnson, K. Mislow, W. D. Hounshell, J. F. Blount, *J. Am. Chem. Soc.* **1981**, *103*, 957–958. (e) C. A. Johnson, A. Guenzi, K. Mislow, *J. Am. Chem. Soc.* **1981**, *103*, 6240–6242. (f) C. A. Johnson, A. Guenzi, R. B. Nachbar Jr., J. F. Blount, O. Wennerstroem, K. Mislow, *J. Am. Chem. Soc.* **1982**, *104*, 5163–5168. (g) Y. Kawada, H. Iwamura, *J. Am. Chem. Soc.* **1983**, *105*, 1449–1459. (h) Y. Kawada, H. Iwamura, *J. Am. Chem. Soc.* **1981**, *103*, 958–960. (i) Y. Kawada, H. Iwamura, *Tetrahedron Lett.* **1981**, *22*, 1533–1536. (j) Y. Kawada, H. Yamazaki, G. Koga, S. Murata, H. Iwamura, *J. Org. Chem.* **1986**, *51*, 1472–1477. (k) Y. Kawada, J. Ishikawa, H. Yamazaki, G. Koga, S. Murata, H. Iwamura, *Tetrahedron Lett.* **1987**, *28*, 44533–448.

16. (a) J. M. Chance, J. H. Geiger, K. Mislow, *J. Am. Chem. Soc.* **1989**, *111*, 2326–2327. (b) J. M. Chance, J. H. Geiger, Y. Okamoto, R. Aburatani, K. Mislow, *J. Am. Chem. Soc.* **1990**, *112*, 3540–3547.

17. (a) N. Koga, Y. Kawada, H. Iwamura, *J. Am. Chem. Soc.* **1983**, *105*, 5498–5499. (b) N. Koga, Y. Kawada, H. Iwamura, *Tetrahedron* **1986**, *42*, 1679–1686.

18. D. K. Frantz, K. K. Baldridge, J. S. Siegel, *Chimia* **2009**, *63*, 201–204.

19. P. K. T. Mew, F. Vögtle, *Angew. Chem. Int. Ed. Engl.* **1979**, *18*, 159–161.

20. (a) S. Toyota, T. Yamamori, M. Asakura, M. Oki, *Bull. Chem. Soc. Jpn.* **2000**, *73*, 205–213. (b) S. Toyota, T. Yamamori, T. Makino, M. Oki, *Bull. Chem. Soc. Jpn.* **2000**, *73*, 2591–2597.

21. (a) Y. Kawada, H. Sakai, M. Oguri, G. Koga, *Tetrahedron Lett.* **1994**, *35*, 139–142. (b) G. Wang, L. Ma, J. Xiang, Y. Wang, X. Chen, Y. Che, H. Jiang, *J. Org. Chem.* **2015**, *80*, 11302–11312.

22. (a) J. C. Bryan, R. A. Sachleben, A. A. Gakh, G. J. Bunick, *J. Chem. Crystallogr.* **1999**, *29*, 513–521. (b) T. F. Magnera, J. Michl, J. *Top. Curr. Chem.* **2005**, *262*, 63–97. (c) D. C. Caskey, B. Wang, X. Zheng, J. Michl, *Collect. Czech. Chem. Commun.* **2005**, *70*, 1970–1985.

23. S. Toyota, T. Shimizu, T. Iwanaga, K. Wakamatsu, *Chem. Lett.* **2011**, *40*, 312–314.
24. D. K. Frantz, A. Linden, K. K. Baldridge, J. S. Siegel, *J. Am. Chem. Soc.* **2012**, *134*, 1528–1535.
25. T. Setaka, T. Nirengi, C. Kabuto, M. Kira, *J. Am. Chem. Soc.* **2008**, *130*, 15762–15763.
26. H. Ube, Y. Yasuda, H. Sato, M. Shionoya, *Nat. Commun.* **2017**, *8*, 14296.
27. F. Huang, G. Wang, L. Ma, Y. Wang, X. Chen, Y. Che, H. Jiang, *J. Org. Chem.* **2017**, *82*, 12106–12111.
28. K. Sanada, H. Ube, M. Shionoya, *J. Am. Chem. Soc.* **2016**, *138*, 2945–2948.
29. S. Toyota, K. Kawahata, K. Sugahara, K. Wakamatsu, T. Iwanaga, *Eur. J. Org. Chem.* **2017**, 5696–5707.
30. M. Nakamura, K. Kishimoto, Y. Kobori, T. Abe, K. Yoza, K. Kobayashi, *J. Am. Chem. Soc.* **2016**, *138*, 12564–12577.
31. T. R. Kelly, M. C. Bowyer, K. V. Bhaskar, D. Bebbington, A. Garcia, F. Lang, M. H. Kim, M. P. Jette, *J. Am. Chem. Soc.* **1994**, *116*, 3657–3658.
32. (a) K. Nikitin, C. Bothe, H. Müller-Bunz, Y. Ortin, M. J. McGlinchey, *Organometallics* **2012**, *31*, 6183–6198. (b) G. Wang, H. Xiao, J. He, J. Xiang, Y. Wang, X. Chen, Y. Che, H. Jiang, *J. Org. Chem.* **2016**, *81*, 3364–3371.
33. D. Zhang, Q. Zhang, J. Sua, H. Tian, *Chem. Commun.* **2009**, *13*, 1700–1702.
34. (a) J.-S. Yang, Y.-T. Huang, J.-H. Ho, W.-T. Sun, H.-H. Huang, Y.-C. Lin, S.-J. Huang, S.-L. Huang, H.-F. Lu, I. Chao, *Org. Lett.* **2008**, *10*, 2279–2282. (b) M. C. Basheer, Y. Oka, M. Mathews, N. Tamaoki, *Chem. Eur. J.* **2010**, *16*, 3489–3496. (c) W.-T. Sun, S.-L. Huang, H.-H. Yao, I-C. Chen, Y.-C. Lin, J.-S. Yang, *Org. Lett.* **2012**, *14*, 4154–4157. (d) W. S. Tan, P.-Y. Chuang, C.-H. Chen, C. Prabhakar, S.-J. Huang, S.-L. Huang, Y.-H. Liu, Y.-C. Lin, S.-M. Peng, J.-S. Yang, *Chem. Asian J.* **2015**, *10*, 989–997.
35. (a) P. V. Jog, R. E. Brown, D. K. Bates, *J. Org. Chem.* **2003**, *68*, 8240–8243. (b) T. Tseng, H.-F. Lu, C.-Y. Kao, C.-W. Chiu, I. Chao, C. Prabhakar, J.-S. Yang, *J. Org. Chem.* **2017**, *82*, 5354–5366.
36. (a) K. Tashiro, K. Konishi, T. Aida, *Angew. Chem. Int. Ed. Engl.* **1997**, *36*, 856–858. (b) K. Tashiro, K. Konishi, T. Aida, *J. Am. Chem. Soc.* **2000**, *122,* 7921–7926. (c) M. Takeuchi, T.

Imada, S. Shinkai, *Angew. Chem. Int. Ed.* **1998**, *37*, 2096–2099. (d) M. Ikeda, M. Takeuchi, S. Shinkai, F. Tani, Y. Naruta, *Bull. Chem. Soc. Jpn.* **2001**, *74*, 739–746. (e) M. Ikeda, M. Takeuchi, S. Shinkai, F. Tani, Y. Naruta, S. Sakamoto, K. Yamaguchi, *Chem. Eur. J.* **2002**, *8*, 5541–5550. (f) M. Ikeda, Y. Kubo, K. Yamashita, T. Ikeda, M. Takeuchi, S. Shinkai, *Eur. J. Org. Chem.* **2007**, 1883–1886.

37. (a) S. K. Samanta, M. Schmittel, *J. Am. Chem. Soc.* **2013**, *135*, 18794–18797. (b) S. K. Samanta, J. W. Bats, M. Schmittel, *Chem. Commun.* **2014**, *50*, 2364–2366. (c) S. K. Samanta, A. Rana, M. Schmittel, *Angew. Chem. Int. Ed.* **2016**, *55*, 2267–2272.
38. (a) B. E. Dial, R. D. Rasberry, B. N. Bullock, M. D. Smith, P. J. Pellechia, S. Profeta, Jr., K. D. Shimizu, *Org. Lett.* **2011**, *13*, 244–247. (b) B. E. Dial, P. J. Pellechia, M. D. Smith, K. D. Shimizu, *J. Am. Chem. Soc.* **2012**, *134*, 3675−3678. (c) Y. Suzuki, M. Kageyama, R. Morisawa, Y. Dobashi, H. Hasegawa, S. Yokojima O. Kitagawa, *Chem. Commun.* **2015**, *51*, 11229–11232.
39. (a) C.-H. Yang, C. Prabhakar, S.-L. Huang, Y.-C. Lin, W. S. Tan, N. C. Misra, W.-T. Sun, J.-S. Yang, *Org. Lett.* **2011**, *13*, 5632–5635. (b) G. Chen, Y. Zhao, *Org. Lett.* **2014**, *16*, 668–671. (c) L. Greb, A. Eichhöfer, J.-M. Lehn, *Eur. J. Org. Chem.* **2016**, 1243–1246.

2. Sextuple Triptycene Gearing System

2-1. Introduction

As mentioned in section **1-2** in **Chapter 1**, "gearing" enables long-distance motion transmission of rotation, and is also used for adjusting the rotational speed and torque, controlling the direction of rotation, and dividing and integrating power by assembling multiple gears. A gear plays an important role in a macroscopic machine, and it is an interesting topic whether or not a molecular gear at the nanoscale can act in the same manner as a macroscopic machine.

Some molecular gearing systems have been previously reported,[1a–1d] however, there are only a limited number of examples using more than two gears in one system.[2a–2e] This may be because, as the number of gears in a molecule increases, the design and synthesis of the molecule become more and more difficult.

In this study, I have designed and synthesized a sextuple triptycene gearing system and evaluated its motion transmission efficiency and the effect of metal coordination on the molecular motion.

2-2. Design and Synthesis of a Gearing System 1

I designed a gear molecule **1** in which six triptycene gears are attached to a central benzene ring *via* an acetylene linker (Figure 2-2-1). Long dodecyloxy side chains are introduced at the bridgehead of each triptycene to increase the solubility of the gear molecule **1**.

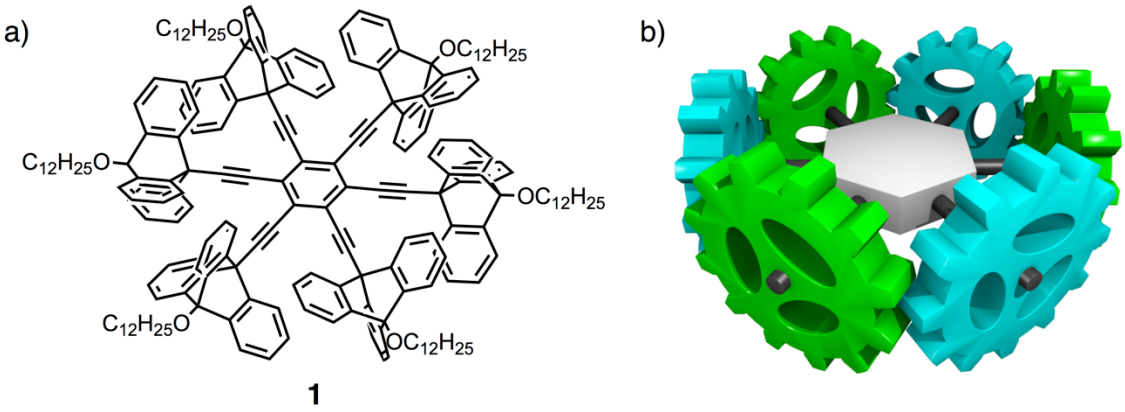

Figure 2-2-1. a) Molecular structure and b) schematic representation of the target gear molecule **1**.

By arranging the triptycenes circularly, the design and synthesis of the molecule become easier because of its high symmetry. Even number of gears is required for the concerted rotation in a circularly closed system. In this design, the degree of meshing between the adjacent gears can be tuned by adjusting the linker length. In fact, I designed and synthesized a similar molecule **1'** in my master course, which possesses a longer phenylene moiety as a linker. In the molecule, a loosely meshed structure was predicted by a Molecular Mechanics (MM) method. (Figure 2-2-2).

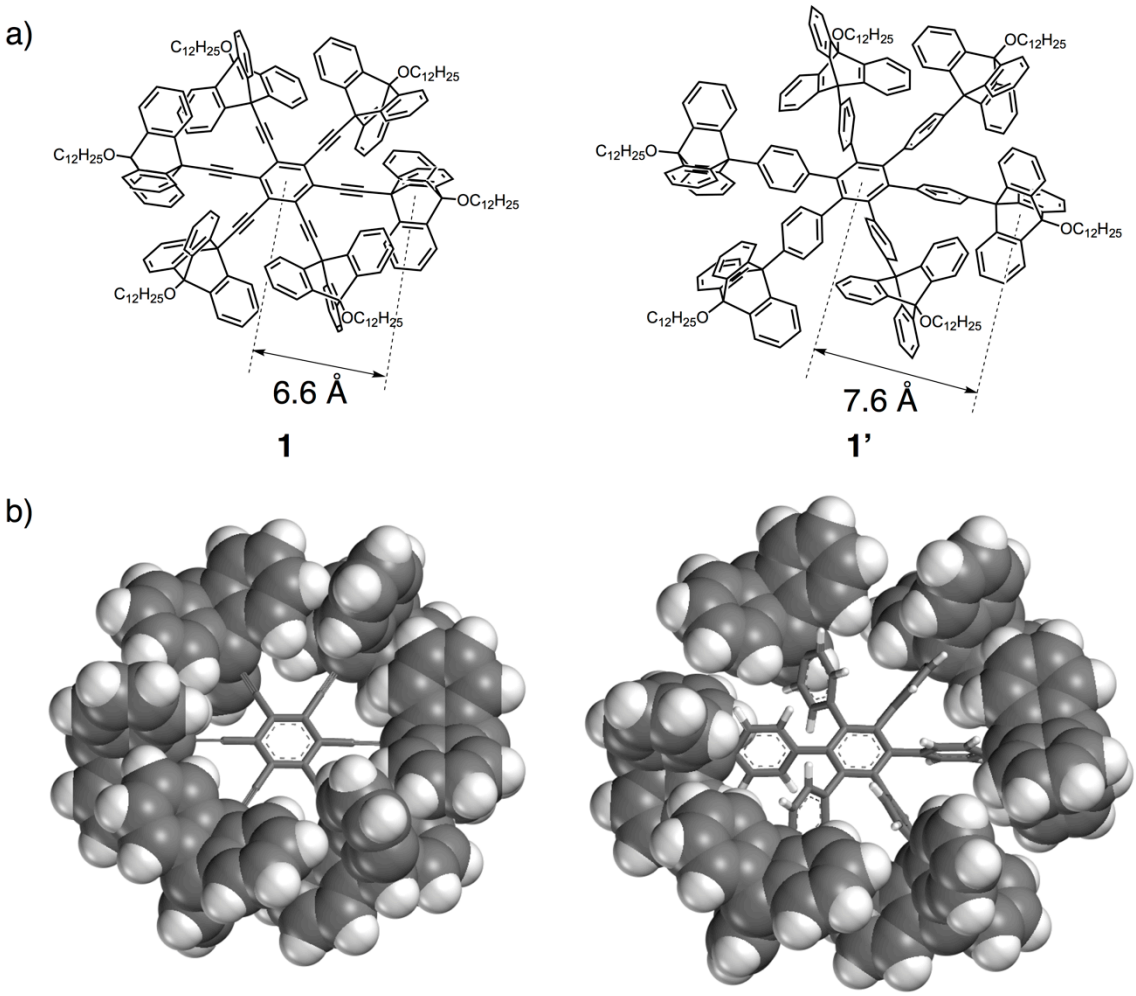

Figure 2-2-2. a) Comparison of distances between the centers of the molecule and the triptycene moiety for **1** and **1'**. The distance for **1'** with phenylene moieties is longer than that for **1** with acetylene moieties. b) MM structures of **1** and **1'**. It is also apparent from the comparison between **1** and **1'** that the gear system **1** provides a closer gearing system. The core parts are shown in a stick model and the triptycene moieties are shown in a space filling model. Side chains are omitted for clarity.

The retrosynthetic route is shown in Figure 2-2-3. The target molecule **1** can be obtained by trimerization reaction of the bis-substituted alkyne as an important precursor. In this study, I introduced dodecyloxy side chains to the triptycene gears to enhance the solubility of the molecule.

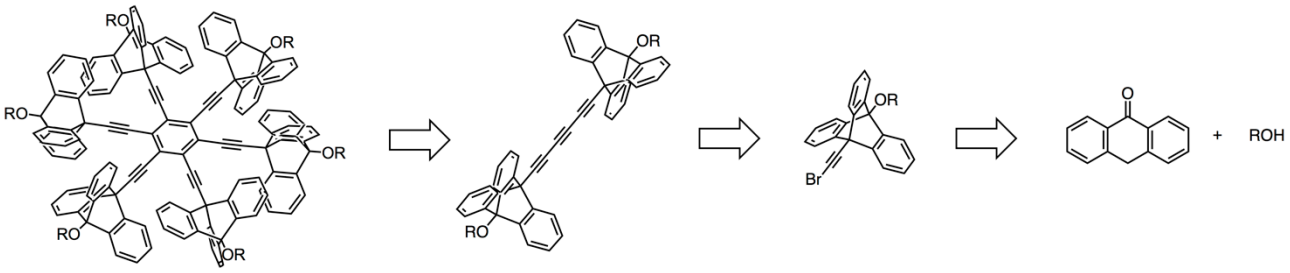

Figure 2-2-3. The retrosynthetic route of the target gear molecule **1**.

The detailed synthetic route is shown in Scheme 2-2-1. I chose anthron as a starting material. First, 9-dodecyloxyanthracene (**2**) was synthesized by condensation reaction of anthron with 1-dodecanol. Then, an acetylene linker was introduced by Sonogashira reaction. The triptycene framework was prepared by Diels-Alder reaction of **4** with benzyne. Deprotection and bromination were carried out to obtain bromoacetylene **7**. This synthetic intermediate **7** was converted to triyne **10** by using Cadiot-Chodkiewicz coupling twice. Then obtained triyne **10** was finally trimerized in the presence of a cobalt catalyst, $Co_2(CO)_8$, under microwave irradiation to afford the desired compound **1**. Thus gear molecule **1** with high symmetry was obtained in 10 steps in 13% overall yield. The molecular structure of **1** was fully characterized by various 1D and 2D NMR spectroscopies, ESI-TOF mass spectrometry, X-ray structure analysis, and elemental analysis.

Scheme 2-2-1. Synthesis of the target gear molecule **1**.

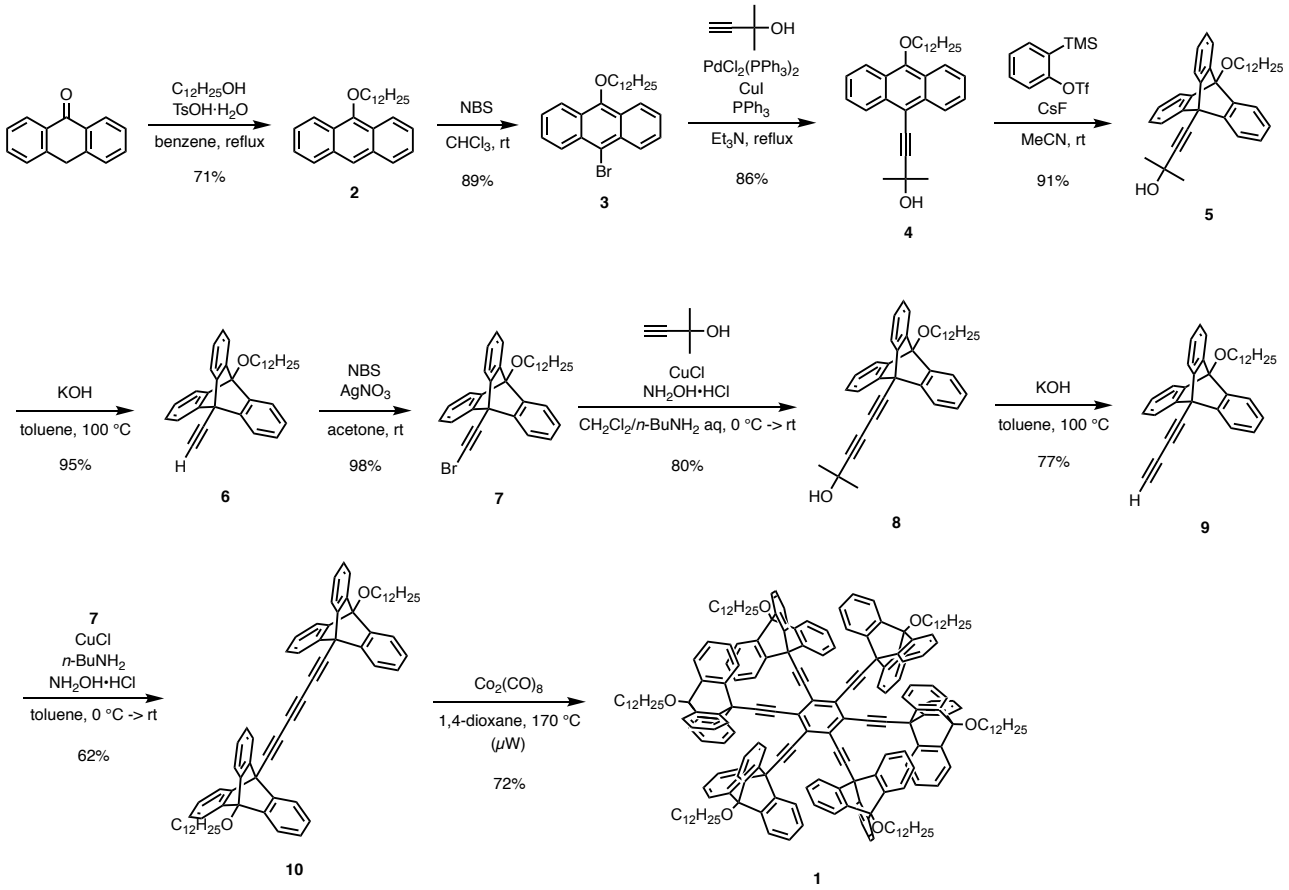

All signals in ^{1}H NMR were assigned by 2D NMR (COSY and NOESY) spectroscopy. In the aromatic region, the signals for protons *b* and *c* were significantly up-field shifted. For instance, the signal of proton *b* was observed around 5.3 ppm, which is up-field shifted by 1.7 ppm compared with that of the precursor triyne. This is due to the strong shielding effect from the adjacent triptycene, suggesting the tightly meshed gearing structure of **1**. Proton *b* showed a more up-field shifted signal than proton *c* compared with non-substituted triptycene (^{1}H NMR chemical shifts of *b* and *c* for non-substituted triptycene are observed at 6.97 ppm in $CDCl_3$[3]) due to the cyclic arrangement of triptycene, that is, the degree of meshing around proton *b* is greater than proton *c* which is located outside.

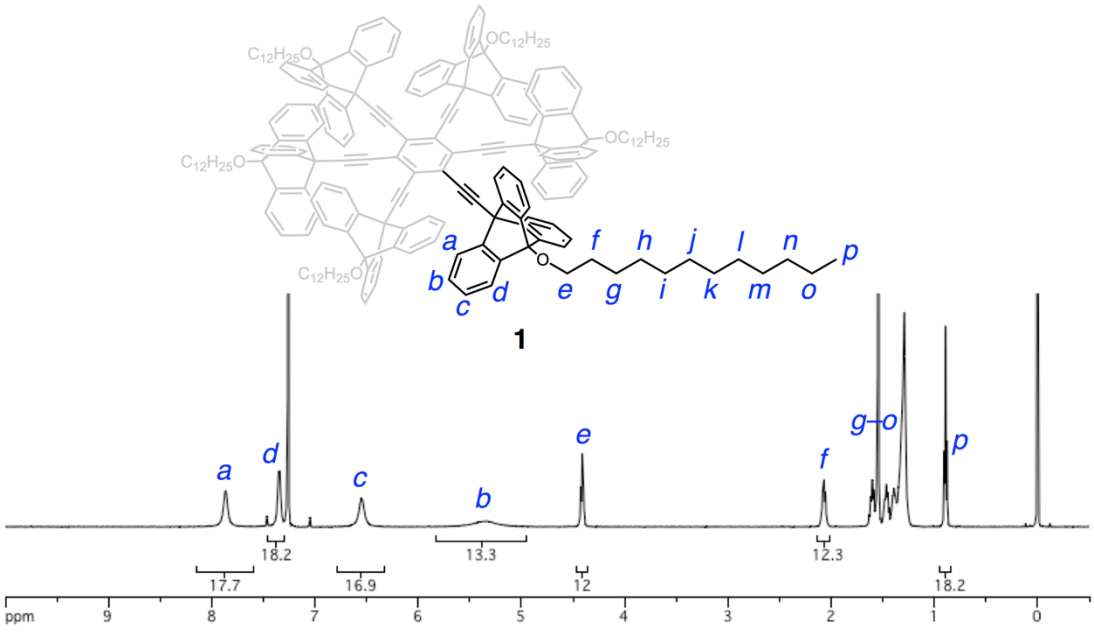

Figure 2-2-4. ^{1}H NMR spectrum of gear molecule **1** (500 MHz, $CDCl_3$, 300 K).

The signals of protons *a–d* in the triptycene moiety were significantly broadened at 300 K compared with the protons *e–p* of the side chains. This indicates that the rotational speed of triptycene moieties is comparable to the NMR timescale (the detailed dynamics will be discussed later in section **2-3**). Moreover, the signals of the three phenylene rings of one triptycene give the appearance that they are chemically equivalent, which suggests that the triptycene moieties of **1** rotate slightly faster than NMR timescale at 300 K. The tightly meshed structure of **1** would lead to the higher activation barrier of the rotational motion of the triptycene moiety than a meshing-free triptycene rotor in which the activation barrier is normally too low to be measured experimentally.[4]

A single crystal of gear molecule **1** suitable for X-ray structural analysis was obtained by vapor diffusion with $CHCl_3$/acetone (Figure 2-2-5). The side chain moieties are largely disordered as shown in Figure 2-2-5-a or 2-2-5-c, but the core structure is clearly observed. In the crystal state, the molecule takes D_{3d} symmetry and the adjacent gears are alternately arranged upwards and downwards as shown in Figure 2-2-6-a. The triptycenes tightly mesh with each other, but there

were no strain as judged from the bond distances and angles (Figure 2-2-6-b). The distance between the phenylene rings of the adjacently meshing triptycenes was 3.14 Å, which indicated their strong π–π interaction. Neither intermolecular gearing nor rotational motion was observed in the crystalline state due to the densely packed dodecyloxy side chains as shown in Figure 2-2-7. No obvious gearing motions were observed in the crystal state under the condition of measurement, although there are several reports on solid-state molecular rotational motion.[5]

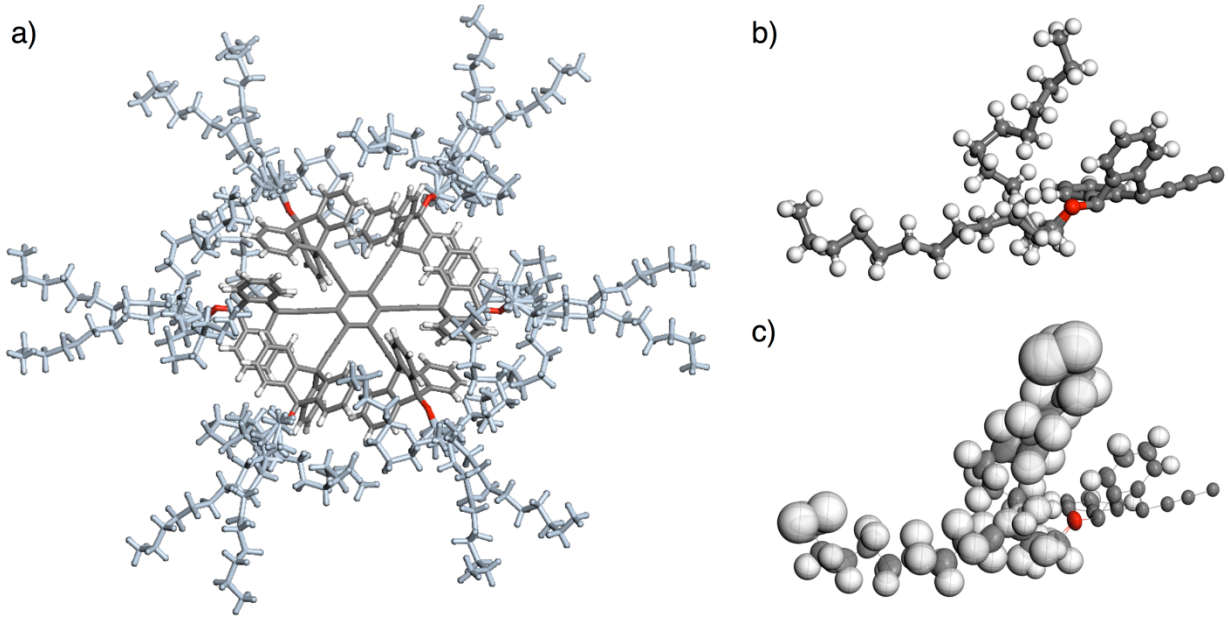

Figure 2-2-5. a) Crystal structure of **1** in a stick model. Disordered dodecyl groups are colored in light blue. The others are colored based on CPK coloring. Color code; C gray, H white, O red. b) An asymmetric unit of crystal structure of **1** in a ball and stick model. c) b) in the ORTEP diagram with thermal ellipsoids setting at the scale factor = 1.53 (50% probability).

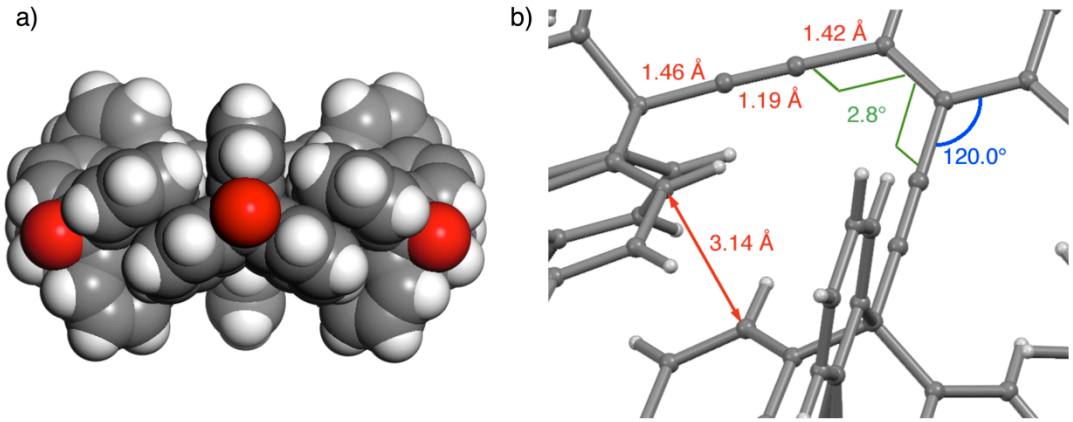

Figure 2-2-6. a) Crystal structure of **1** as a side view in a space filling model. The adjacent triptycenes are alternately arranged upwards and downwards and tightly meshing with each other. Disordered dodecyl groups are omitted for clarity. b) Selected bond lengths and angles of **1** in a ball and stick model, suggesting that there are no strains in the crystal state.

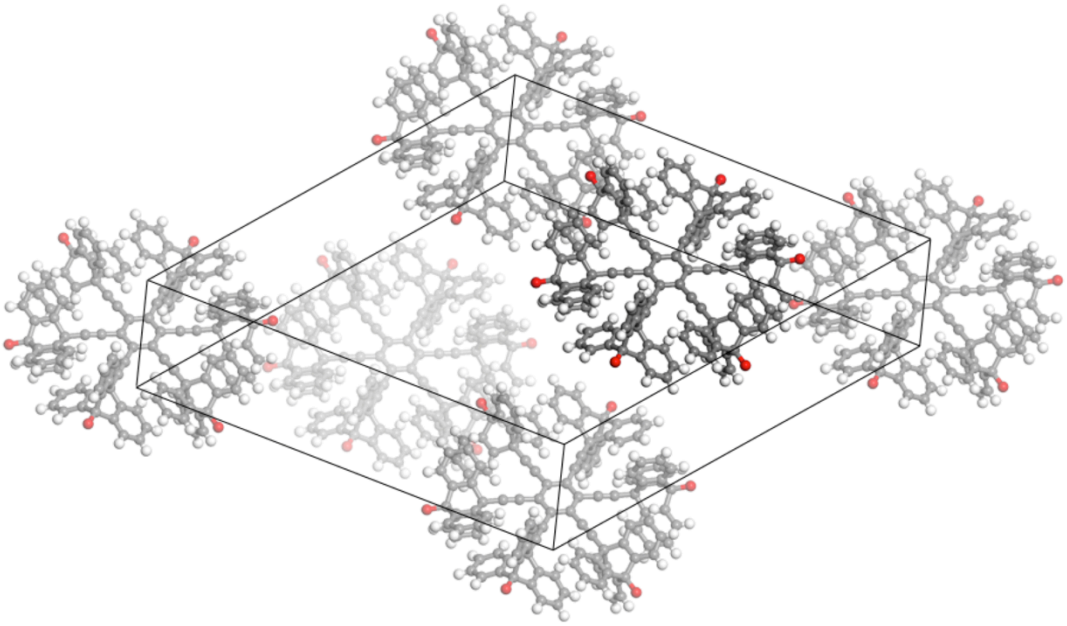

Figure 2-2-7. Unit cell of **1** in a ball and stick model shows its packing structure. Omitted dodecyl groups are filled in the vacant space. Intermolecular gearing is impossible in the crystal state.

2-3. Motion Evaluation of the Gearing System 1

Variable temperature-(VT-)NMR spectroscopy provides an excellent way to evaluate molecular motions in solution.[6] A reversible molecular process that results in a detectable change in NMR spectra in a range from –150 to +150 °C with a rate constant from *ca.* 10 to 10,000 sec^{-1} ($\Delta G^{\ddagger}$ corresponds to from *ca.* 5 to 26 kcal/mol) can be studied by variable temperature dynamic NMR (DNMR) spectroscopy. The range of evaluable free energy highly depends on the difference between frequencies (or chemical shifts) of the exchanging signals.

DNMR spectroscopy can deal with only a process in equilibrium. Most of the studies have focused on *degenerate* processes, that is, the starting material and product are identical and therefore K_{eq} is 1. *Non-degenerate* processes can also be studied by DNMR but both species (= both signals) should exist at equilibrium in an observable amount (Figure 2-3-1).

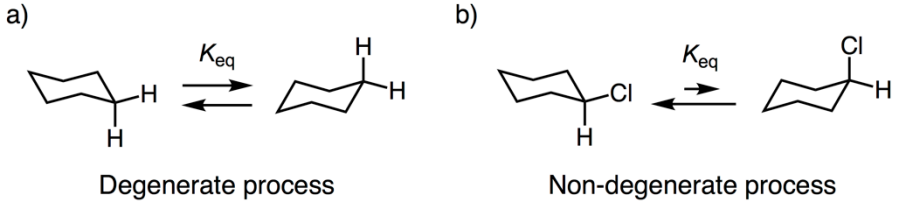

Figure 2-3-1. Examples of evaluable dynamics by DNMR spectroscopy. a) Cyclohexane inversion as a degenerate system. b) Chlorocyclohexane inversion as a non-degenerate system.

When the molecule has some different, exchangeable conformations and the exchange rate is comparable to or faster than the NMR timescale, a coalesced signal is obtained. On the other hand, when the molecular motion becomes slower than the NMR timescale at low temperatures, the signals of the different conformations become independent and split (Figure 2-3-2).

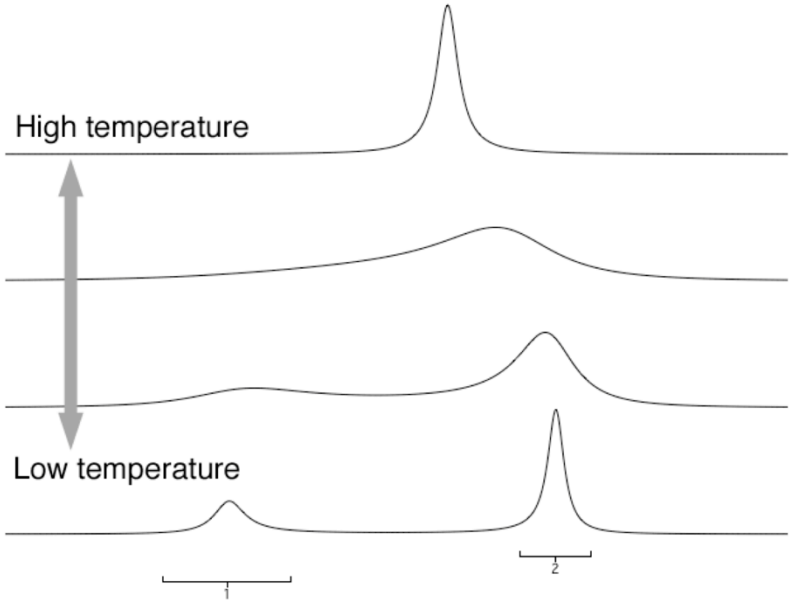

Figure 2-3-2. Outline drawing of temperature-dependent NMR spectral changes when the rate of molecular conformational exchanges is comparable to the NMR timescale. NMR signals coalesced at higher temperatures and split at lower temperatures.

To apply the DNMR spectroscopy, high quality spectral measurement at given temperatures is required within a range of two independent signals broadend and coalesced into one signal. An estimated rate constant at each temperature could be calculated from the spectral data using several approximate formulas.[7]

Approximate DNMR formulas are shown below.

For broadening of a single peak well below coalescence, *i.e.*, before the peaks begin to overlap,

$$k = \pi(\Delta\nu - \Delta\nu_{ref}).$$

For uncoupled equal intensity nuclei at coalescence,

$$k = \frac{\pi}{\sqrt{2}} \quad \nu_{AB}.$$

For residual broadening of a peak after coalescence,

$$k = \frac{\pi \nu_{AB}^{2}}{2(\Delta\nu - \Delta\nu_{ref})} .$$

Here,

$\Delta\nu$: peak width at half height of exchanging singlet (in Hz).

$\Delta\nu_{ref}$: peak width at half height of non-exchanging reference singlet.

ν_{AB} : chemical shift (in Hz) between A and B.

k : rate constant in sec^{-1}.

These formulas include the effects of motional narrowing.

The VT-NMR spectra of **1** are shown in Figure 2-3-3. The signals of side chain moieties (proton *e*–*p*) did not exhibit temperature dependence. On the other hand, the signals of triptycene moiety were significantly changed depending on temperature. Averaged signals at higher temperatures were split into two independent signals at lower temperatures. Coalescence of the signals was observed around 260 K.

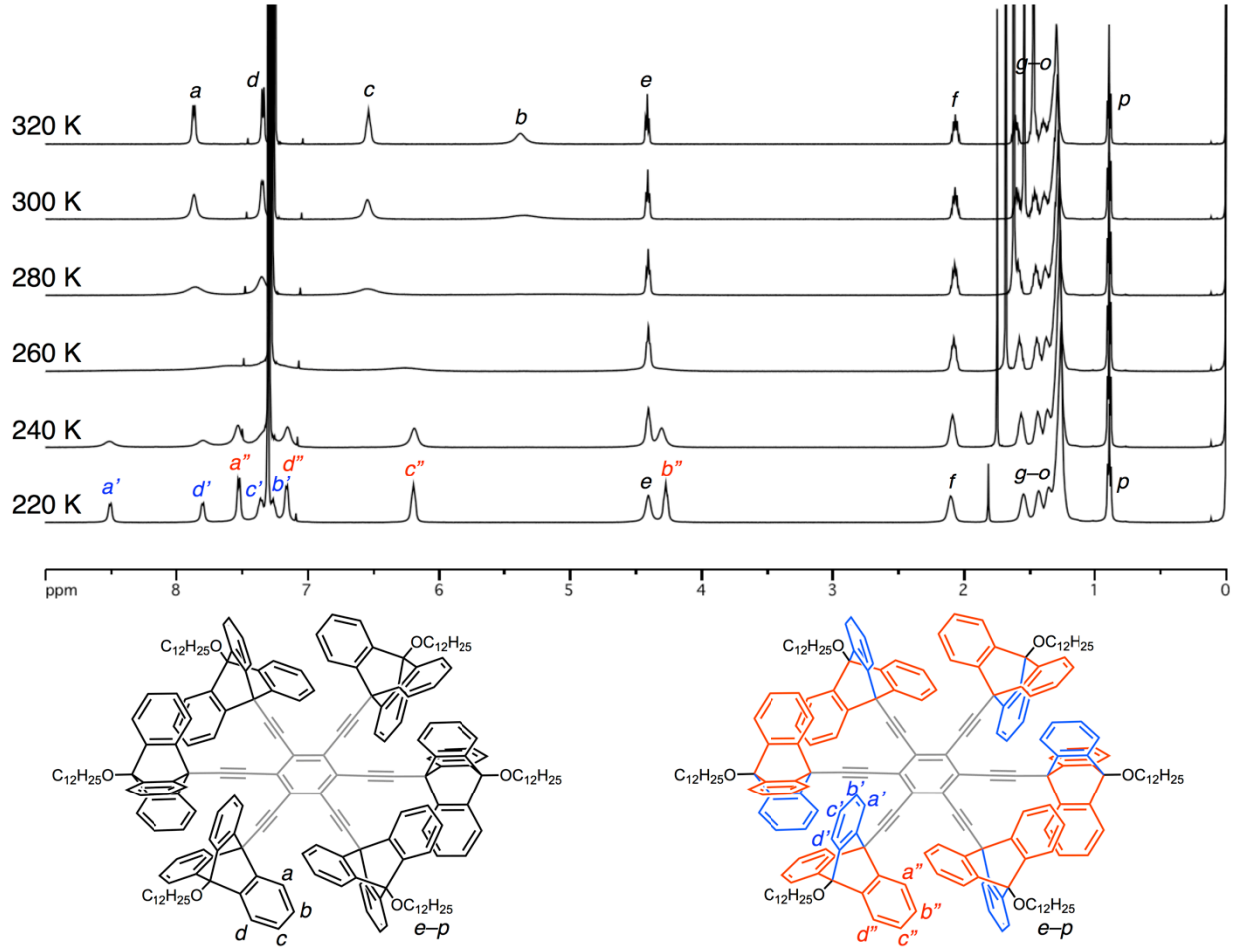

Figure 2-3-3. VT-^{1}H NMR spectra of **1** (500 MHz, $CDCl_3$) with signal assignment.

There are 3 × 6 = 18 phenylene rings that belong to the six triptycene moieties, however, only four kinds of protons were observed at high temperatures (T > 260 K). This indicates that the motion of the triptycene moieties (the exchange of phenylene rings) is faster than the NMR timescale at these temperatures, and consequently only one set of averaged signals was obtained.

On the other hand, two sets of signals for the triptycene moieties were observed in an integral ratio of 1:2 at low temperatures (T < 260 K), indicating the 18 phenylene rings were divided into 6 and 12. It is quite unlikely that six triptycene moieties behave in a different manner because of the molecular symmetry, so this signal separation would be derived from desymmetrization of each triptycene moiety at low temperatures.

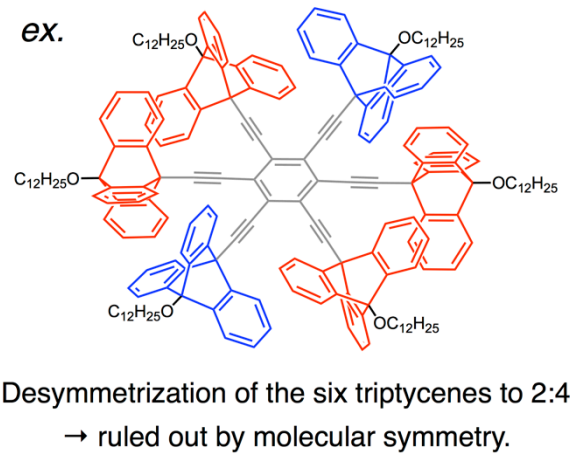

Figure 2-3-4. Signal splitting in a 1:2 integral ratio at low temperature can be explained by dividing the six triptycenes into two groups, however, this possibility is unlikely due to the symmetry of the molecule.

When focusing on one triptycene in the gear system **1**, three phenylene rings cannot locate in the same environment at once because of its symmetry (Figure 2-3-5). If the rotation of the tripytence was faster than NMR timescale, phenylene rings would be observed as coalesced signals. On the other hand, independent signals would be obtained if the triptycene rotates slower.

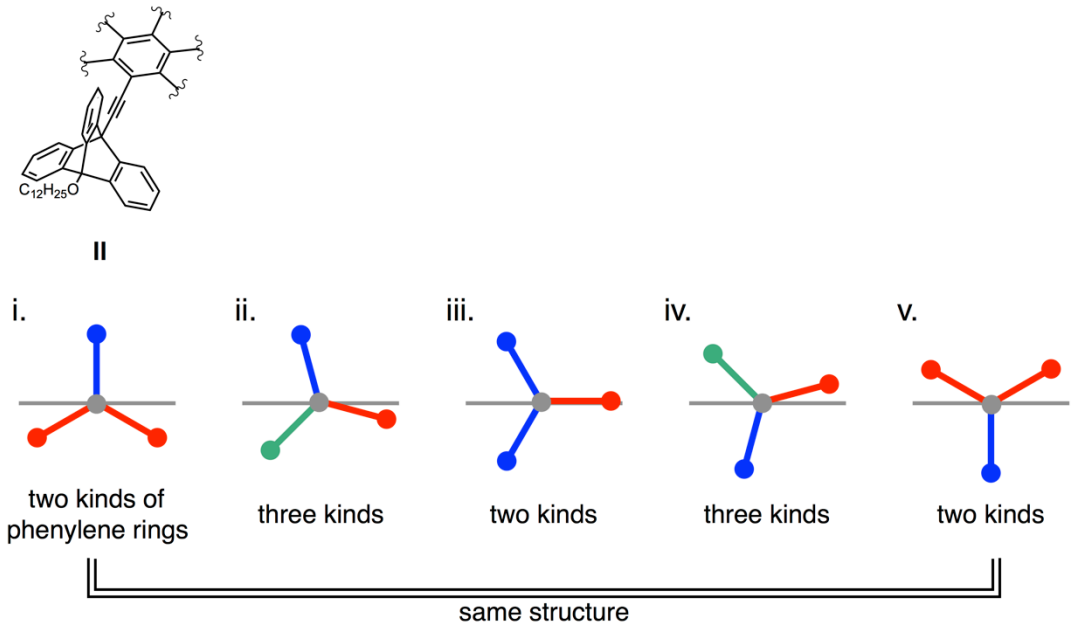

Figure 2-3-5. Schematic representation of one triptycene gear in the gear system **1**. Three phenylene rings of one triptycene should locate at least two kinds of environments at a certain moment.

From the fact that the coalesced signals at high temperatures were split in a 1:2 integral ratio at low temperatures, the averaged conformation of each triptycene at low temperatures can be regarded as structure i (v) or iii in Figure 2-3-5.

Considering the whole molecule, there are four possible conformations, which is consistent with the experimental result (Figure 2-3-6-b–e). Because of the large steric hindrance, conformations b) and e) would be obviously excluded.

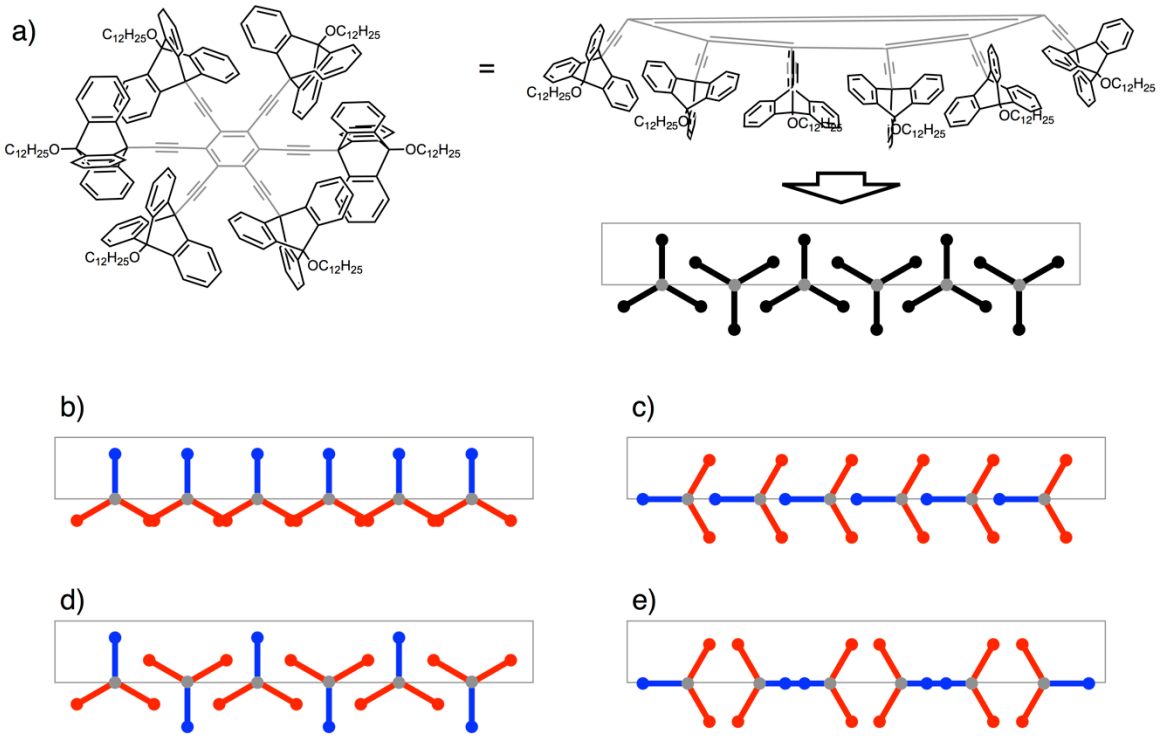

Figure 2-3-6. a) Schematic representation of triptycene gears in the gear system **1**. b)–e) Four possible conformations of triptycenes consistent with a 1:2 integral ratio.

Major signals were observed in the higher magnetic field, whereas minor signals were observed in the lower magnetic field compared to the signals at higher temperatures (Figure 2-3-3). This result indicates that the averaged conformation at low temperatures can be regarded as an alternate structure d), which is the same as the crystal structure. As for protons *b* and *c*, the signals were widely split as a result of the larger up-field shift for protons *b"* and *c"*, due to the shielding effect from the phenylene rings of the adjacent triptycenes. On the other hand, the down-field shift for proton *a'* due to the deshielding effect from the adjacent tripycene largely contributes to the signal splitting of proton *a*.

From the obtained spectra, theoretical dynamic NMR simulation was conducted using iNMR software (version 5)[8] (Figure 2-3-7). The obtained spectra were simulated using a two-state exchange model, and from the evaluated data, the rate constant *k* of the exchange of the triptycene blade at each temperature was calculated according to the formulas on page 33.

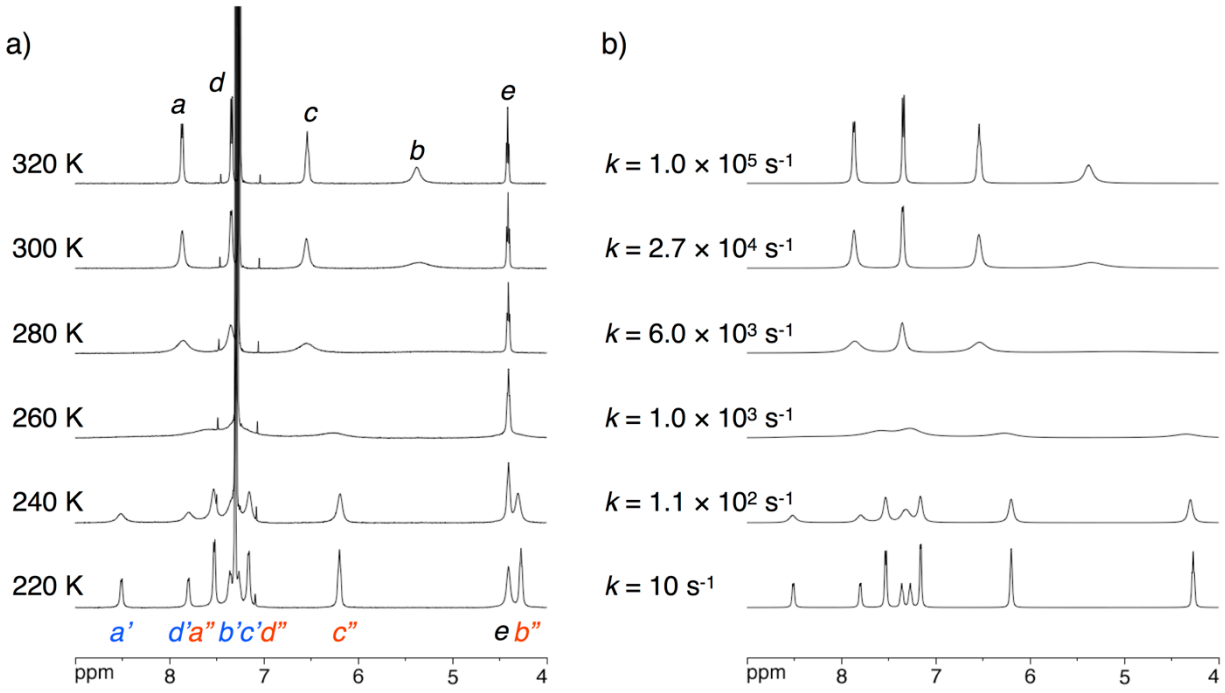

Figure 2-3-7. a) Partially experimental VT-^{1}H NMR spectra of **1** (500 MHz, $CDCl_3$) and b) their theoretical dynamic NMR simulation. Only the signals of triptycene moiety (*a*–*d*) are simulated. Assignment of the signals is the same as Figure 2-3-3.

Two-state exchange model is set to evaluate the interconversion from one conformation to the other conformation in equilibrium. In the case of cyclohexane, for example, interconversion from one chair conformation to another chair conformation through a series of intermediate structures of higher energy (half-chair, twist-boat, boat) is applicable (Figure 2-3-8).[9]

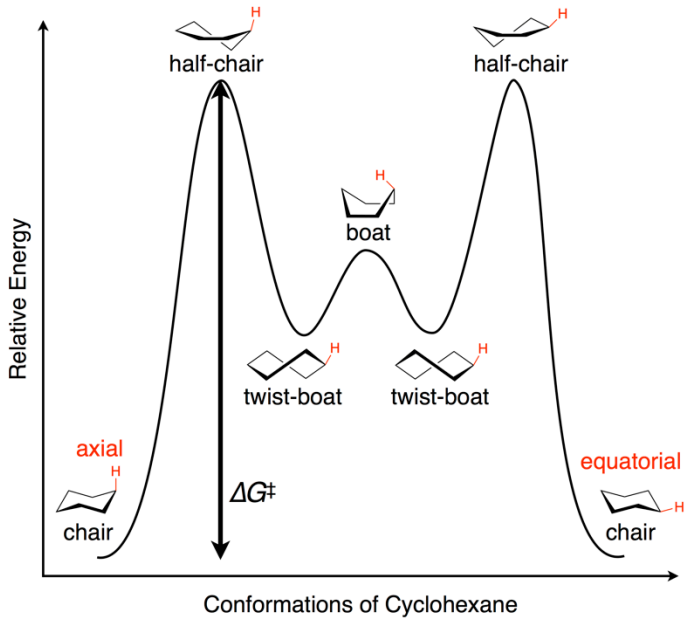

Figure 2-3-8. Conformational changes during the inversion of cyclohexane. Axial and equatorial protons interconvert through the process. There are several intermediates in the reaction coordinate.

Only the free energy difference between the initial and transition states can affect the rate of interconversion between the stable conformations in equilibrium, and the reaction path or the intermediates have nothing to do with the reaction rate. In other words, the rate constant k for interconversion can be calculated depending on the activation free energy $\Delta G^{\ddagger}$ only.

In the gearing system here, a certain phenylene ring (or a certain proton) can exist in either of the two environments at equilibrium, which means the two-state exchange model is applicable. The exchange rate constants between stable conformations at each temperature are shown in Figure 2-3-7.

There are two possible pathways for the exchange of the triptycene blades, that is, "geared rotation" and "gear slippage"[1c] (Figure 2-3-4). In the geared rotation, adjacent triptycene gears rotate in the opposite directions *via* a *tounge-and-groobe* transition state. Gear slippage is an undesired rotation where the phase of meshing is changed from the initial state. In general, geared rotation has lower energy barrier than gear slippage motion,[1b] however, these motions couldn't be distinguished in this case. To evaluate the frequency of the gear slippage, some substituents should be introduced on the triptycene blades, and the exchange between the phase isomers has to be discussed.

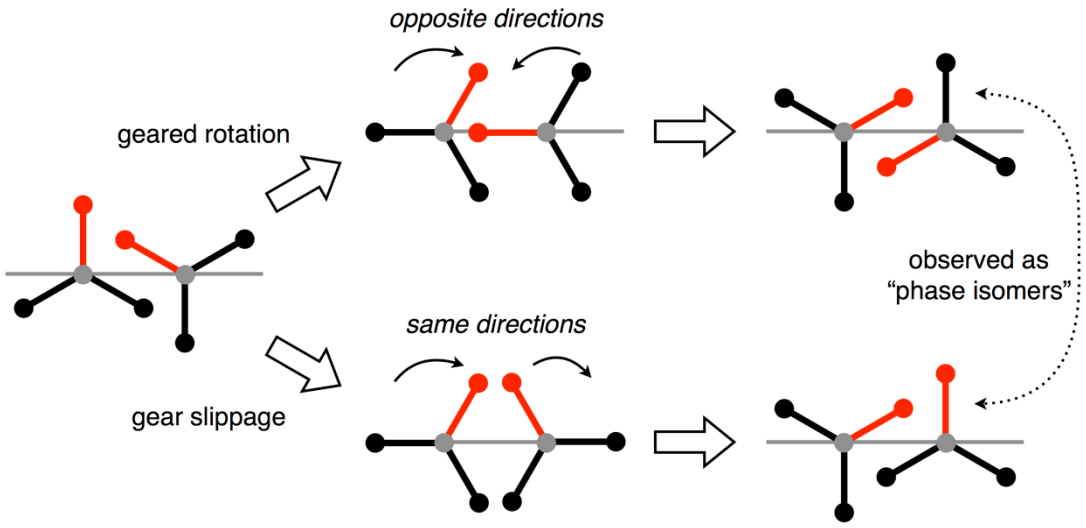

Figure 2-3-9. Schematic representation of "geared rotation" and "gear slippage". Depending on the pathway, the phase of the gear should be changed.

It should be noted that the rate constant *k* represents the frequency of 60° flipping between the phenylene blades, which would include "geared rotation" and "gear slippage" mentioned above (Figure 2-3-10).

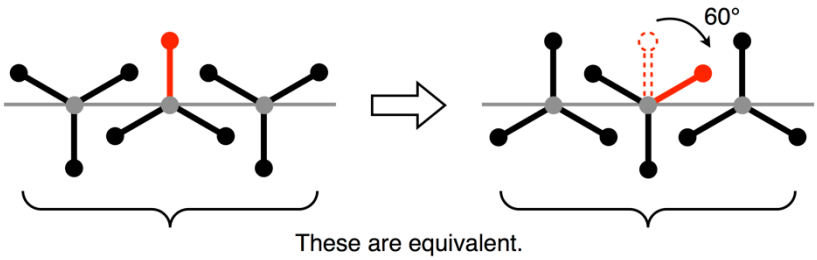

Figure 2-3-10. Schematic representation of 60° rotation. Because of the structural symmetry of gear molecule **1**, 60° rotation is enough for the recovery of the initial states.

By applying Eyring plots, the activation enthalpy and entropy can be estimated.

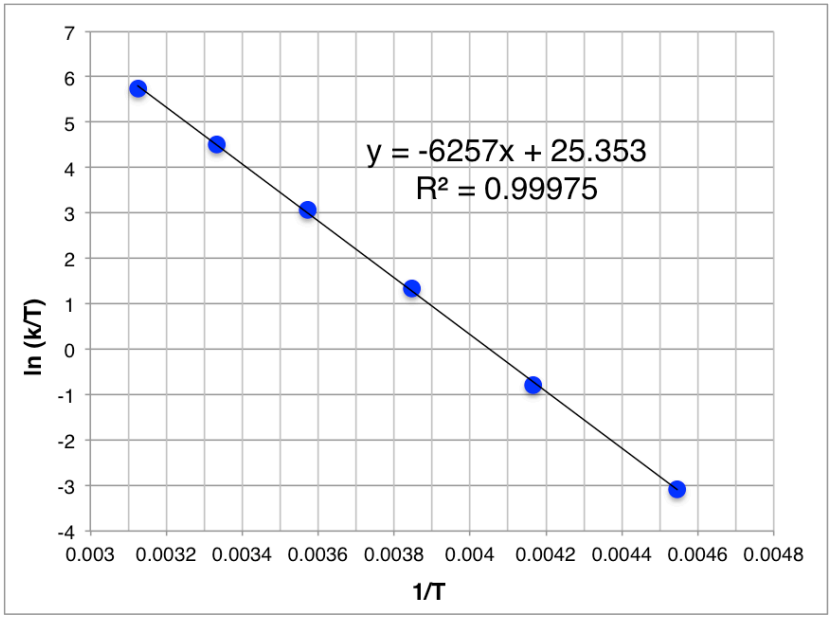

Figure 2-3-11. Eyring plots calculated from the simulated spectra with its approximate straight line and the coefficient of determination.

From the Eyring equation, the rate constant k can be written as below.

$$k = \kappa \frac{k_B T}{h} \exp\left(\frac{-\Delta G^{\ddagger}}{RT}\right)$$

Here, κ: transmission factor, k_B: Boltzmann's constant, T: absolute temperature, h: Planck's constant, $\Delta G^{\ddagger}$: Gibbs energy of activation, R: gas constant.

Therefore,

$$k = \kappa \frac{k_B T}{h} \exp\left(\frac{-\Delta H^{\ddagger}}{RT}\right) \exp\left(\frac{\Delta S^{\ddagger}}{R}\right) ,$$

($\Delta H^{\ddagger}$: enthalpy of activation, $\Delta S^{\ddagger}$: entropy of activation)

$$\ln \frac{k}{T} = \frac{-\Delta H^{\ddagger}}{R} \cdot \frac{1}{T} + \ln \kappa \frac{k_B}{h} + \frac{\Delta S^{\ddagger}}{R} .$$

The transmission factor κ, which reflects how much of the transition state molecule proceeds to the product, is assumed to be one. This means that every molecule at the transition state goes through to form the product.

The plot of $\ln(k/T)$ versus $1/T$ gives straight line (Figure 2-3-11), where enthalpy of activation ($\Delta H^{\ddagger}$) can be derived from slopes and entropy of activation ($\Delta S^{\ddagger}$) can be derived from intercepts of the approximate straight line.

From the obtained approximate straight line (y = –6257x + 25.353), the kinetic parameters were calculated as below.

$$\Delta H^{\ddagger} = +12.4 \pm 0.1 \text{ kcal·mol}^{-1}$$

$$\Delta S^{\ddagger} = +3.2 \pm 0.4 \text{ cal·mol}^{-1}\text{·K}^{-1}$$

There are only a few reports in which the activation parameters are evaluated for the rotation of molecular gears.[10,11]

In the cases of porphyrin gear systems below,[10] both the activation enthalpy and entropy were lower than those obtained in this study, which suggests smoother motion of the gears. It cannot be unconditionally compared since it is a completely different system between triptycene and porphyrin, including the number of the gear teeth, the lower energy barriers for rotational motion might be because the molecule itself is large and the degree of meshing is looser compared to this study.

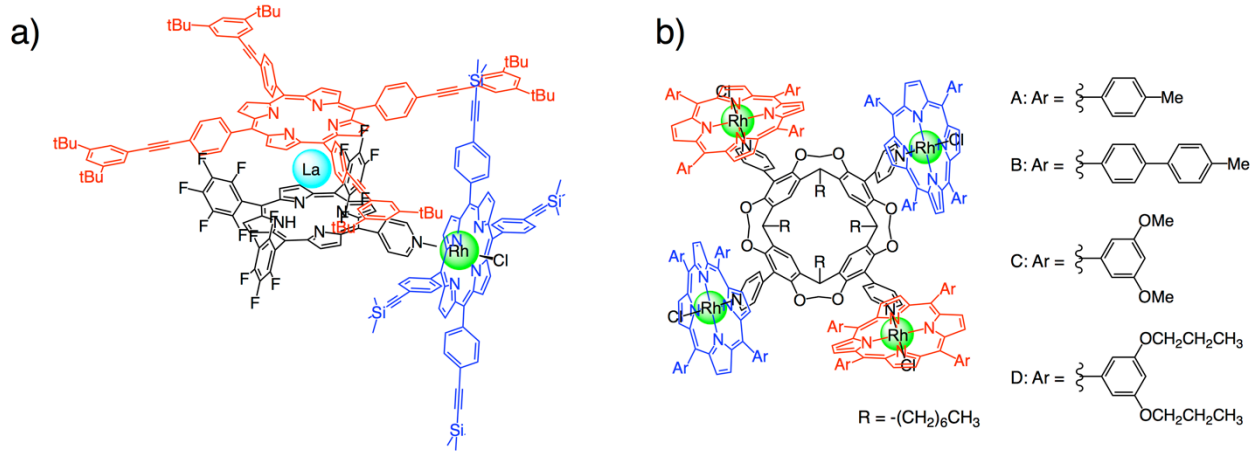

Rotor	$\Delta H^{\ddagger}$ (kcal mol^{-1})	$\Delta S^{\ddagger}$ (cal mol^{-1} K^{-1})
top	6.64	–28.7
side	6.79	–25.3

complex	$\Delta H^{\ddagger}$ (kcal mol^{-1})	$\Delta S^{\ddagger}$ (cal mol^{-1} K^{-1})
A	5.92	–17.25
B	2.96	–28.87
C	5.38	–18.05
D	6.79	–15.05

Figure 2-3-12. Activation parameters for the motion of porphyrin gear systems.[10] These values were calculated from the NMR spectra measured in CD_2Cl_2 in both cases.

To the best of my knowledge, the activation parameters for the rotational motions of the triptycene gears are experimentally evaluated in only two examples below.[11] Here theoretical calculations or the system evaluating only gear slippage motions are excluded. In most of the studies, the activation parameters for the rotational motions are too low to estimate by VT-NMR measurements. Examples below adopted sterically hindered amide bond or circularly closed system to increase the activation energy for rotation. The activation barriers are comparable to that of this study.

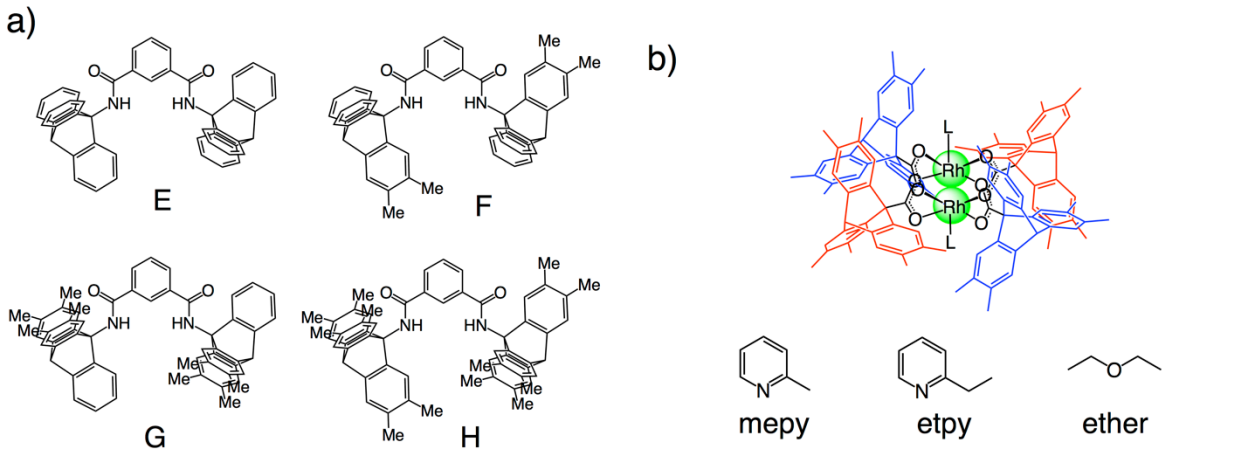

compound	$\Delta H^{\ddagger}$ (kcal mol^{-1})	$\Delta S^{\ddagger}$ (cal mol^{-1} K^{-1})
E	12.3 ± 0.4	11.0 ± 2.0
F	9.2 ± 0.1	–5.9 ± 0.4
G	12.3 ± 0.3	11.0 ± 1.2
H	8.9 ± 0.2	–6.3 ± 0.7

L	$\Delta H^{\ddagger}$ (kcal mol^{-1})	$\Delta S^{\ddagger}$ (cal mol^{-1} K^{-1})
mepy	14.5 ± 1.2	6 ± 5
etpy	18.0 ± 0.5	16.6 ± 1.9
ether	11.4 ± 0.2	–0.9 ± 0.8

Figure 2-3-13. Activation parameters for the motion of triptycene gearing systems.[11]

The positive value of the activation entropy for the gearing system **1** means that the entropy at the transition state is higher than the stable conformation, which can be explained by the molecular symmetry.

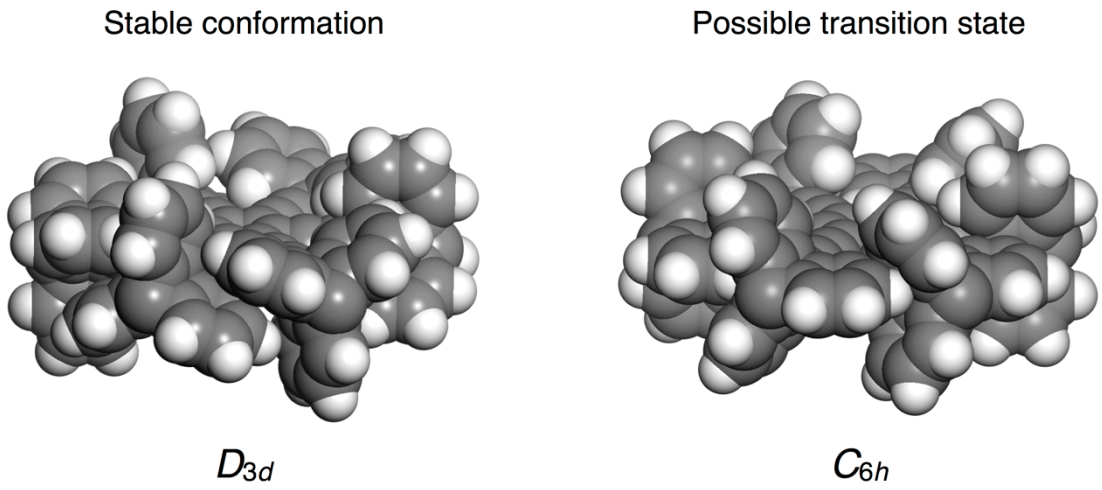

Figure 2-3-14. Molecular structure of stable conformation and possible transition states. Ideally, the molecule adopts D_{3d} or C_{6h} symmetry. Side chains are omitted for clarity.

Comparing the symmetry of the molecule, the transition state would take a lower symmetrical conformation than stable conformation (Figure 2-3-14). Moreover, the conformation of the transition state is ideally C_{6h}, but there is steric hindrance between adjacent triptycene gears, suggesting more desymmetrized structure is favored at the transition state. Other factors such as solvent releasing effect might also affect the activation entropy.

2-4. Metal-mediated Control of the Gearing System 1

Ruthenium-Cp* (Cp* = pentamethylcyclopentadienyl) complex is known to react with a phenylene ring of triptycene molecule (Scheme 2-4-1).[12] I expected that the ruthenium complex would attach to a triptycene moiety of the molecule, and it would block the rotational motion of the RuCp*-attached triptycene (Figure 2-4-1). The whole motion in the molecule would be then sterically inhibited through gearing and the interlocking motion should be directly demonstrated as a gradual change in the motional rate depending on the distance from RuCp*.

Scheme 2-4-1. Reaction of triptycene with ruthenium-Cp* complex.[12]

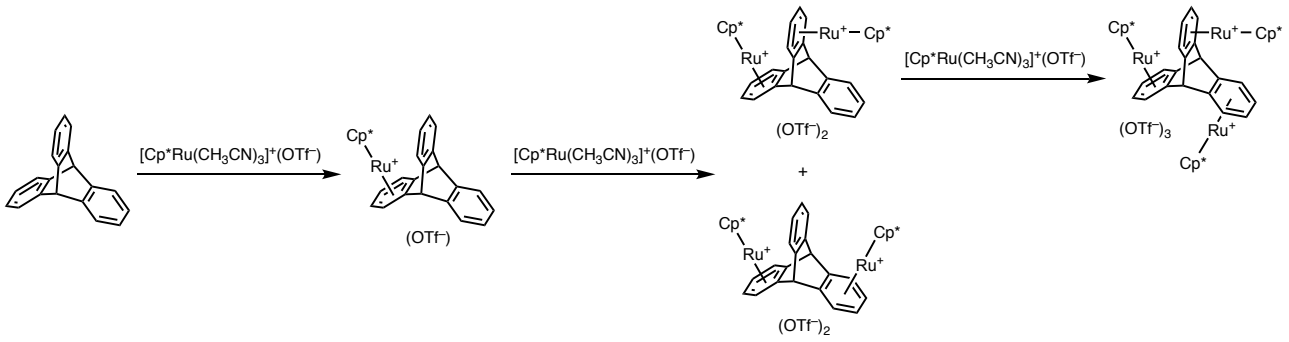

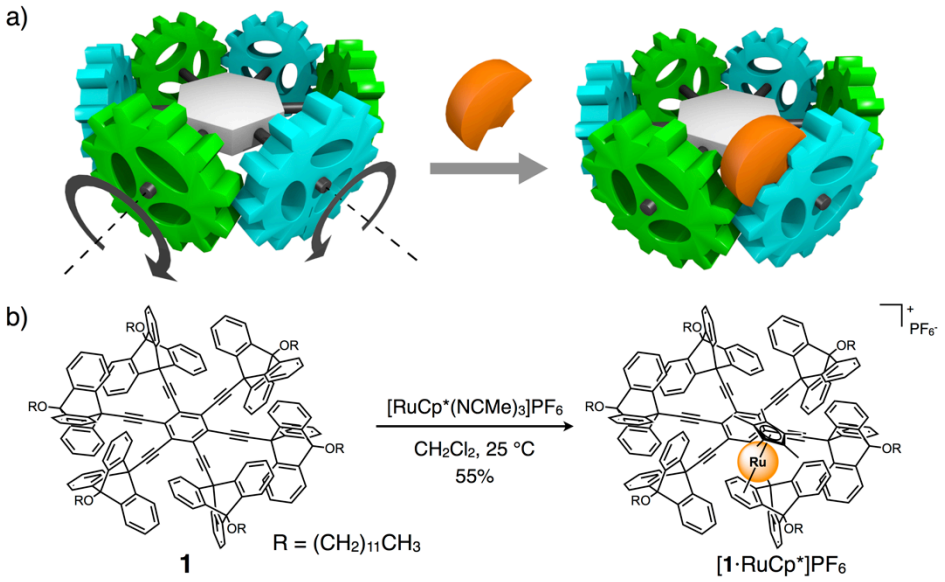

Figure 2-4-1. a) Schematic representation of a bulky "stopper" on the gear system. b) Synthetic scheme of complexation between **1** and $[RuCp^*(NCMe)_3]PF_6$.

By mixing the gear molecule **1** with $[RuCp^*(NCMe)_3]PF_6$ in dichloromethane at room temperature, a 1:1 complex $[\mathbf{1}\cdot RuCp^*]PF_6$ was formed as a racemic mixture. A mononuclear complex was successfully isolated, and identified by various NMR spectroscopies, ESI-TOF mass spectrometry, and elemental analysis. The ESI-TOF mass spectrum after purification of the product clearly supported the isolation of a 1:1 complex $[\mathbf{1}\cdot RuCp^*]^+$ between RuCp* and the gear molecule.

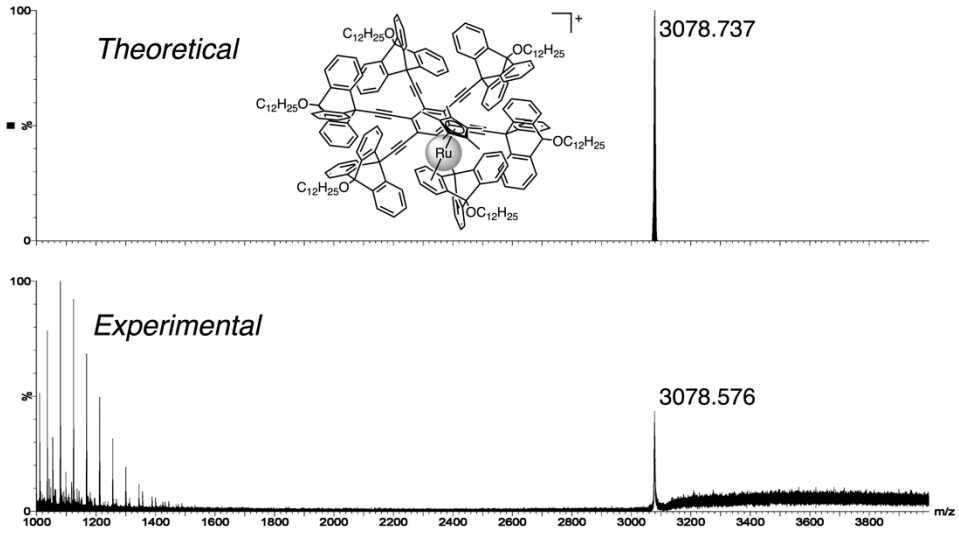

Figure 2-4-2. ESI-TOF mass spectrum of $[\mathbf{1}\cdot RuCp^*]PF_6$.

^{1}H NMR spectra of the complex are shown in Figure 2-4-3. The signals became complicated after complexation, which suggests that triptycenes of one molecule were significantly desymmetrized by addition of the metal complex. This clearly indicates that the RuCp* complex binds not to the central benzene ring but to one phenylene ring of one triptycene gear. It should be noted that the obtained ruthenium complex is a chiral molecule, which means that all the six triptycenes are potentially inequivalent if the RuCp*-bound triptycene does not rotate. I assigned every signal by 2D NMR measurements, and RuCp*-bound triptycene showed distinctive signals (shown in red), and the other five triptycenes showed merged signals (shown in brown circle).

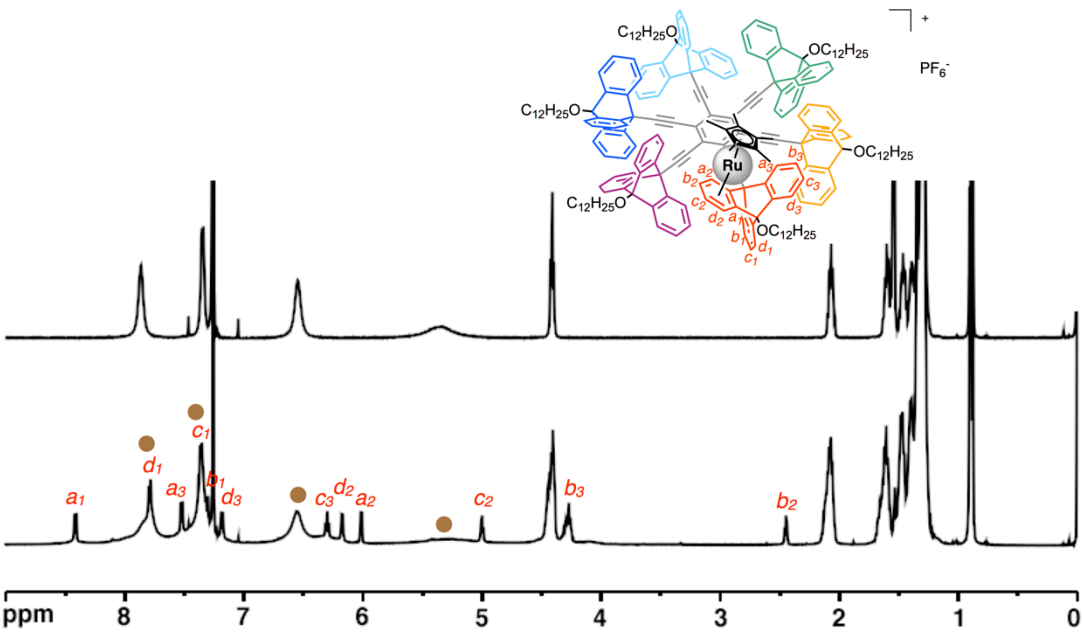

Figure 2-4-3. ^{1}H NMR spectra (500 MHz, $CDCl_3$, 300 K). Top: before complexation. Bottom: after complexation with ruthenium.

The VT-NMR spectra of the ruthenium complex [**1**·RuCp*]PF_6 at different temperatures are shown in Figure 2-4-4. Similar to the previous metal-free gearing system, the shape of the spectra varies with temperature. All the signals at each temperature were assigned by 2D NMR measurements. For example, NOE signals were observed between phenylene rings of adjacent triptycenes.

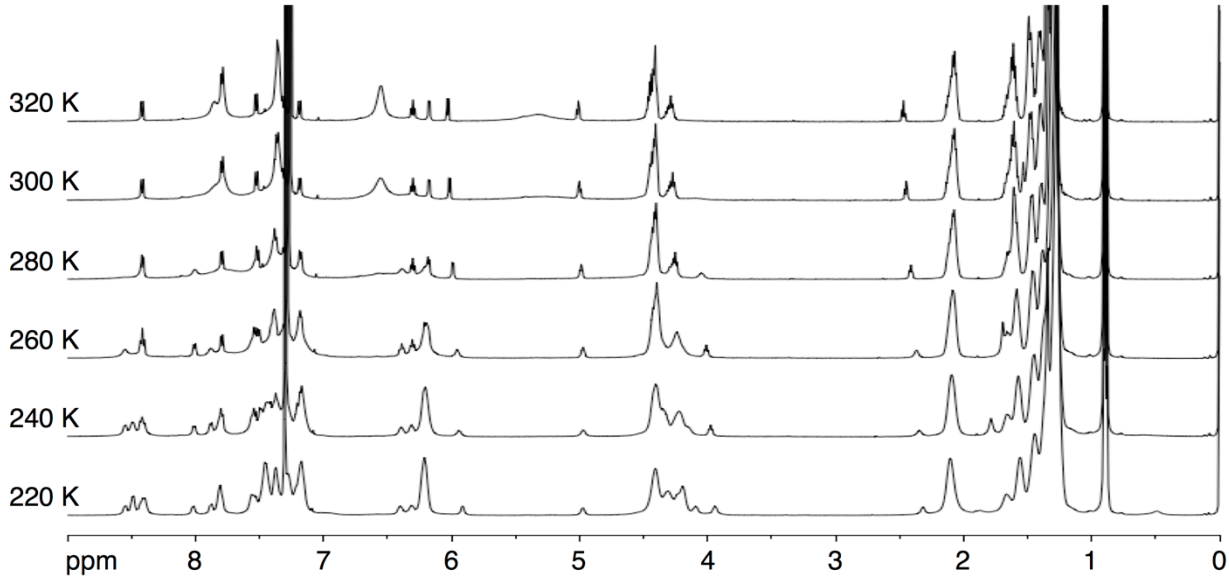

Figure 2-4-4. VT-^{1}H NMR spectra of [**1**·RuCp*]PF_6 (500 MHz, $CDCl_3$).

VT-NMR indicated that the coalescence temperatures of all the signals for triptycenes were raised compared with the RuCp*-free **1**, suggesting that whole motion in the molecule is substantially restricted. For example, proton signals assigned for "a_4–a_{18}" were observed from 7.7–7.9 ppm at 320 K (Figure 2-4-5). Upon cooling, these signals are broadened, and the 1:2 splitting of the signals was observed blow 260 K.

From the obtained results, the VT-NMR spectra of the ruthenium complex [**1**·RuCp*]PF_6 were partially simulated similarly to the previous section (**2-3**). Here only the signals of proton "*a*" (eighteen inner protons of six triptycenes) are simulated for simplification.

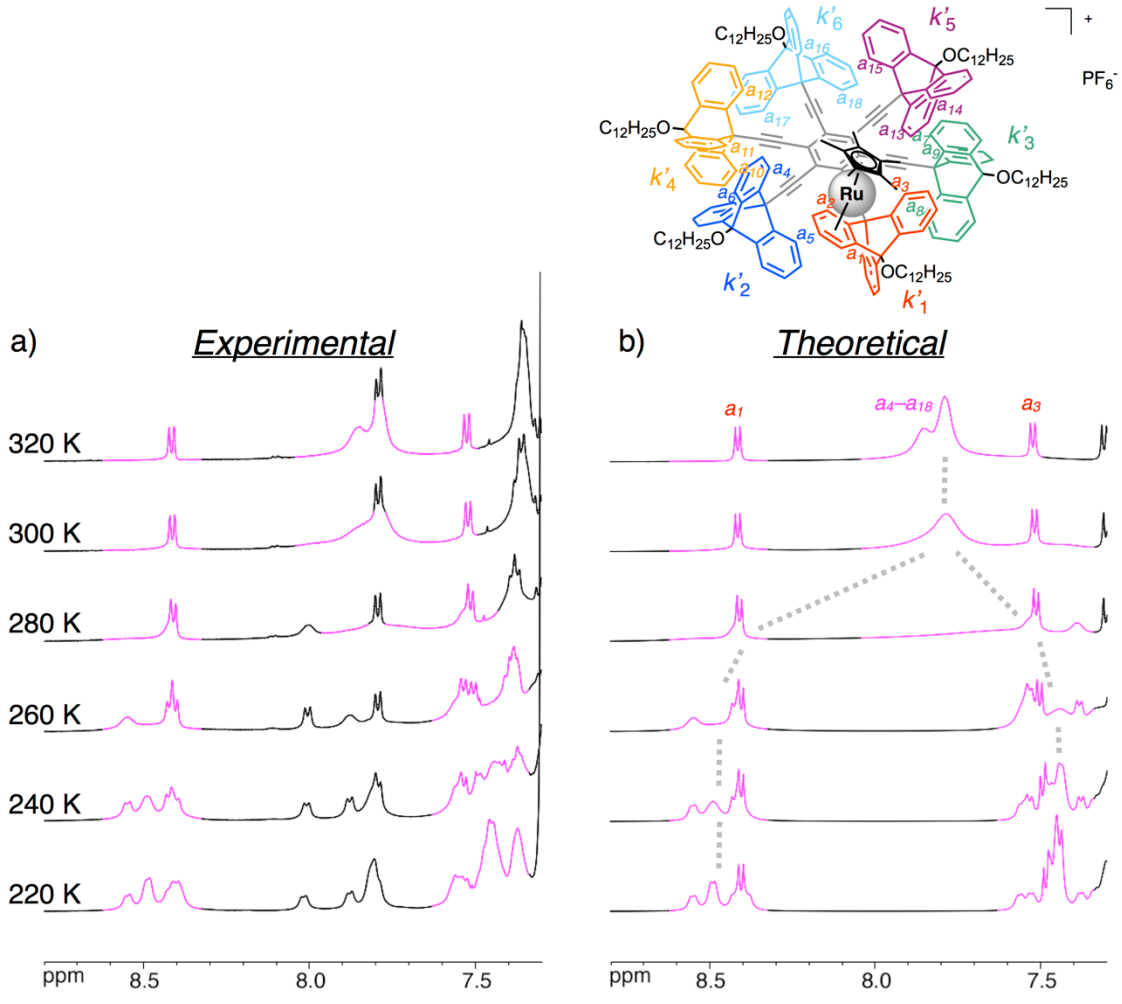

c)

	k'_1	k'_2	k'_3	k'_4	k'_5	k'_6
320 K	0	5.0×10^2	2.0×10^3	1.0×10^4	1.5×10^4	1.5×10^4
300 K	0	1.0×10^2	8.0×10^2	4.0×10^3	7.0×10^3	7.0×10^3
280 K	0	20	1.5×10^2	5.0×10^2	1.0×10^3	1.0×10^3
260 K	0	5.0	20	50	1.2×10^2	1.2×10^2
240 K	0	5.0	10	25	25	25
220 K	0	10	10	10	10	10

Figure 2-4-5. a) Partially experimental VT-^{1}H NMR spectra of [**1**·RuCp*]PF_6 (500 MHz, $CDCl_3$). b) Their theoretical dynamic NMR simulation. Only the signals of proton *a* (shown in pink region) are simulated. c) Table of the estimated rate constants (*k'*) for the rotational motion of each triptycene at each temperature.

These spectra were simulated based on one important assumption; the exchange rate constant of the RuCp*-bound triptycene was assumed to be zero in the range of applied temperatures, because RuCp* is bulky enough to prevent the rotation of the attached triptycene. This assumption is also supported by ^{13}C NMR measurement. If the RuCp*-bound triptycene rotates faster than the NMR times scale, only four signals of the central ring should be observed in a ^{13}C NMR spectrum (Figure 2-4-6). However, sharp signals of six carbon atoms assigned for the central benzene ring were observed at 300 K, suggesting that the rotation of the RuCp*-bound triptycene is considerably slow compared with the NMR timescale.

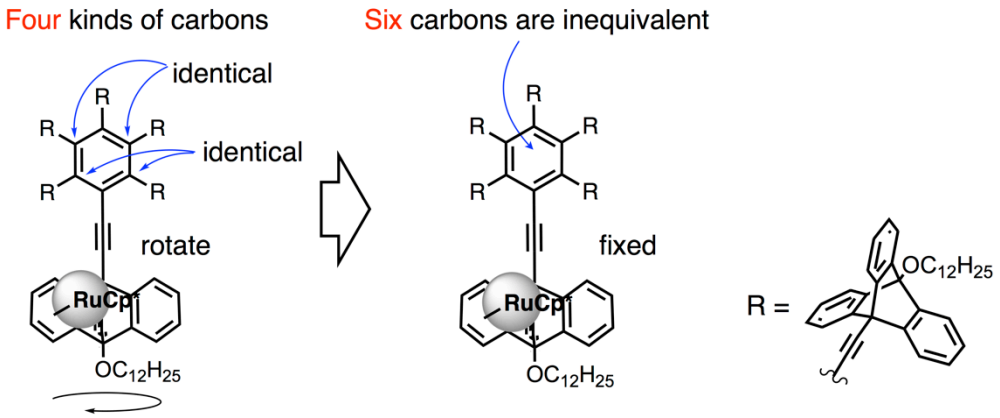

Figure 2-4-6. Only four kinds of signals would be observed if the RuCp*-bound triptycene rotates faster than the NMR time scale. On the other hand, when RuCp*-bound triptycene rotates slower than the NMR time scale, six kinds of signals for central benzene ring should be observed because the molecule is chiral.

This assumption is necessary for simulating the spectra for practical reasons, because without this assumption, for example, proton a_4 exchanges not only to a_5 or a_6 but also to a_7–a_9, which leads a too complicated system to analyze (Figure 2-4-7).

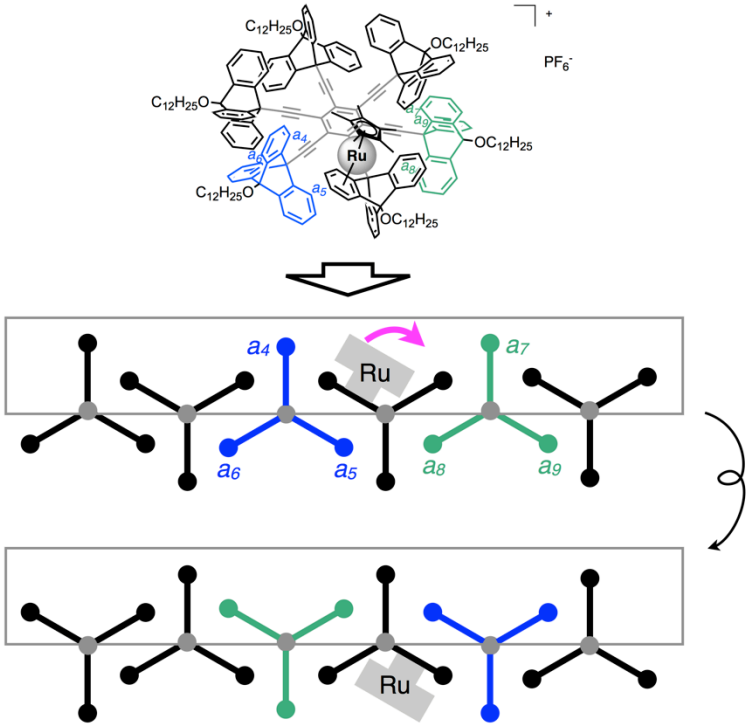

Figure 2-4-7. If RuCp*-bound triptycene rotates, not only *intra*-triptycene proton exchange ($a_4 \leftrightarrow a_5 \leftrightarrow a_6$) but also *inter*-triptycene proton exchange ($a_4 \leftrightarrow a_5 \leftrightarrow a_6 \leftrightarrow a_7 \leftrightarrow a_8 \leftrightarrow a_9$) should be considered.

If the molecular gears are tightly meshed with each other and no gear slippage occurred, the whole motion is restricted and all the k' value should be zero. However, the exchange rate constants showed an increasing tendency with the distance from RuCp*-bound triptycene regardless of the presence of the bulky RuCp*; $k'_1 < k'_2 < k'_3 < k'_4 < k'_5$, k'_6 (Figure 2-4-5-c). This result suggests that the gears are not completely meshed with each other but a "gear slippage" takes place to some extent.

Compering the values of k'_2 and k'_3, k'_2 showed smaller values at every temperature, indicating that stronger π-π interactions would occur between the Ru-bound phenylene ring and contacted rings due to the electro-deficient nature of Ru-bound phenylene ring.

When the Ru-bound triptycene was fixed, the other triptycene gears can rotate only at every 120° because of the steric repulsion, which means that the exchanging rate constants for the Ru-attached systems were given as a **120° flipping motion**. In addition, two triptycenes adjacent to the Ru-bound one show slippage motion only without gearing (Figure 2-4-8). The motions of the other three triptycene gears would include both geared rotation and gear slippage.

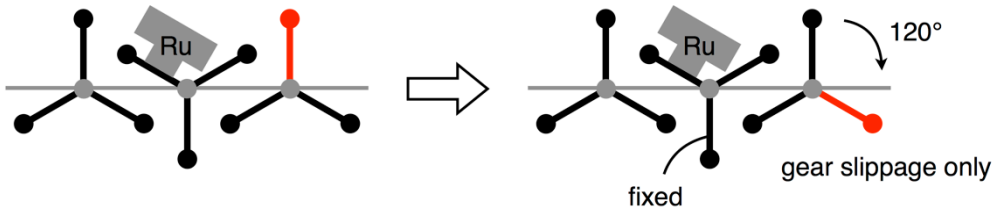

Figure 2-4-8. Both sides of a RuCp*-bound triptycene show only gear slippage, and the rate constant in this system means the exchange rate for a 120° flipping.

Before comparing the rotational speed of a metal-free gearing system **1** and Ru-attached system, the definition of *k* and *k'* should be confirmed.

A non-metal coordinated gear molecule **1** is achiral, and two "equatorial" phenyele rings in each tripycene gear in **1** at low temperatures are in the same environment (we cannot distinguish the two phenlyene rings in NMR). Here the rate constant *k* is defined as an exchange rate between **one "axial" phenylene blade** and **two "equatorial" phenylene blades** (Figure 2-4-9-a).

On the contrary, the molecule becomes chiral after metal complexation. As a result, two "equatorial" phenlylene rings of each tripycene gear at low temperatures are in different environments (we can distinguish the two phenlyene rings in NMR). Here the rate constant *k'* is defined as an exchange rate between **three phenylene blades** (Figure 2-4-9-b).

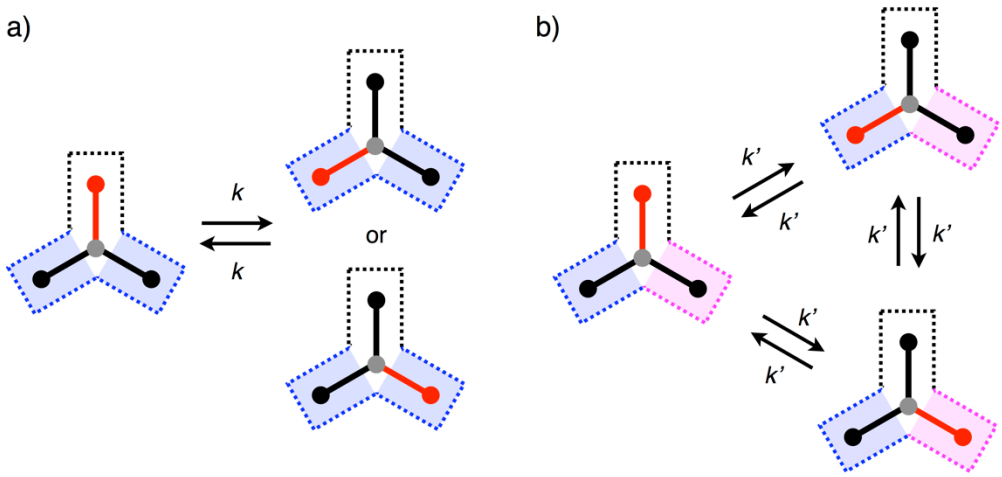

Figure 2-4-9. a) Rate constant *k* of **1**. b) Rate constant *k'* after complexation.

If the triptycene gears move at the same rotational speed in both cases, the formula below should be established.

$$k = 2k'$$

The rotational speed of the triptycene gear in the two systems can easily be compared by converting the rate constants to the frequency of rotation.

In the case of metal-free gear molecule **1**, the exchanging rate constants *k* were determined for **a 60° flipping** motion. Then, the 360° rotational frequency f_{free} in this system is given by

$$f_{free} = \frac{60°}{360°} k = \frac{k}{6} .$$

However, the direction of the 60° flipping is based on the same statistical probability.

On the other hand, the rate constant *k'* after metal complexation is defined as an exchange rate between three phenylene blades as a 120° flipping motion. Therefore, the rotational frequency f_{Ru} in this system is given by

$$f_{Ru} = \frac{120°}{360°}\ k = \frac{2k'}{3}\ .$$

This rotational frequency was based on the assumption that the RuCp*-bound triptycene could not rotate at all (k_1 was assumed to be zero). If the assumption was not correct ($k_1 \neq 0$), the exchanging rate constants of the complex were determined for a **60° flipping**. This means a smaller motion for each movement, that is, a slower rotational rate. Rotational frequency *f* in this case is given by

$$f_{Ru} = \frac{60°}{360°}\ k = \frac{k'}{3}\ .$$

Figure 2-4-10 shows the rotational frequencies *f* before and after metal complexation. Although the rotational frequencies of f_5 and f_6 are almost comparable to Ru-free **1**, the values for f_4 showed significantly smaller values than Ru-free **1**, indicating that the RuCp* complex would act as a chemical inhibitor to restrict the motion of an unadjacent triptycene *via* the mechanical meshing of the triptycene gears.

The rotational frequencies for f_2–f_6 of the ruthenium complex [**1**·RuCp*]PF_6 at 220 K showed larger values than Ru-free **1**. This may originate from the error caused by overestimation of exchange rate as the broadening of the spectrum, which is actually derived from more asymmetric structures caused by structural fluctuation at lower temperatures. The actual values of exchange rate constants were expected to be much smaller than the estimated one.

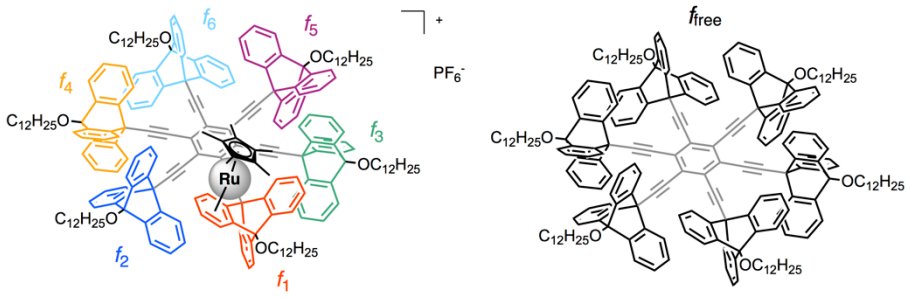

	f_1	f_2	f_3	f_4	f_5	f_6	f_{free}
320 K	0	1.7×10^2	1.3×10^3	8.0×10^3	1.0×10^4	1.0×10^4	1.7×10^4
300 K	0	67	5.3×10^2	1.7×10^3	5.0×10^3	5.0×10^3	4.5×10^3
280 K	0	13	1.0×10^2	3.3×10^2	6.7×10^2	6.7×10^2	1.0×10^3
260 K	0	3.3	13	17	80	80	1.7×10^2
240 K	0	3.3	6.7	17	17	17	18
220 K	0	6.7	6.7	6.7	6.7	6.7	1.7

Figure 2-4-10. Table of rotational frequencies f of the ruthenium complex [**1**·RuCp*]PF_6 and metal-free **1** at each temperature. The values for Ru-attached system were estimated on the high side ($f_{Ru} = 2/3\ k'$).

From the obtained results, although it is incomplete due to the gear slippage, the rotational motion is definitely transmitted through the gearing process.

2-5. Conclusion

In conclusion, I have designed and synthesized a circularly arranged sextuple triptycene gearing system **1**, which was synthesized in 10 steps in 13% overall yield. The key reaction to construct such a crowded structure was a trimerization reaction of bis-substituted alkynes in the final step. A dodecyloxy side chain attached to each triptycene moiety also plays an important role for the reaction to enhance the solubility of the synthetic intermediate as well as the target molecule **1** in general organic solvents.

A single crystal X-ray structural analysis revealed that the six triptycene moieties are tightly meshed with each other in the molecule.

Dynamic behaviors of the gear system **1** in solution were analyzed by VT-^{1}H NMR spectroscopy. The rotational speeds of the triptycene moieties in solution at each temperature were calculated by the comparison with simulated spectra, and the various thermodynamic parameters were determined by applying Eyring plots.

The effect of a ruthenium complex coordinatively attached to the gear system **1** was examined on the speed of rotational motion. A mononuclear 1:1 [**1**·RuCp*]PF_6 complex was isolated and characterized, and its dynamic behaviors in solution were analyzed by VT-^{1}H NMR spectroscopy. The rate constant *k'* of each triptycene was determined by the comparison with simulated NMR spectra. The rate constant *k'* becomes larger as distant from the Ru-attached triptycene, which suggests that the gear slippage motions take place to some extent. The result also demonstrates that the motions of unadjacent triptycenes to the Ru-attached position would be affected through gearing of the triptycene moieties, although it is incomplete due to the gear slippage.

The transmission of stimulus through mechanical interlocking of gear molecules was demonstrated for the first time in this study.

Scheme 2-5-1. Key reactions in this chapter. a) Synthesis of gear molecule **1**. b) Metal complexation between **1** and ruthenium for motion inhibition.

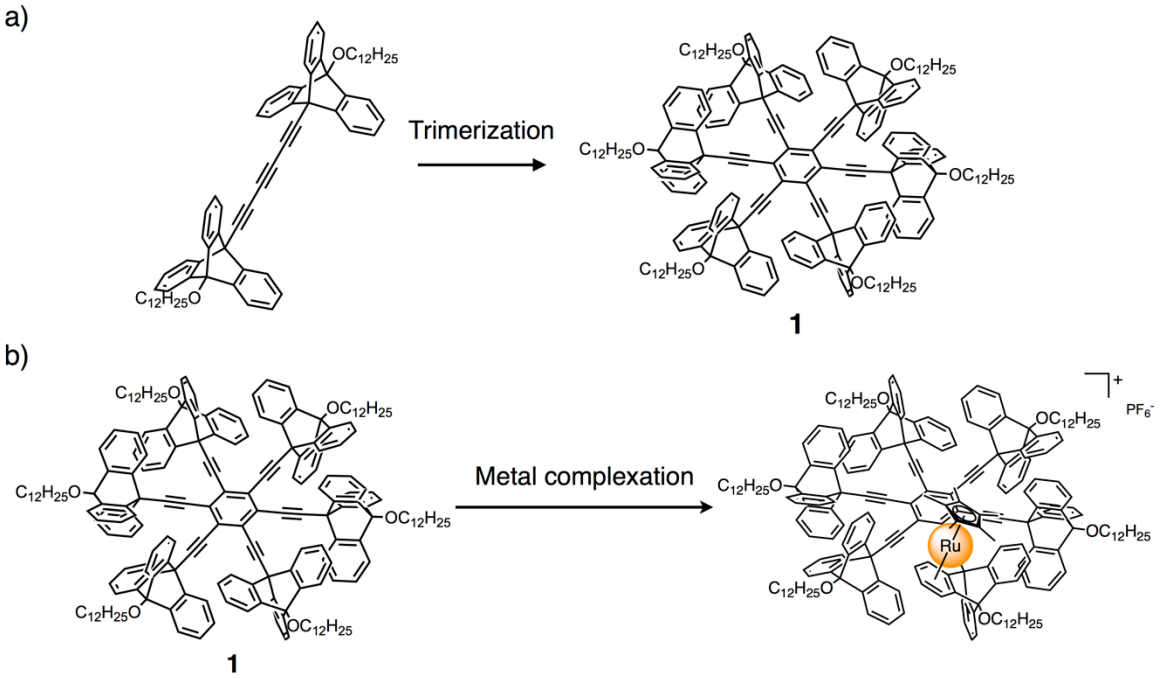

2-6. Experimental Section

Materials and methods

Unless otherwise noted, solvents and reagents were purchased from TCI Co., Ltd., WAKO Pure Chemical Industries Ltd., Kanto Chemical Co., and Sigma-Aldrich Co., and used without further purification. 2-(trimethylsilyl)phenyl trifluoromethanesulfonate was prepared according to the literature,[13] Unstable $Co_2(CO)_8$ was handled in a vacuum glove box (UNICO UN-650F) under nitrogen atmosphere with an air filter (Glovebox Japan GBJPWS3-00). Microwave synthesis was conducted using an Anton Paar Monowave 300. Gel permeation chromatography (GPC) was performed on a recycling preparative HPLC (Japan Analytical Industry; LC-9204) with a JAIGEL-2H-40 column.

^{1}H, ^{13}C, ^{19}F, ^{31}P, and other 2D NMR spectra were recorded on a Bruker AVANCE III-500 (500 MHz) spectrometer. Tetramethylsilane was used as an internal standard (δ 0 ppm) for ^{1}H and ^{13}C NMR measurements when $CDCl_3$ was used as a solvent. Abbreviations: s, singlet; d, doublet; t: triplet; br, broad. Pulse width: 12 μsec. Delay time: 1 s. The compounds did not show any concentration dependence. A single-crystal X-ray crystallographic analysis was performed using a Rigaku XtaLAB PRO MM007DW PILATUS diffractometer with CuKα radiation, and obtained data were processed by using CrysAlisPro 1.171.39.7e (Rigaku OD, 2015) software, analyzed by CrystalStructure 4.2.1 (Rigaku, 2015) software, using SHELXL-2014/7,[14] Crystallographic data in this paper can be obtained free of charge from the Cambridge Crystallographic Data Centre (http://www.ccdc.cam.ac.uk/data_request/cif).

ESI-TOF mass data were recorded on a Micromass LCT Premier XE mass spectrometer. Unless otherwise noted, experimental conditions were as follows (Ion mode, positive; Capillary

voltage, 3000 V; Sample cone voltage, 30 V; Desolvation temperature, 150 °C; Source temperature, 80 ºC). Melting point was measured by a Yanaco Micro Melting Point Apparatus MP-500D. IR spectra were recorded on a Jasco FT/IR 4200 with an ATR PRO410-S equipment. UV-vis spectra were recorded on a HITACHI U-3500 UV-Vis spectrophotometer. Experimental conditions were as follows (1.0 cm glass cell; λ = 240–850 nm; scanning rate, 120 nm/min; data acquisition intervals, 0.5 nm). Emission and excitation spectra were recorded on a HITACHI F-4500 fluorescence spectrophotometer. Experimental conditions were as follows (1.0 cm glass cell; λ = 450–800 nm; scanning rate, 240 nm/min; data acquisition intervals, 1.0 nm; excitation light slit, 5.0 nm; emission light slit, 2.5 nm; photo multiplier voltage, 950 V).

Elemental analysis was conducted in the Microanalytical Laboratory, Department of Chemistry, School of Science, the University of Tokyo.

Synthesis of gear molecule 1

Synthesis of 9-dodecyloxyanthracene (2)[15]

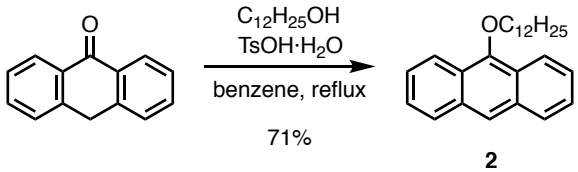

2

Compound **2** was reported previously,[15] however, synthesized by a modified procedure. A three-necked 500 mL flask equipped with a Dean-Stark trap and a magnetic stirring bar was filled with argon gas. To the flask were added anthrone (11.7 g, 60.0 mmol, 1.0 eq), 1-dodecanol (22.4 g, 120 mmol, 2.0 eq), *p*-toluenesulfonic acid monohydrate (381 mg, 2.00 mmol, 3 mol%) and benzene (250 mL). The reaction mixture was heated to reflux and the water generated during the reaction was removed azeotropically by the Dean-Stark trap. After a month, the reaction mixture was cooled to room temperature and solid precipitated was filtered. The solution was diluted with diethyl ether, washed with 1.0 M NaOH aqueous solution (100 mL), water (100 mL) and brine (100 mL), and dried over $MgSO_4$. After filtration, the solvents were evaporated. Obtained orange sticky liquid (40.3 g) was purified by short path silica gel column chromatography (Merck 70–230 mesh, *n*-hexane) twice to give **2** as a pale yellow solid (15.5 g, 42.7 mmol, 71%). Analytical sample was obtained by further purification by recrystallization from a small amount of *n*-pentane.

^{1}H NMR ($CDCl_3$, 500 MHz, 300 K): δ 8.31–8.28 (m, 2H), 8.21 (s, 1H), 8.01–7.97 (m, 2H), 7.49–7.44 (m, 4H), 4.20 (t, J = 6.7 Hz, 2H), 2.09–2.02 (m, 2H), 1.69–1.62 (m, 2H), 1.48–1.28 (m, 16H), 0.89 (t, J = 6.9 Hz, 3H); ^{13}C NMR ($CDCl_3$, 126 MHz, 300 K): δ 151.6, 132.5, 128.4, 125.4, 125.0, 124.8, 122.5, 121.9, 76.2, 31.9, 30.7, 29.70, 29.67, 29.63, 29.4, 26.3, 22.7, 14.1; mp: 48–50 °C; FT-IR: 3054.7 (aromatic C-H stretch), 2949.6, 2867.6 (methyl C-H stretch), 2919.7, 2849.3 (methylene C-H stretch), 1466.6, 736.7 (methylene C-H bend), 1278.6, 1085.7 (C-O-C stretch),

1621.8, 1440.6, 1415.5 (aromatic C=C stretch) cm^{-1}; HRMS ($CHCl_3/CH_3OH$, positive): $[\mathbf{2}\cdot H]^+$ ($C_{26}H_{34}O$) *m/z* 363.2621 (required, 363.2604).

Synthesis of 9-bromo-10-dodecyloxyanthracene (3)

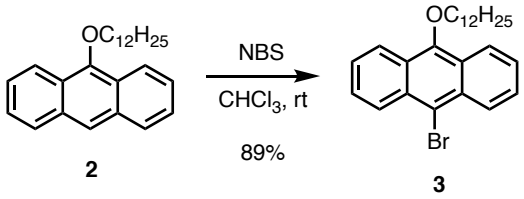

A three-necked 1000 mL flask equipped with a magnetic stirring bar was replaced with nitrogen gas. To the flask were added 9-dodecyloxyanthracene (**2**) (13.8 g, 38.2 mmol, 1.0 eq) and dry chloroform (400 mL), and degassed. *Caution; amylene stabilized chloroform should be used. Ethanol stabilized one caused side-chain exchange reaction.* Next, *N*-bromosuccinimide (7.13 g, 40.0 mmol, 1.05 eq) was added and the reaction mixture was stirred at room temperature for 15 min. The reaction mixture was then quenched with water (300 mL), and the organic layer was separated and the aqueous layer was extracted with 150 mL of dichloromethane twice. The organic layers were combined, washed with water (200 mL) for three times and brine (200 mL), dried over $MgSO_4$, filtrated and then evaporated. The obtained yellow solid (17.4 g) was purified by silica gel column chromatography (Merck 70–230 mesh, *n*-hexane) to give **3** as a yellow solid (15.1 g, 34.1 mmol, 89%).

^{1}H NMR ($CDCl_3$, 500 MHz, 300 K): δ 8.52 (dd, J = 8.9, 0.6 Hz, 2H), 8.32 (d, J = 8.6 Hz, 2H), 7.61–7.58 (m, 2H), 7.53–7.50 (m, 2H), 4.17 (t, J = 6.7 Hz, 2H), 2.08–2.02 (m, 2H), 1.69–1.62 (m, 2H), 1.47–1.31 (m, 16H), 0.89 (t, J = 6.8 Hz, 3H); ^{13}C NMR ($CDCl_3$, 126 MHz, 300 K): δ 151.9, 131.1, 127.9, 127.3, 125.6, 125.4, 122.8, 116.9, 76.6, 31.9, 30.6, 29.69, 29.66, 29.60, 29.4, 26.2,

22.7, 14.1; mp: 44–45 °C; FT-IR: 3074.9, 3047.0 (aromatic C-H stretch), 2955.4, 2871.5 (methyl C-H stretch), 2917.8, 2850.3 (methylene C-H stretch), 1619.9, 1435.7, 1416.5 (aromatic C=C stretch), 1470.5, 753.1 (methylene C-H bend), 1256.4, 1095.4 (C-O-C stretch), cm^{-1}; HRMS ($CHCl_3/CH_3OH$, positive): $[\mathbf{3}\cdot Na]^+$ ($C_{26}H_{33}BrONa$) *m/z* 463.1630 (required, 463.1607).

Synthesis of 4-(10-dodecyloxy-9-anthracenyl)-2-methyl-3-butyn-2-ol (4)

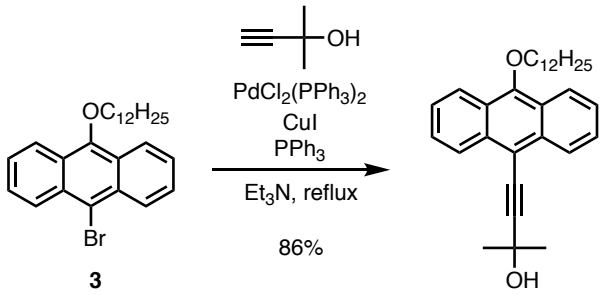

A three-necked 100 mL flask equipped with a reflux condenser and a magnetic stirring bar was filled with argon gas. To the flask were added 9-bromo-10-dodcyloxyanthracene (**3**) (8.83 g, 20.0 mmol, 1.0 eq), 2-methyl-3-butyn-2-ol (3.9 mL, 40 mmol, 2.0 eq), bis(triphenylphosphine)palladium(II) dichloride (56.4 mg, 80 mmol, 0.4 mol%), copper iodide (57.2 mg, 300 μmol, 1.5 mol%), triphenylphosphine (84.1 mg, 321 μmol, 1.6 mol%) and triethylamine (50 mL), and degassed. The reaction mixture was refluxed for 22 h. After cooling, the mixture was poured into saturated NH_4Cl aqueous solution (50 mL) and extracted with dichloromethane (50 mL) three times. The combined organic layer was washed with water (80 mL) for three times and brine (80 mL), dried over $MgSO_4$. After filtration, the solvents were removed under reduced pressure. The red residue (15.0 g) was purified by silica gel column chromatography (Merck 70–230 mesh, *n*-hexane/dichloromethane = 1:0 ~ 1:2) to give **4** as an orange solid (7.69 g,

17.3 mmol, 86%). It can be further purified by recrystallization from hot *n*-hexane.

^{1}H NMR ($CDCl_3$, 500 MHz, 300 K): δ 8.50 (d, J = 8.6 Hz, 2H), 8.30 (d, J = 8.6 Hz, 2H), 7.58–7.55 (m, 2H), 7.52–7.49 (m, 2H), 4.18 (t, J = 6.7 Hz, 2H), 2.24 (s, 1H), 2.08–2.01 (m, 2H), 1.84 (s, 6H), 1.68–1.61 (m, 2H), 1.47–1.28 (m, 16H), 0.89 (t, J = 6.9 Hz, 3H); ^{13}C NMR ($CDCl_3$, 126 MHz, 300 K): δ152.6, 133.6, 126.9, 126.7, 125.3, 124.5, 122.8, 112.3, 104.4, 78.9, 76.6, 66.3, 31.94, 31.91, 30.6, 29.69, 29.65, 29.59, 29.4, 26.2, 22.7, 14.1; mp: 66–69 °C; FT-IR: 3310.2 (O-H stretch), 3059.5 (aromatic C-H stretch), 2917.8, 2847.4 (methylene C-H stretch), 2211.0 (C≡C stretch), 1619.9, 1434.8, 1403.9 (aromatic C=C stretch), 1463.7, 722.2 (methylene C-H bend), 1224.6, 1058.7 (C-O-C stretch), 752.1 (aromatic C-H bend (4)) cm^{-1}; HRMS ($CHCl_3$/CH_3OH, positive): [**4**·Na]$^+$ ($C_{31}H_{40}O_2Na$) *m/z* 467.2941 (required, 467.2921).

Synthesis of 4-(10-dodecyloxy-9-triptycyl)-2-methyl-3-butyn-2-ol (5)

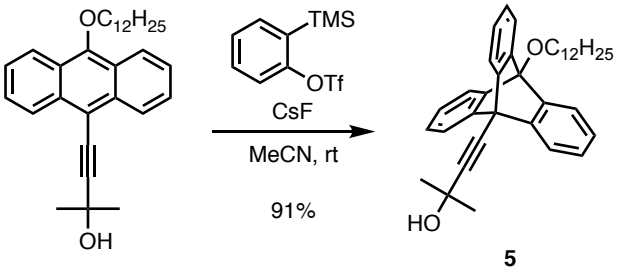

4 **5**

A three-necked 500 mL flask equipped with a magnetic stirring bar was filled with nitrogen gas. To the flask were added 4-(10-dodcyloxy-9-anthracenyl)-2-methyl-3-butyn-2-ol (**4**) (4.45 g, 10.0 mmol, 1.0 eq), cesium fluoride (4.6 g, 30 mmol, 3.0 eq) and dry acetonitrile (300 mL). Next, 2-(trimethylsilyl)phenyl trifluoromethanesulfonate (3.65 mL, 15.0 mmol, 1.5 eq) was added dropwise to the reaction mixture and the resulting mixture was stirred at room temperature for 23 h. Then the volatile was removed by evaporation and the residue was passed through a plug column

on silica gel with dichloromethane. After evaporation, obtained a yellow solid (5.50 g) was purified by washing with ethyl acetate to give **5** as a slightly yellow solid (4.75 g, 9.12 mmol, 91%).

^{1}H NMR ($CDCl_3$, 500 MHz, 300 K): δ 7.67 (dd, J = 7.2, 1.3 Hz, 3H), 7.62 (dd, J = 7.3, 1.1 Hz, 3H), 7.10–7.03 (m, 6H), 4.58 (t, J = 6.9 Hz, 2H), 2.25 (s, 1H), 2.18–2.12 (m, 2H), 1.87 (s, 6H), 1.70–1.64 (m, 2H), 1.54–1.29 (m, 16H), 0.89 (t, J = 6.9 Hz, 3H); ^{13}C NMR ($CDCl_3$, 126 MHz, 300 K): δ 144.8, 143.4, 125.4, 125.1, 121.9, 121.2, 98.3, 85.5, 76.6, 67.4, 65.9, 52.0, 32.1, 32.0, 31.8, 29.74, 29.70, 29.4, 26.3, 22.7, 14.1; HRMS ($CHCl_3$/CH_3OH, positive): [**5**·Na]$^+$ ($C_{37}H_{44}O_2Na$) *m/z* 543.3258 (required, 543.3234).

Synthesis of 9-dodecyloxy-10-ethynyltriptycene (6)

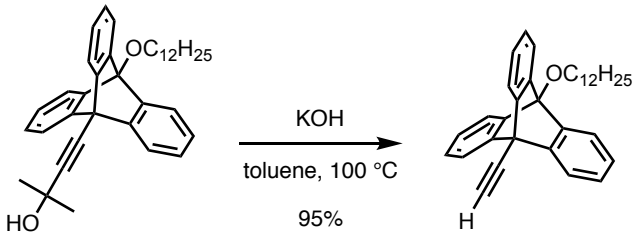

5 **6**

A three-necked 300 mL flask equipped with a reflux condenser and a magnetic stirring bar was filled with argon gas. To the flask were added 4-(10-dodcyloxy-9-triptycyl)-2-methyl-3-butyn-2-ol (**5**) (4.69 g, 9.0 mmol, 1.0 eq), potassium hydroxide (760 mg, 13.5 mmol, 1.5 eq) and dry toluene (100 mL). The reaction mixture was heated at 100 °C for 4 h. After cooling, the mixture was quenched with water (50 mL), the organic layer was separated and the aqueous layer was extracted with 50 mL of dichloromethane twice. The organic layers were combined, washed with water (100 mL) and brine (100 mL), dried over $MgSO_4$, filtered and evaporated. The obtained a pale yellow solid (4.31 g) was purified by short path silica gel column chromatography (Merck 70–230 mesh,

n-hexane) to give **6** as a slightly yellow solid (3.94 g, 8.52 mmol, 95%).

^{1}H NMR ($CDCl_3$, 500 MHz, 300 K): δ 7.75 (dd, J = 7.2, 1.3 Hz, 3H), 7.63 (dd, J = 7.3, 1.2 Hz, 3H), 7.10–7.04 (m, 6H), 4.59 (t, J = 6.9 Hz, 2H), 3.27 (s, 1H), 2.18–2.12 (m, 2H), 1.70–1.64 (m, 2H), 1.54–1.29 (m, 16H), 0.89 (t, J = 6.9 Hz, 3H); ^{13}C NMR ($CDCl_3$, 126 MHz, 300 K): δ 144.7, 143.0, 125.5, 125.2, 121.9, 121.2, 85.5, 80.9, 78.3, 67.4, 52.2, 31.95, 31.82, 29.74, 29.69, 29.4, 26.3, 22.7, 14.1; mp: 108–109 °C; FT-IR: 3292.9 (alkyne C-H stretch), 2916.8, 2849.3 (methylene C-H stretch), 1447.3, (aromatic C=C stretch), 1465.6, 720.3 (methylene C-H bend), 1094.4 (C-O-C stretch), 749.2 (aromatic C-H bend (4)), 641.2 (alkyne C-H bend) cm^{-1}; HRMS ($CHCl_3$/CH_3OH, positive): [**6**·Na]$^+$ ($C_{34}H_{38}ONa$) *m/z* 485.2791 (required, 485.2815).

Synthesis of 9-(bromoethynyl)-10-doecyloxytriptycene (7)

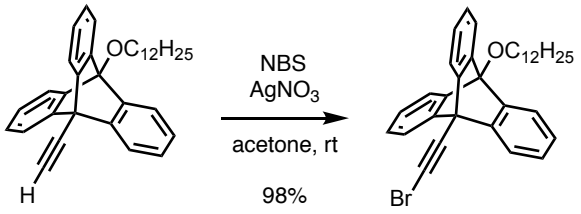

A three-necked 200 mL flask equipped with a magnetic stirring bar was filled with nitrogen gas. To the flask were added 9-dodecyloxy-10-ethynyltriptycene (**6**) (3.70 g, 8.00 mmol, 1.0 eq) and dry acetone (100 mL). *N*-Bromosuccinimide (1.60 g, 9.00 mmol, 1.1 eq) and silver nitrate (136 mg, 0.801 mmol, 0.1 eq) were added in order and the reaction mixture was stirred at room temperature for 4 h. The reaction mixture was then quenched with ice-water (100 mL) and the organic layer was separated. The aqueous layer was extracted with 50 mL of diethyl ether for three times, and the combined organic layers were washed with water (100 mL) twice and brine (100 mL), dried over $MgSO_4$, filtered and evaporated. The obtained a slightly yellow solid (4.23 g, 7.82 mmol, 98%) was

pure enough for the next step without further purification.

^{1}H NMR ($CDCl_3$, 500 MHz, 300 K): δ 7.68 (dd, J = 7.1, 1.4 Hz, 3H), 7.62 (dd, J = 7.2, 1.3 Hz, 3H), 7.11–7.04 (m, 6H), 4.58 (t, J = 6.9 Hz, 2H), 2.18–2.11 (m, 2H), 1.70–1.63 (m, 2H), 1.53–1.29 (m, 16H), 0.89 (t, J = 6.9 Hz, 3H); ^{13}C NMR ($CDCl_3$, 126 MHz, 300 K): δ 144.6, 143.1, 125.5, 125.2, 121.9, 121.3, 85.4, 75.1, 67.4, 53.3, 51.4, 31.9, 31.8, 29.74, 29.69, 29.4, 26.3, 22.7, 14.1; HRMS ($CHCl_3$/CH_3OH, positive): [**7**·Na]$^+$ ($^{13}CC_{33}H_{37}BrONa$) *m/z* 565.1957 (required, 565.1959).

Synthesis of 6-(10-dodecyloxy-9-triptycyl)-2-methyl-3,5-hexadiyn-2-ol (8)

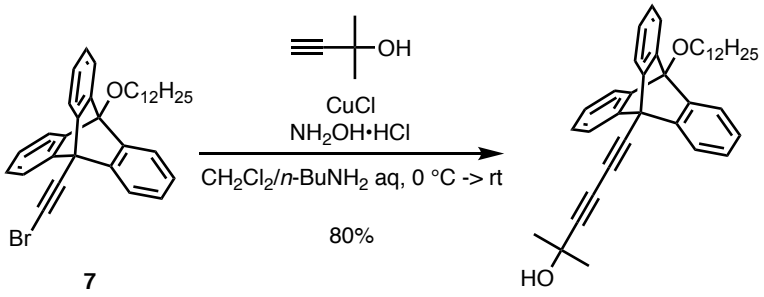

A three-necked 200 mL flask equipped with a magnetic stirring bar was filled with argon gas. To the flask was added an aqueous solution of *n*-butylamine (30%, 50 mL) and degassed. Copper(I) chloride (99.6 mg, 1.01 mmol, 0.2 eq) was added to the solution at 0 °C, and a few crystals of hydroxylamine hydrochloride were added to the flask until the blue color of the solution was discharged. A solution of 2-methyl-3-butyn-2-ol (0.98 mL, 10 mmol, 2.0 eq) in dichloromethane (25 mL) was added to the solution. 9-bromoethynyl-10-dodcyloxytriptycene (**7**) (2.71 g, 5.00 mmol, 1.0 eq) in dichloromethane (50 mL) was added dropwise to the solution over 1 h. During the addition, a small amount of hydroxylamine hydrochloride was added occasionally to keep the color of the reaction light yellow. After the addition, the reaction was stirred while warming up to room

temperature for overnight and then quenched with water (50 mL). The organic layer was separated and the aqueous layer was further extracted with 50 mL of dichloromethane for three times. The combined organic layers were washed with water (100 mL) and brine (100 mL), dried over $MgSO_4$, filtered, and concentrated under reduced pressure. The pale yellow residue (4.31 g) was purified by silica gel column chromatography (Merck 70–230 mesh, *n*-hexane/dichloromethane/ethyl acetate = 10:1:0 ~ 5:0:1) to afford **8** as a colorless solid (2.18 g, 3.99 mmol, 80%).

^{1}H NMR ($CDCl_3$, 500 MHz, 300 K): δ 7.70 (dd, J = 7.2, 1.4 Hz, 3H), 7.62 (dd, J = 7.3, 1.2 Hz, 3H), 7.11–7.04 (m, 6H), 4.57 (t, J = 6.9 Hz, 2H), 2.18–2.11 (m, 2H), 2.08 (s, 1H), 1.68–1.63 (m, 8H), 1.54–1.26 (m, 16H), 0.89 (t, J = 6.9 Hz, 3H); ^{13}C NMR ($CDCl_3$, 126 MHz, 300 K): δ 144.6, 143.0, 125.6, 125.3, 122.0, 121.3, 85.4, 83.5, 76.2, 74.8, 67.4, 66.8, 65.8, 52.8, 31.9, 31.8, 31.2, 29.73, 29.69, 29.4, 26.3, 22.7, 14.1; mp: 131–133 °C; HRMS ($CHCl_3$/CH_3OH, positive): [**8**·Na]$^+$ ($C_{39}H_{44}O_2Na$) *m/z* 567.3210 (required, 567.3234).

Synthesis of 9-(1,3-butadiyn-1-yl)-10-dodecyloxytriptycene (9)

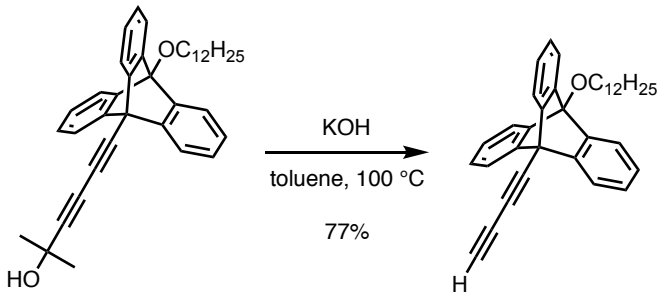

8 **9**

A two-necked 30 mL flask equipped with a reflux condenser and a magnetic stirring bar was filled with argon gas. To the flask were added 6-(10-dodcyloxy-9-triptycyl)-2-methyl-3,5-hexadiyn-2-ol (**8**) (436 mg, 800 μmol, 1.0 eq),

potassium hydroxide (70 mg, 1.2 mmol, 1.5 eq) and dry toluene (10 mL). The reaction mixture was heated at 100 °C for 20 min. After cooling, the mixture was quenched with water (10 mL), the organic layer was separated and the aqueous layer was extracted with 10 mL of dichloromethane twice. The organic layers were combined, washed with water (30 mL) and brine (30 mL), dried over $MgSO_4$, filtered and evaporated. The obtained a pale orange solid (376 mg) was purified by short path silica gel column chromatography (Merck 70–230 mesh, *n*-hexane) to give **9** as a colorless solid (301 mg, 617 μmol, 77%).

^{1}H NMR ($CDCl_3$, 500 MHz, 300 K): δ 7.70 (dd, J = 7.2, 1.4 Hz, 3H), 7.62 (dd, J = 7.3, 1.3 Hz, 3H), 7.12–7.05 (m, 6H), 4.57 (t, J = 6.9 Hz, 2H), 2.40 (s, 1H), 2.18–2.11 (m, 2H), 1.70–1.63 (m, 2H), 1.54–1.29 (m, 16H), 0.89 (t, J = 6.9 Hz, 3H); ^{13}C NMR ($CDCl_3$, 126 MHz, 300 K): δ 144.5, 142.8, 125.6, 125.3, 121.9, 121.4, 85.4, 76.4, 71.7, 68.4, 67.7, 67.4, 52.6, 31.9, 31.8, 29.74, 29.69, 29.4, 26.3, 22.7, 14.1; mp: 138 °C (decomposition); HRMS ($CHCl_3$/CH_3OH, positive): [**9**·Na]$^+$ ($C_{36}H_{38}ONa$) *m/z* 509.2790 (required, 509.2815).

Synthesis of 1,6-bis(10-dodecyloxy-9-triptycyl)-1,3,5-hexatriyne (10)

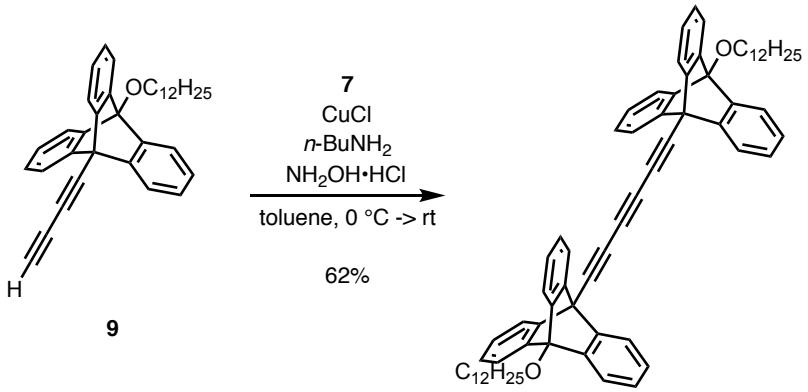

A two-necked 20 mL flask equipped with a magnetic stirring bar was filled with argon gas. To

the flask were added 9-(1,3-butadiyn-1-yl)-10-dodcyloxytriptycene (**9**) (730 mg, 1.50 mmol, 1.0 eq) and dry toluene (6.0 mL) and degassed. Copper(I) chloride (29.8 mg, 301 μmol, 0.20 eq), hydroxylamine hydrochloride (41.8 mg, 602 μmol, 0.40 eq), *n*-butylamine (300 μL, 3.04 mmol, 2.0 eq) was added to the solution at 0 °C in this order. 9-Bromoethynyl-10-dodcyloxytriptycene (**7**) (813 mg, 1.50 mmol, 1.0 eq) in toluene (3.0 mL) was added dropwise to this solution over 30 min. During the addition, a small amount of hydroxylamine hydrochloride was added potionwise to keep the color of the reaction light yellow. After the addition, the reaction mixture was stirred while warming up to room temperature for overnight and then quenched with water (50 mL). The organic layer was separated and the aqueous layer was further extracted with dichloromethane (50 mL) for three times. The organic layers combined were washed with water (50 mL) twice and brine (100 mL), dried over $MgSO_4$ and filtered. After the solvent was evaporated, the obtained pale brown solid (1.44 g) was passed through a plug column on silica gel with dichloromethane, and purified by GPC to give **10** as a colorless solid (883 mg, 932 μmol, 62%).

^{1}H NMR ($CDCl_3$, 500 MHz, 300 K): δ 7.78–7.75 (m, 6H), 7.67–7.63 (m, 6H), 7.14–7.09 (m, 12H), 4.59 (t, J = 6.9 Hz, 4H), 2.19–2.13 (m, 4H), 1.71–1.65 (m, 4H), 1.54–1.26 (m, 32H), 0.89 (t, J = 6.9 Hz, 6H); ^{13}C NMR ($CDCl_3$, 126 MHz, 300 K): δ 144.5, 142.7, 125.8, 125.4, 121.9, 121.5, 85.4, 77.6, 74.5, 67.4, 63.1, 52.9, 32.0, 31.8, 29.8, 29.7, 29.4, 26.3, 22.7, 14.1; mp: 266–267 °C; HRMS ($CHCl_3$/CH_3OH, positive): [**10**·Na]$^+$ ($C_{70}H_{74}O_2Na$) *m/z* 969.5604 (required, 969.5581).

Synthesis of hexakis((10-dodecyloxy-9-triptycyl)ethynyl)benzene (1)

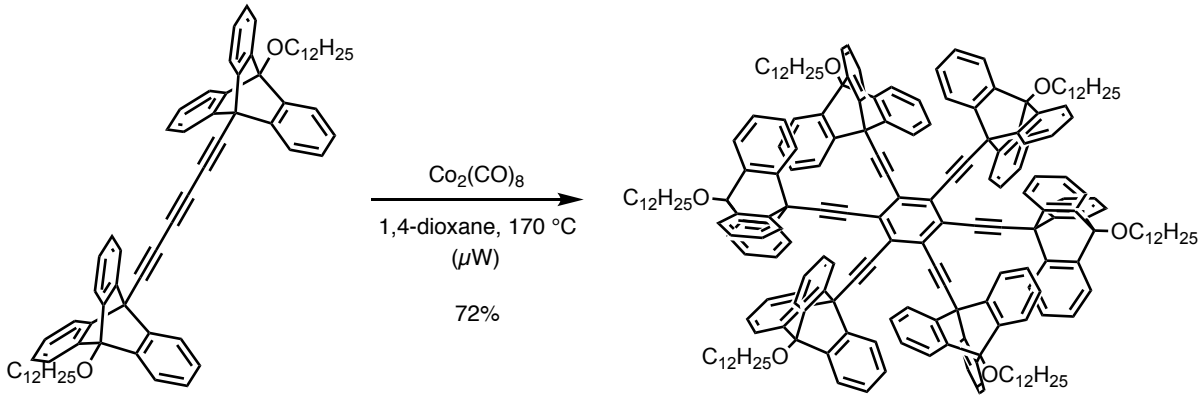

10 **1**

To a pressure bottle equipped with a magnetic stirring bar were added 1,6-bis(10-dodcyloxy-9-triptycyl)-1,3,5-hexatriyne (**10**) (47.4 mg, 50 μmol, 1.0 eq) and dicobalt octacarbonyl (2.8 mg, 8.2 μmol, 16 mol%) in a grove box under nitrogen atmosphere. Dry degassed 1,4-dioxane (5.0 mL) was added, and the reaction mixture was heated at 170 °C for 1.5 h by a microwave reactor. After cooling, the solvent was removed by evaporation and the residue was passed through a plug column on silica gel with chloroform. After evaporation, obtained pale brown solid (45.4 mg) was purified by GPC, recrystallized by chloroform/methanol and chloroform/acetone vapor diffusion for several times to give **1** as colorless crystals (33.1 mg, 11.6 μmol, 70%).

^{1}H NMR ($CDCl_3$, 500 MHz, 300 K): δ 7.87 (brs, 18H), 7.35 (brd, J = 5.9 Hz, 18H), 6.55 (brs, 18H), 5.34 (brs, 18H), 4.41 (t, J = 6.9 Hz, 12H), 2.10–2.04 (m, 12H), 1.63–1.57 (m, 12H), 1.49–1.29 (m, 96H), 0.89 (t, J = 6.9 Hz, 18H); ^{13}C NMR ($CDCl_3$, 126 MHz, 300 K): δ 144.2, 141.8, 129.6, 124.9, 124.2, 123.1, 120.2, 95.9, 90.0, 85.4, 67.3, 53.4, 31.9, 31.8, 29.73, 29.71, 29.69, 29.4, 26.3, 22.7, 14.1; mp: 143–145 °C; HRMS ($CHCl_3$/CH_3CN, positive): [**1**·Ag]$^+$ ($C_{210}H_{222}O_6Ag$) *m/z* 2946.6445 (required, 2946.6112).

NMR spectra of 1

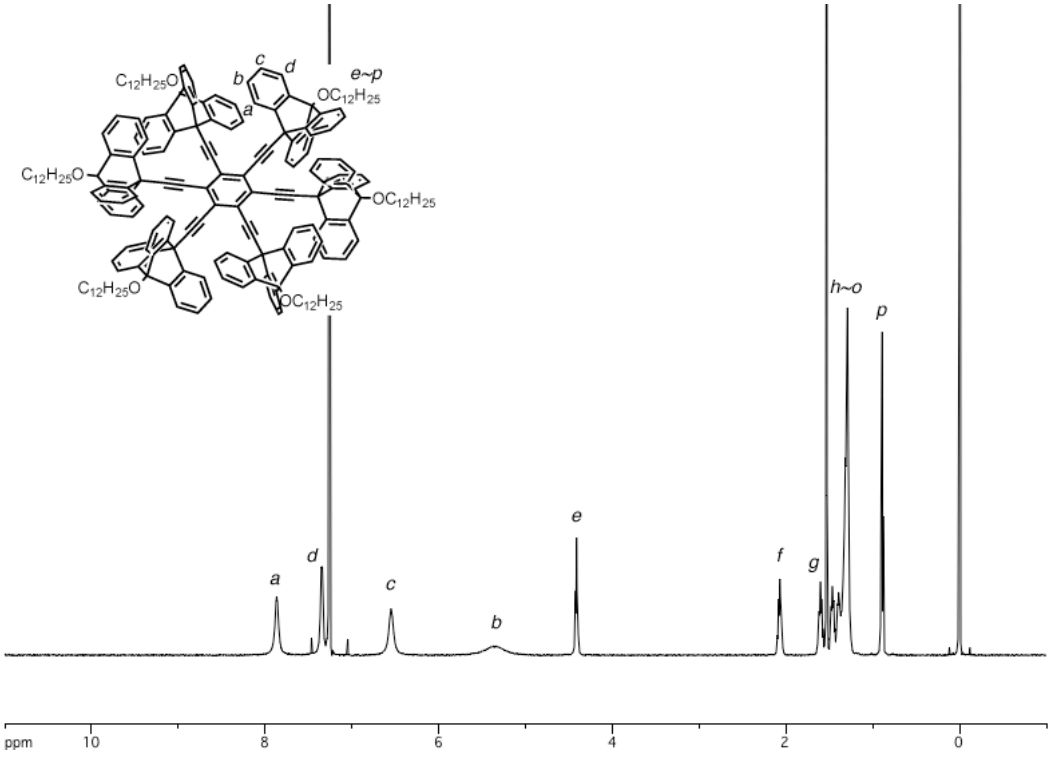

Figure 2-6-1. ^{1}H NMR spectrum of **1** ($CDCl_3$, 500 MHz, 300 K).

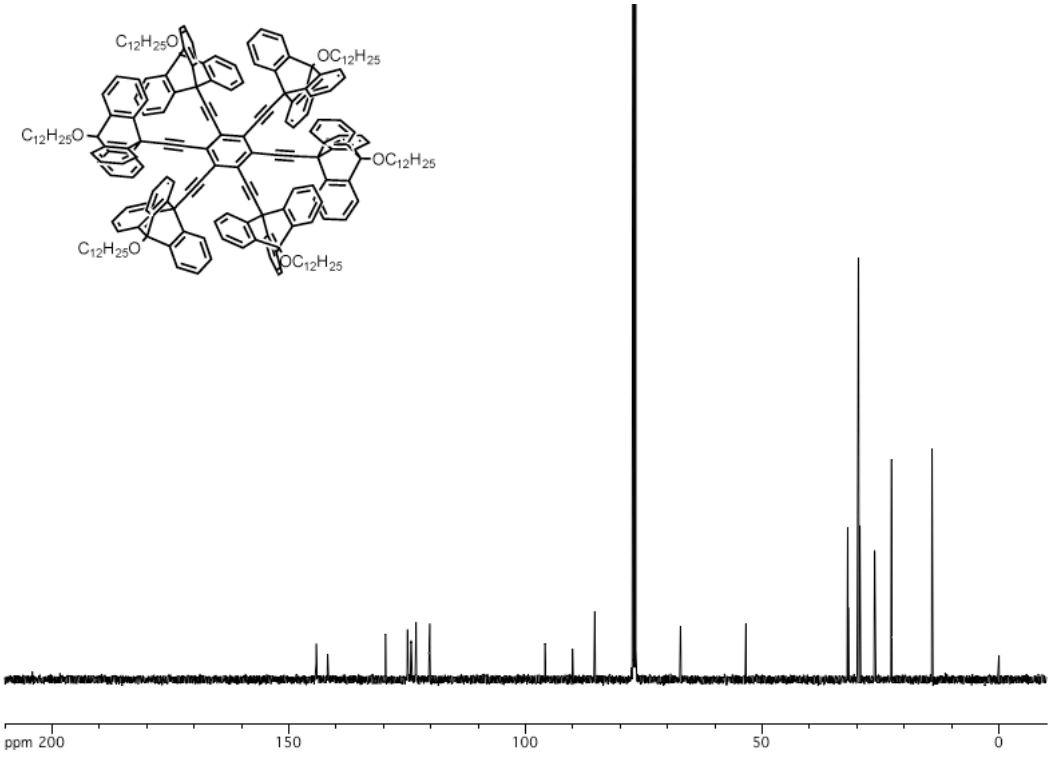

Figure 2-6-2. ^{13}C NMR spectrum of **1** ($CDCl_3$, 126 MHz, 300 K).

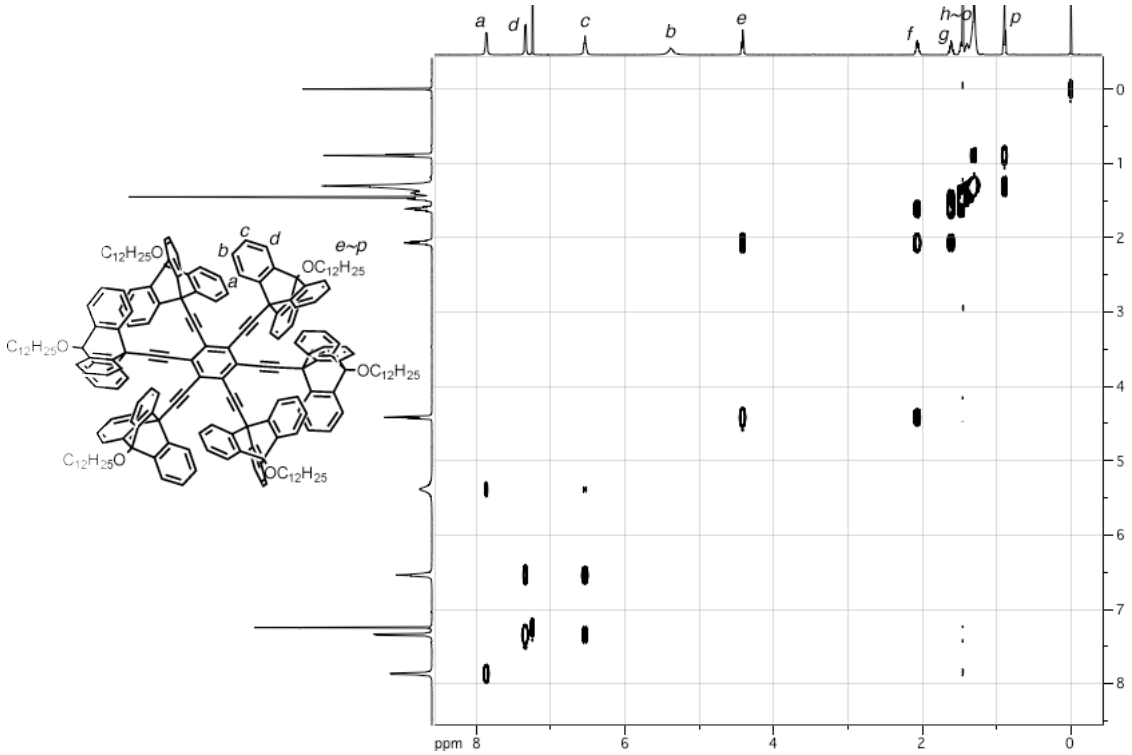

Figure 2-6-3. ^{1}H-^{1}H COSY NMR spectrum of **1** ($CDCl_3$, 500 MHz, 325 K).

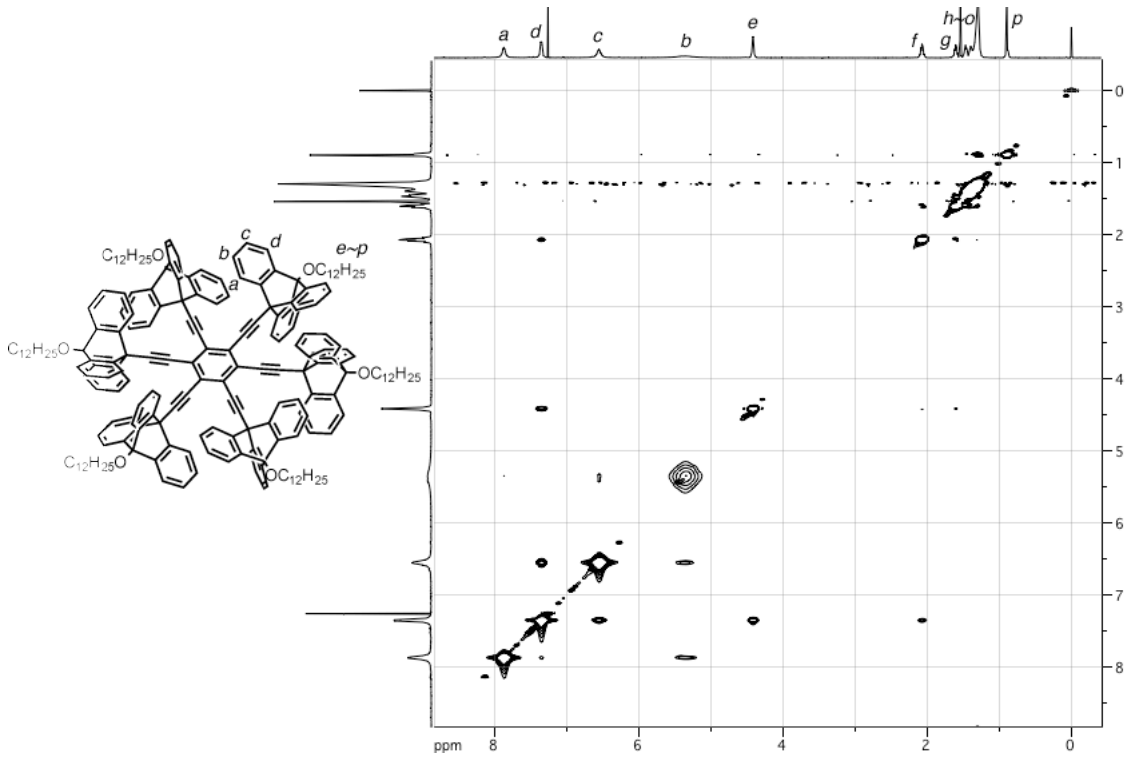

Figure 2-6-4. ^{1}H-^{1}H NOESY NMR spectrum of **1** ($CDCl_3$, 500 MHz, 300 K).

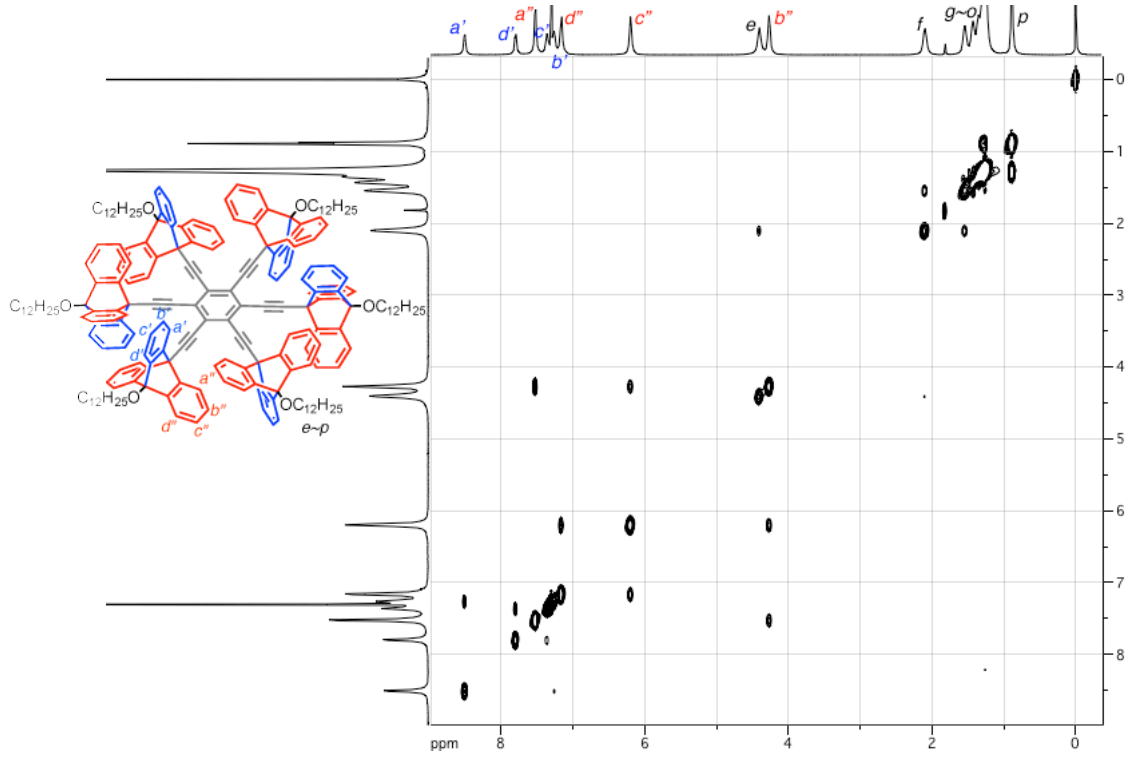

Figure 2-6-5. ^{1}H-^{1}H COSY NMR spectrum of **1** ($CDCl_3$, 500 MHz, 220 K).

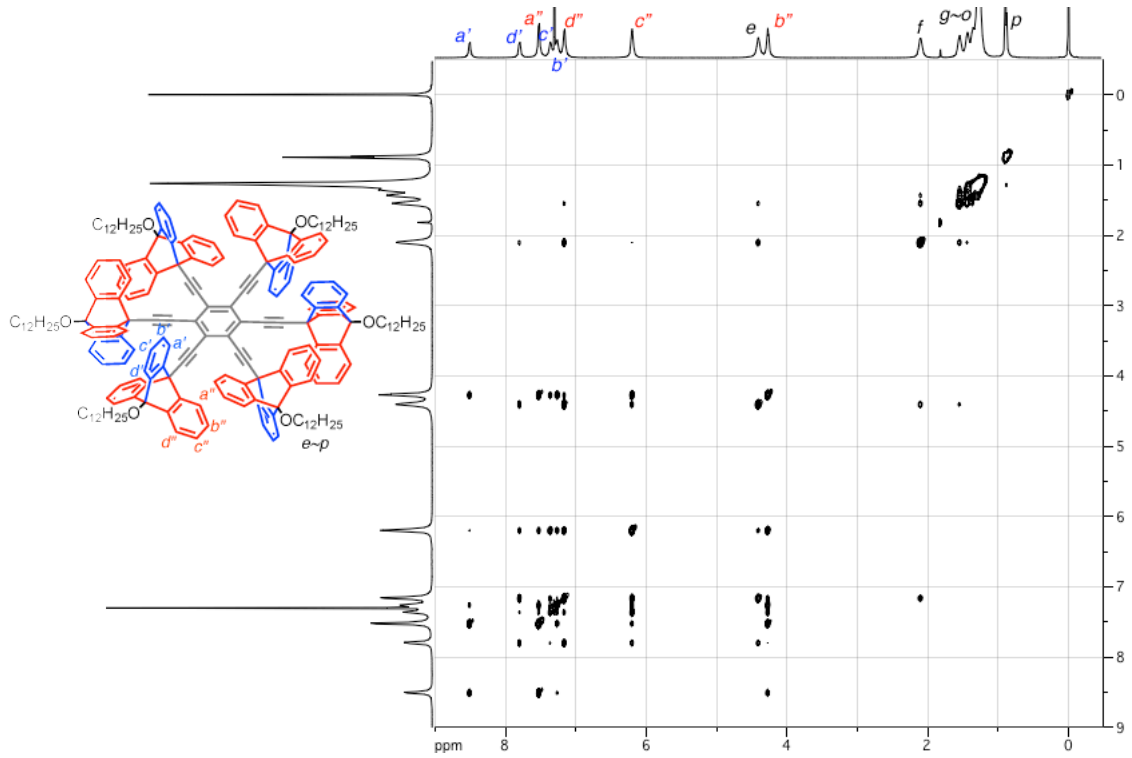

Figure 2-6-6. ^{1}H-^{1}H NOESY NMR spectrum of **1** ($CDCl_3$, 500 MHz, 220 K).

Single-crystal X-ray analysis of 1

A crystal suitable for X-ray analysis was obtained by slow vapor diffusion of acetone into a chloroform solution of **1** at room temperature.

Crystal data for **1**: $C_{210}H_{222}O_6$, Fw = 2842.06, colorless, block, 0.525 × 0.179 × 0.143 mm^3, trigonal, space group R-3m (#166), a = 32.5048(4) Å, c = 13.0046(2) Å, V = 11889.3(3) $Å^3$, Z = 3, r_{calcd} = 1.190 gcm^{-3}, T = 93 K, λ(CuKα) = 1.54187 Å , $2\theta_{max}$ = 149.3°, 2831/14328 reflections collected/unique (R_{int} = 0.0156), R_1 = 0.1081 ($I > 2\sigma(I)$), wR_2 = 0.3545 (for all data), GOF = 1.756, largest diff. peak and hole 0.43/-0.44 $eÅ^{-3}$. CCDC Deposit number 1510134.

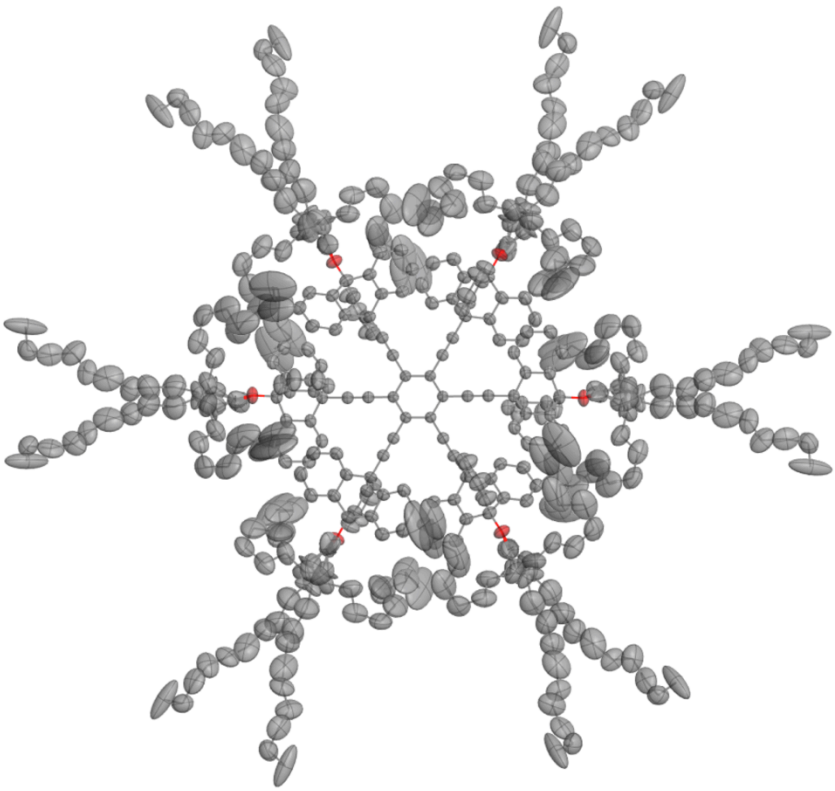

Figure 2-6-7. Crystal structure of **1**. Thermal ellipsoids set at 50% probability. Color code; C gray, O red. Hydrogen atoms are omitted for clarity.

Complexation of 1 with $[RuCp^*(NCMe)_3]PF_6$

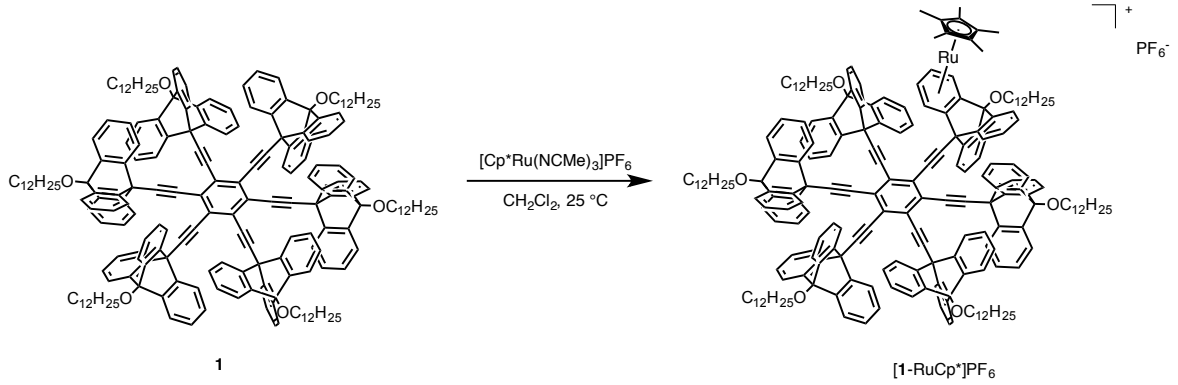

A two-necked 30 mL flask equipped with a magnetic stirring bar was filled with argon gas. Hexakis((10-dodcyloxy-9-triptycyl)ethynyl)benzene (**1**) (28.5 mg, 10.0 μmol, 1.0 eq) was added to the flask and dissolved in dry dichloromethane (10 mL), and the mixture was degassed. Tris(acetonitrile)penta-methylcyclopentadienyl ruthenium(II) hexafluorophosphate (7.6 mg, 15 μmol, 1.5 eq) was added to the solution at 25 °C and the reaction mixture was stirred for 20 h. Then the solvent was removed by evaporation and the residue (36.5 mg) was purified by column chromatography (Merck 70–230 mesh, *n*-hexane/chloroform/methanol = 1:1:0 ~ 0:1:0 ~ 0:50:1). The desired fraction was washed with 100 mM $NaPF_6$ *aq*. (10 mL) and water (10 mL), and evaporated. The crude material was further purified by reprecipitation from chloroform/methanol to obtain [**1**·RuCp*]PF_6 as a colorless solid (17.6 mg, 5.46 μmol, 55%).

^{1}H NMR ($CDCl_3$, 500 MHz, 300 K): δ 9.12–8.25 (m, 3H), 8.25–7.65 (m, 14H), 7.65–6.95 (m, 19H), 6.95–5.92 (m, 22H), 5.92-3.30 (m, 25H), 2.45 (t, J = 5.7 Hz, 1H), 2.35–1.84 (m, 12H), 1.84–1.08 (m, 123H), 1.08–0.75 (m, 18H); ^{13}C NMR ($CDCl_3$, 126 MHz, 300 K): δ 145.2, 144.2, 142.4, 141.6, 141.2, 137.9, 130.6, 130.2, 130.0, 129.8, 129.2, 127.7, 127.5, 126.5, 125.9, 125.1, 124.5, 124.4, 124.1, 122.9, 122.5, 122.0, 121.2, 120.4, 108.2, 108.0, 97.0, 96.8, 96.8, 96.4, 96.0, 95.8, 91.5, 91.3,

90.2, 89.8, 89.8, 89.7, 89.7, 85.4, 85.4, 85.3, 85.3, 85.1, 83.3, 82.9, 82.6, 80.4, 67.6, 67.4, 67.4, 67.3, 53.5, 53.5, 53.4, 53.4, 53.4, 51.3, 31.9, 31.8, 31.8, 31.2, 29.8, 29.7, 29.4, 26.4, 26.3, 26.0, 22.7, 14.1, 10.3; See also *Figure 2-6-8–2-6-19*, NMR data for assignment of [**1**·RuCp*]PF_6. HRMS ($CHCl_3$, positive): [**1**·RuCp*]$^+$ ($C_{220}H_{237}O_6Ru$) *m/z* 3079.7471 (required, 3079.7449).

NMR spectra of [1·RuCp*]PF_6

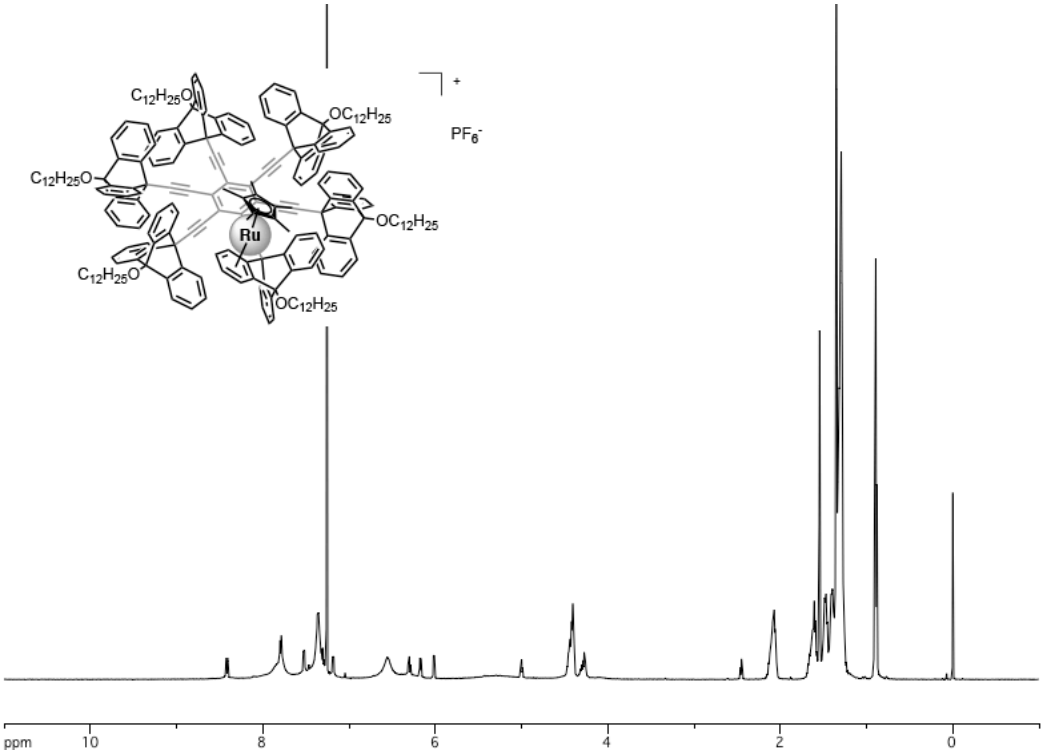

Figure 2-6-8. ^{1}H NMR spectrum of [**1**·RuCp*]PF_6 ($CDCl_3$, 500 MHz, 300 K).

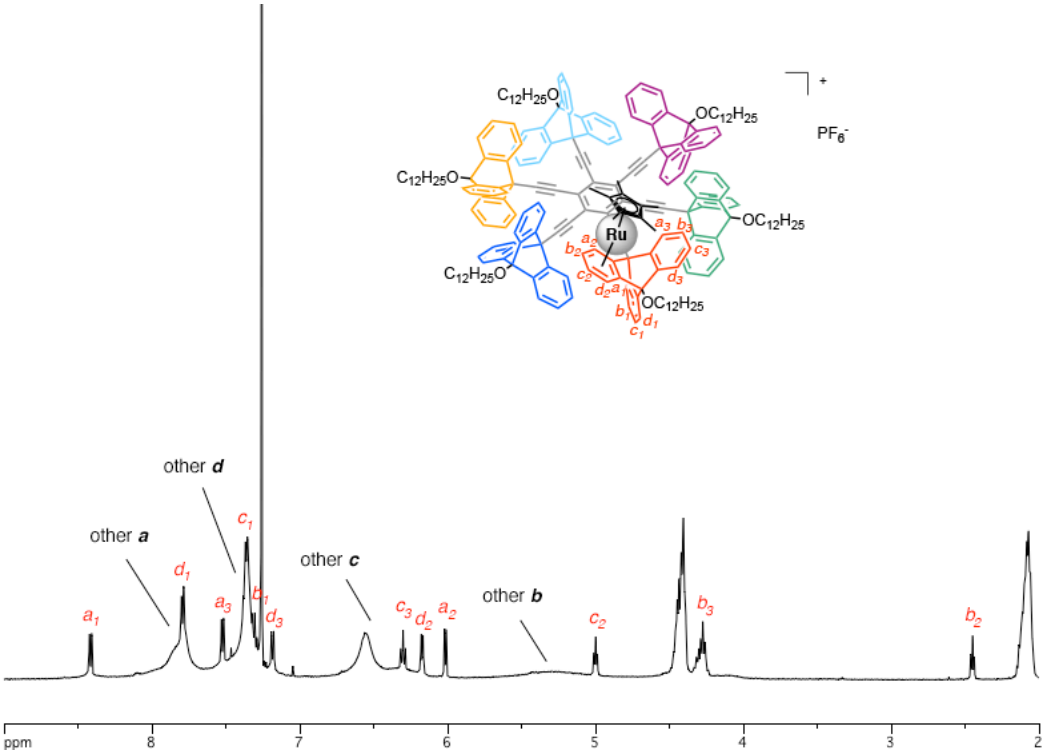

Figure 2-6-9. Partial ^{1}H NMR spectrum of [**1**·RuCp*]PF_6 ($CDCl_3$, 500 MHz, 300 K).

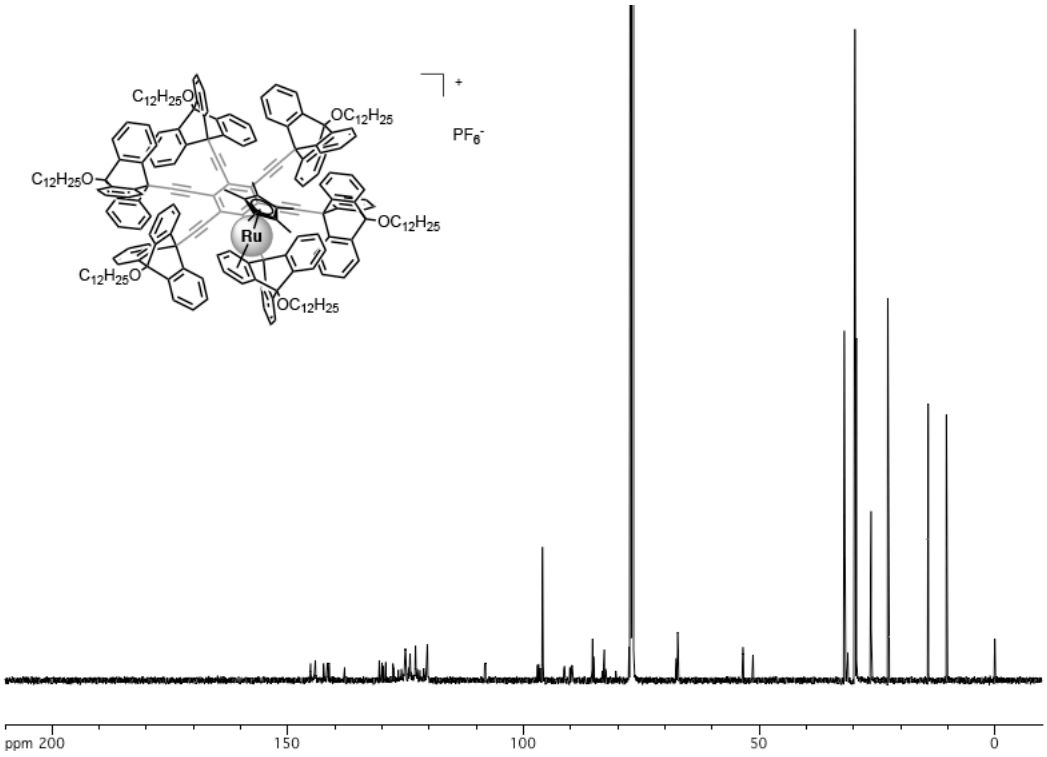

Figure 2-6-10. ^{13}C NMR spectrum of [**1**·RuCp*]PF_6 ($CDCl_3$, 126 MHz, 300 K).

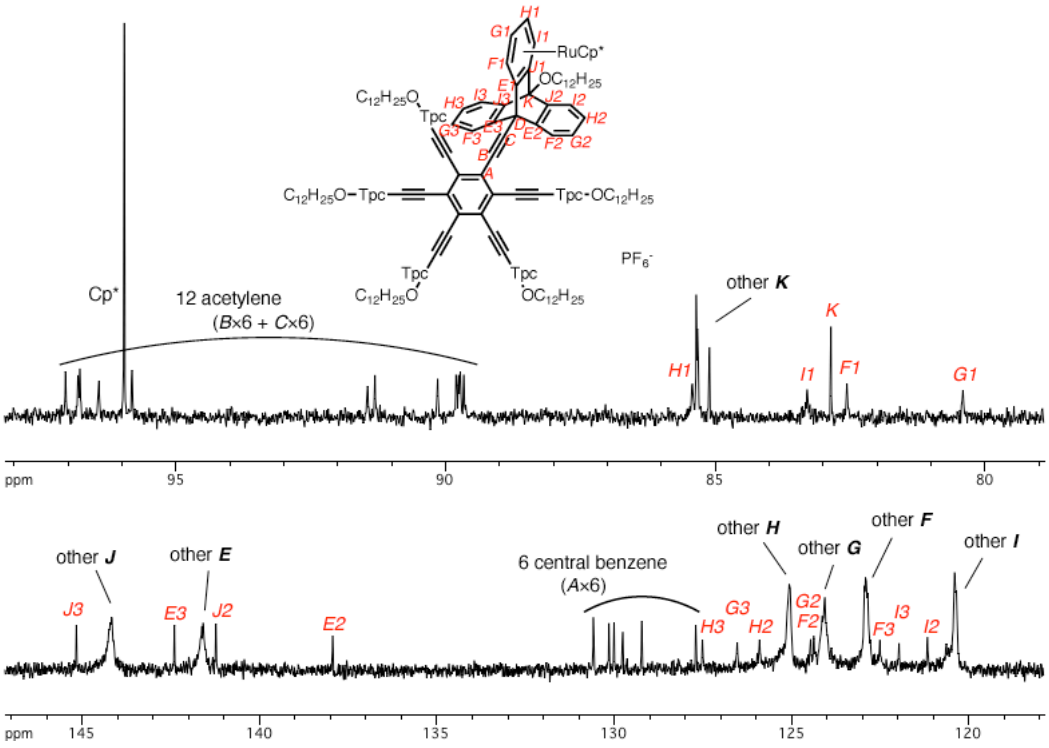

Figure 2-6-11. Partial ^{13}C NMR spectrum of [**1**·RuCp*]PF_6 ($CDCl_3$, 126 MHz, 300 K).

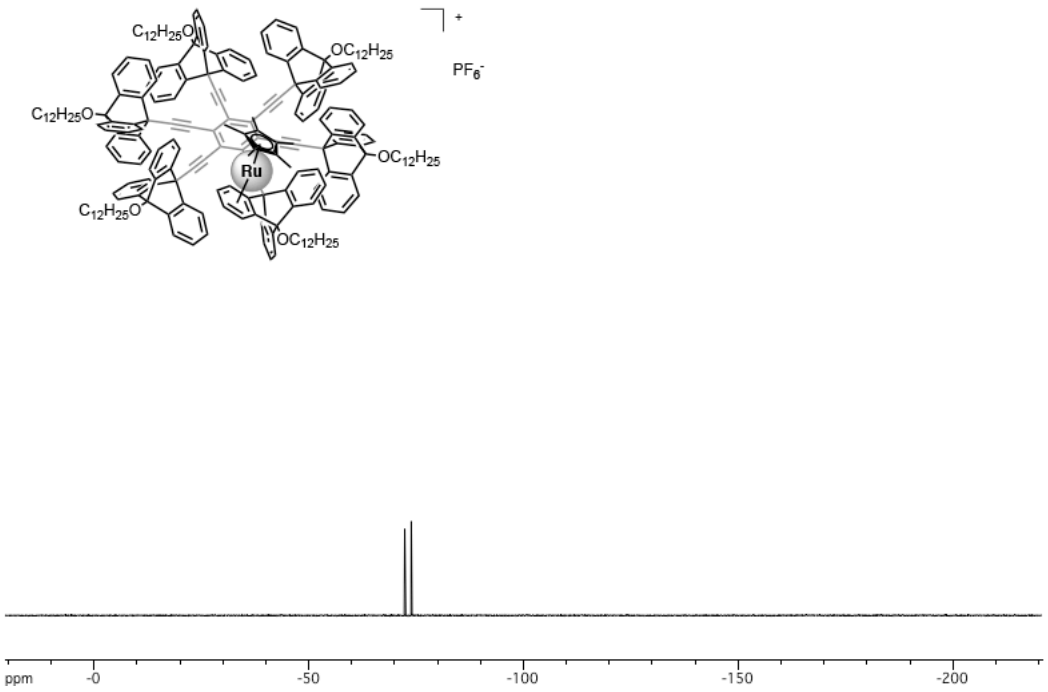

Figure 2-6-12. ^{19}F NMR spectrum of [**1**·RuCp*]PF_6 ($CDCl_3$, 471 MHz, 300 K).

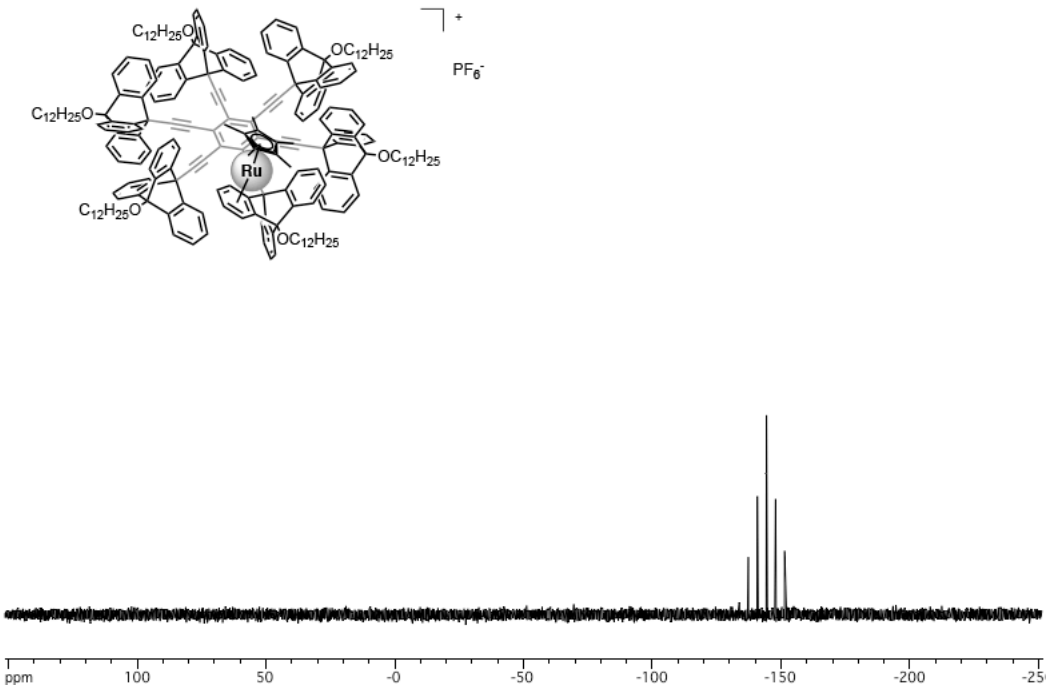

Figure 2-6-13. ^{31}P NMR spectrum of [**1**·RuCp*]PF_6 ($CDCl_3$, 202 MHz, 300 K).

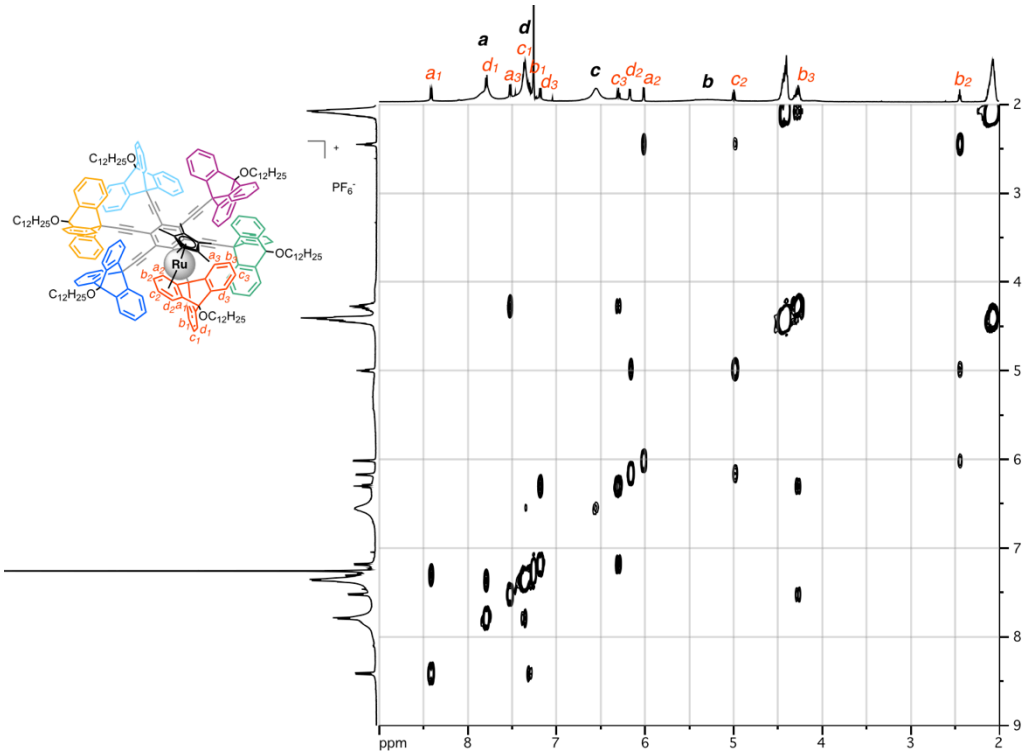

Figure 2-6-14. ^{1}H-^{1}H COSY NMR spectrum of [**1**·RuCp*]PF_6 ($CDCl_3$, 500 MHz, 300 K).

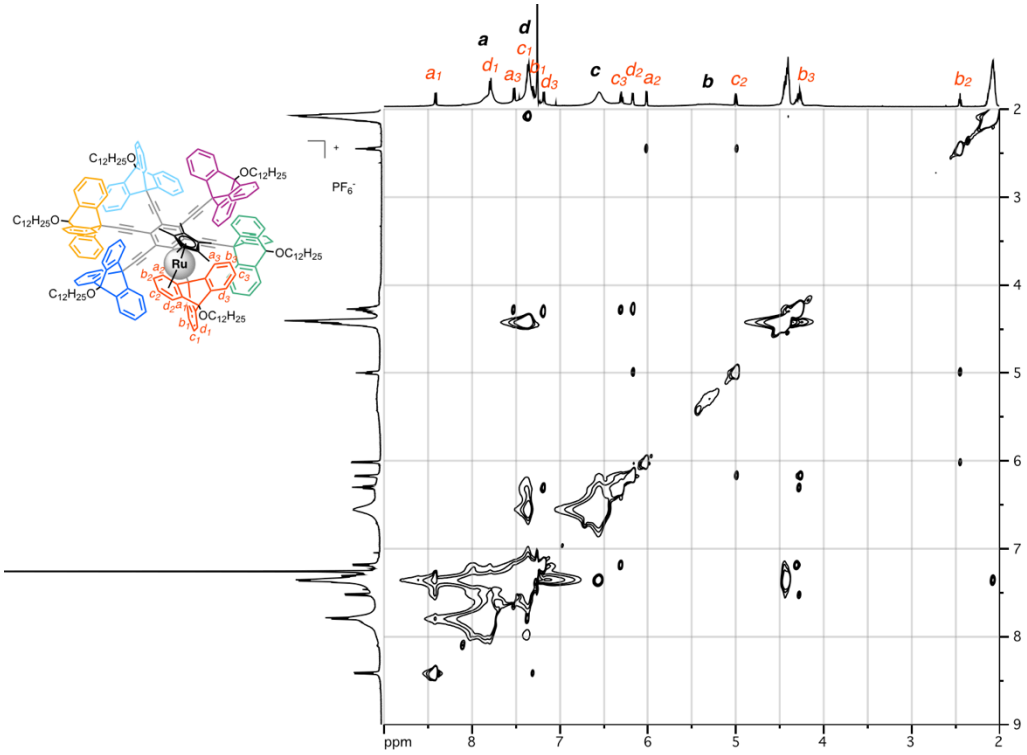

Figure 2-6-15. ^{1}H-^{1}H NOESY NMR spectrum of [**1**·RuCp*]PF_6 ($CDCl_3$, 500 MHz, 300 K).

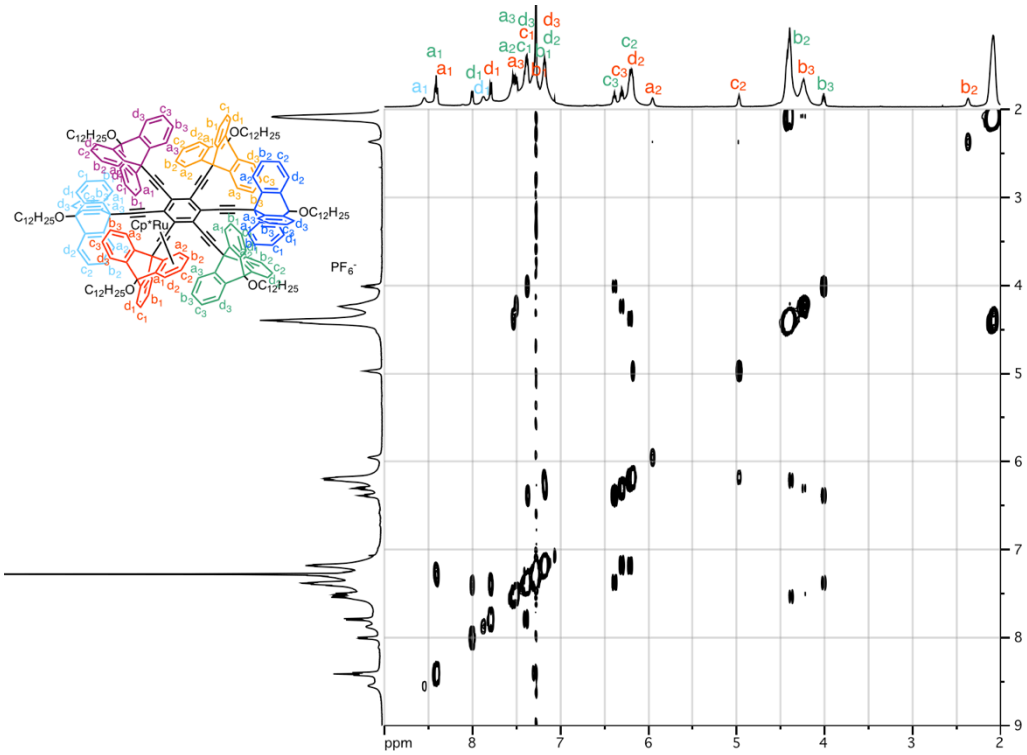

Figure 2-6-16. ^{1}H-^{1}H COSY NMR spectrum of [**1**·RuCp*]PF_6 ($CDCl_3$, 500 MHz, 260 K).

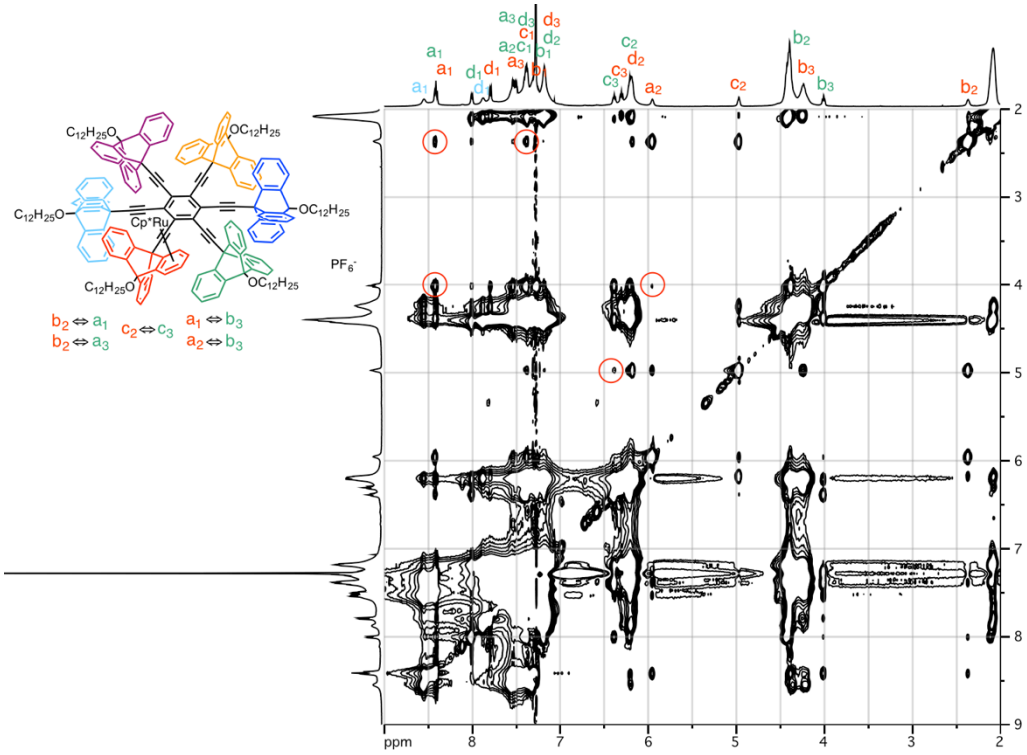

Figure 2-6-17. ^{1}H-^{1}H NOESY NMR spectrum of [**1**·RuCp*]PF_6 ($CDCl_3$, 500 MHz, 260 K).

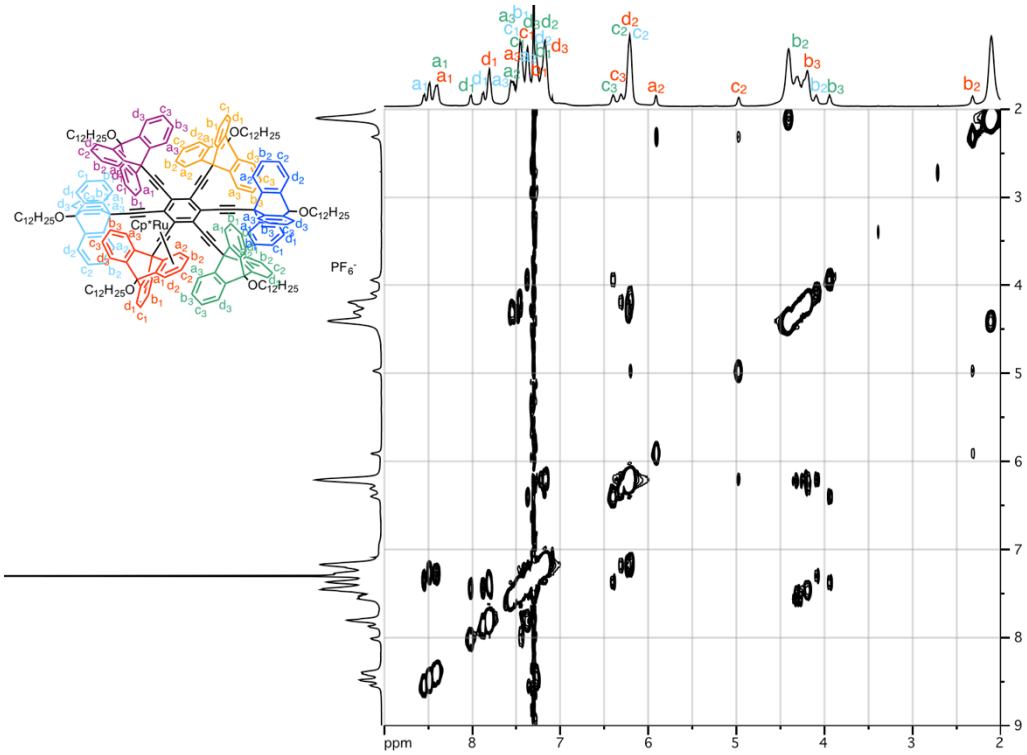

Figure 2-6-18. ^{1}H-^{1}H COSY NMR spectrum of [**1**·RuCp*]PF_6 ($CDCl_3$, 500 MHz, 220 K).

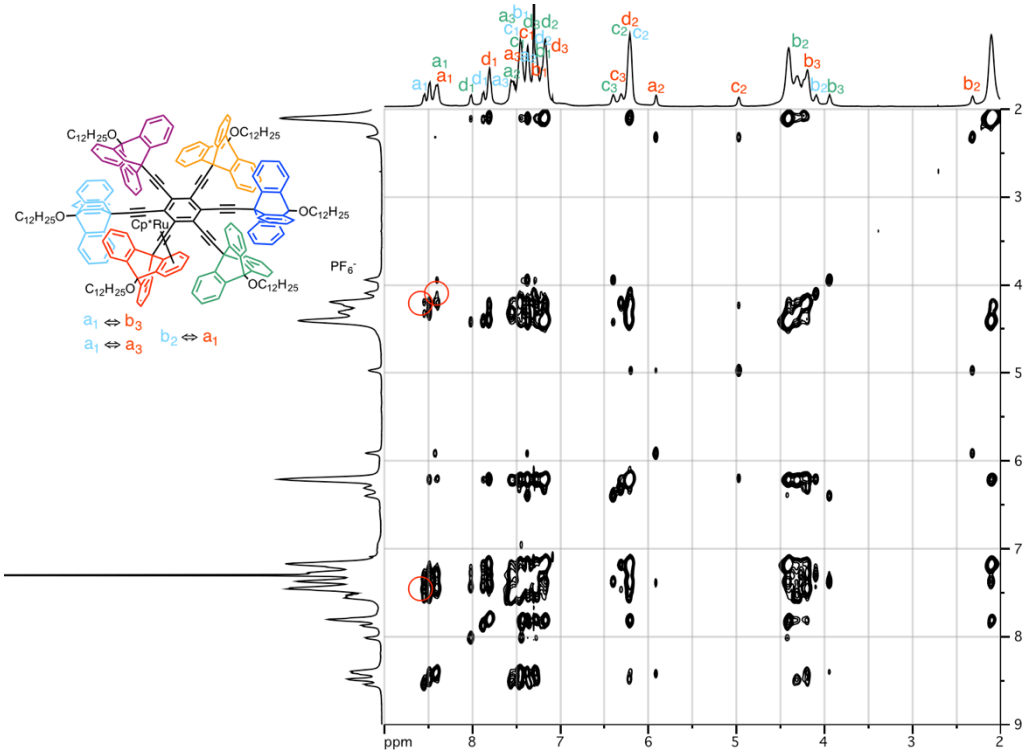

Figure 2-6-19. ^{1}H-^{1}H NOESY NMR spectrum of [**1**·RuCp*]PF_6 ($CDCl_3$, 500 MHz, 220 K).

2-7. References

1. (a) G. S. Kottas, L. I. Clarke, D. Horinek, J. Michl, *Chem. Rev.* **2005**, *105*, 1281–1376. (b) H. Iwamura, K. Mislow, *Acc. Chem. Res.* **1988**, *21*, 175–182. (c) D. K. Frantz, A. Linden, K. K. Baldridge, J. S. Siegel, *J. Am. Chem. Soc.* **2012**, *134*, 1528–1535. (d) H. Ube, Y. Yasuda, H. Sato, M. Shionoya, *Nat. Commun.* **2017**, *8*, 14296.
2. (a) N. Koga, Y. Kawada, H. Iwamura, *Tetrahedron* **1986**, *42*, 1679–1686. (b) S. Ogi, T. Ikeda, R. Wakabayashi, S. Shinkai, M. Takeuchi, *Chem. Eur. J.* **2010**, *16*, 8285–8290. (c) K. Sanada, H. Ube, M. Shionoya, *J. Am. Chem. Soc.* **2016**, *138*, 2945–2948. (d) M. Nakamura, K. Kishimoto, Y. Kobori, T. Abe, K. Yoza, K. Kobayashi, *J. Am. Chem. Soc.* **2016**, *13*8, 12564–12577. (e) S. Toyota, K. Kawahata, K. Sugahara, K. Wakamatsu, T. Iwanaga, *Eur. J. Org. Chem.* **2017**, 5696–5707.
3. F. Imashiro, K. Hirayama, A. Saika, *Magn. Reson. Chem.* **1987**, *25*, 518–520.
4. S. Toyota, *Chem. Rev.* **2010**, *110*, 5398–5424.
5. C. S. Vogelsberg, M. A. Garcia-Garibay, *Chem. Soc. Rev.* **2012**, *41*, 1892–1910.
6. M. Ōki, *Applications of dynamic NMR spectroscopy to organic chemistry*. Vol. 4. Vch Pub, 1985.
7. (a) D. Kost, E. H. Carlson, M. Raban, *J. Chem. Soc. D* **1971**, 656–657. (b) H. S. Gutowsky, C. H. Holm, *J. Chem. Phys.* **1956**, *25*, 1228–1234.
8. http://www.inmr.net
9. D. J. Nelson, N. C. Bramer, *J. Chem. Educ.* **2011**, *88*, 292–294.
10. a) S. Ogi, T. Ikeda, R. Wakabayashi, S. Shinkai, M. Takeuchi, *Chem. Eur. J.* **2010**, *16*, 8285–8290. b) M. Nakamura, K. Kishimoto, Y. Kobori, T. Abe, K. Yoza, K. Kobayashi, *J. Am. Chem. Soc.* **2016**, *138*, 12564–12577.
11. a) G. Wang, L. Ma, J. Xiang, Y. Wang, X. Chen, Y. Che, H. Jiang, *J. Org. Chem.* **2015**, *80*, 11302–11312. b) K. Sanada, H. Ube, M. Shionoya, *J. Am. Chem. Soc.* **2016**, *138*, 2945–2948.
12. P. J. Fagan, M. D. Ward, J. C. Calabrese, *J. Am. Chem. Soc.* **1989**, *111*, 1698–1719.
13. D. Peña, A. Cobas, D. Pérez, E. Guitián, *Synthesis* **2002**, *10*, 1454–1458.

14. G. M. Sheldrick, *Acta Cryst.* **2008**, A*64*, 112–122.

15. W. E. Barnett, L. L. Needham, *J. Org. Chem.* **1971**, *136*, 4134–4136.

3. Conclusions and Perspectives

3-1. Conclusion

In conclusion, I have constructed a circularly arranged sextuple triptycene molecular gearing system and evaluated its static and dynamic properties. The efficient synthetic route of the target molecule **1**, in which six triptycenes are circularly attached to a central benzene ring through an ethynyl linker, was established, and the desired compound was fully characterized by various NMR spectroscopies, ESI-TOF mass spectrometry, and single-crystal X-ray structural analysis. From the results together, the tightly meshed gearing structure was verified both in solution and in the crystal state. The activation energy parameters for the rotational motion of the gearing system were high enough to evaluate experimentally by applying the line-shape analysis of the VT ^{1}H NMR spectra using a two-state exchange model.

When one bulky RuCp* complex was attached to the triptycene moiety of the gearing system **1**, the whole rotational motion of the molecule was significantly affected through gearing, which was the first example of demonstrating transmission of stimulus through gear meshing. However, the results also suggested that the transmission efficiency through gearing was lowered to some extent due to the gear slippage motions.

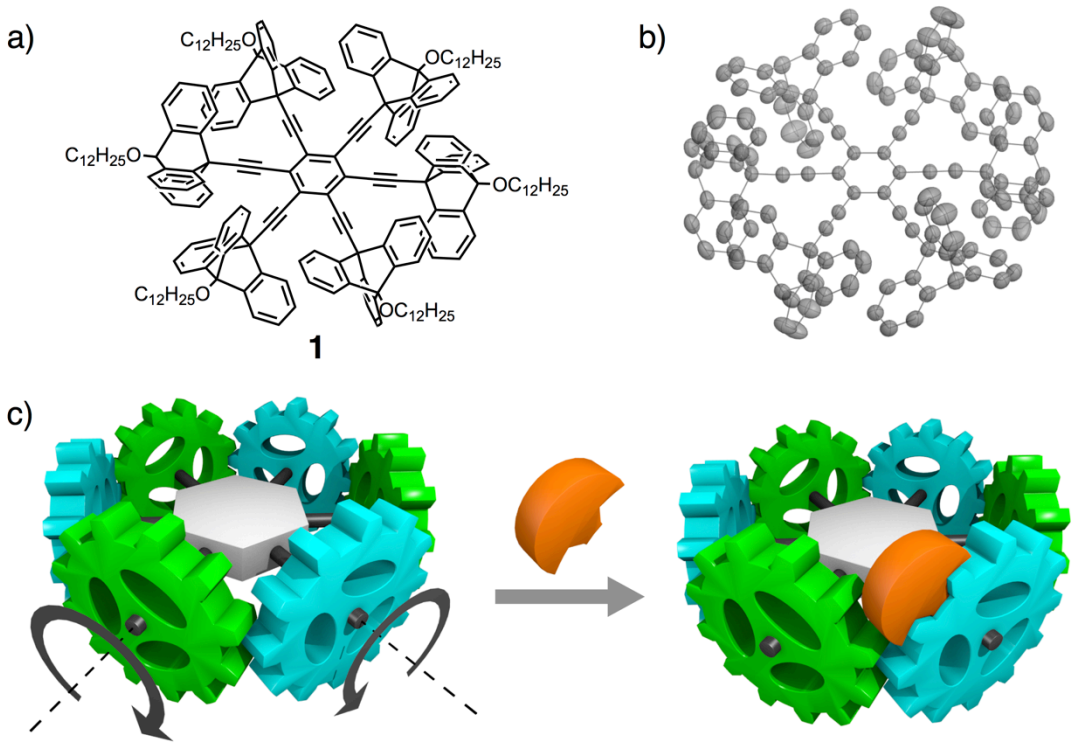

Figure 3-1-1. Overview of **Chapter 2**. a) A chemical structure of **1**. b) Crystal structure of **1** in ORTEP diagram. Side chains are omitted for clarity. c) Schematic representation of metal complexation with a chemical stopper.

3-2. Perspectives

As mentioned in **Section 2-3**, two kinds of motions, "geared rotation" and "gear slippage", are possible in the exchange of the triptycene blades. Quantitative evaluation of these motions would offer multifaceted insight into the transmission efficiency through molecular gearing.

To evaluate the frequency of the gear slippage, some substituents should be introduced into triptycenes, and the exchange between the phase isomers has to be discussed in detail. However, the size of the substituents and the electronic effects should be also carefully considered.

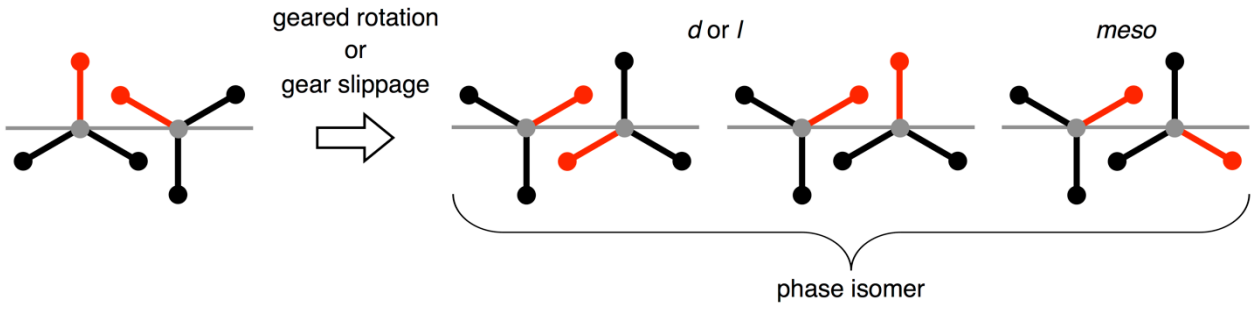

Figure 3-2-1. Phase isomers resulted from "geared rotation" and "gear slippage".

Substituted triptycene molecules could be easily synthesized by Diels-Alder reaction with substituted benzyne, which would be converted to substituted triyne. Trimerization reaction of this substituted triyne with non-substituted triyne at a ratio of 1:2 would provide gearing system in which substituents are introduced into the adjacent triptycenes (Scheme 3-2-1).

Scheme 3-2-1. Synthesis of substituted gear molecule

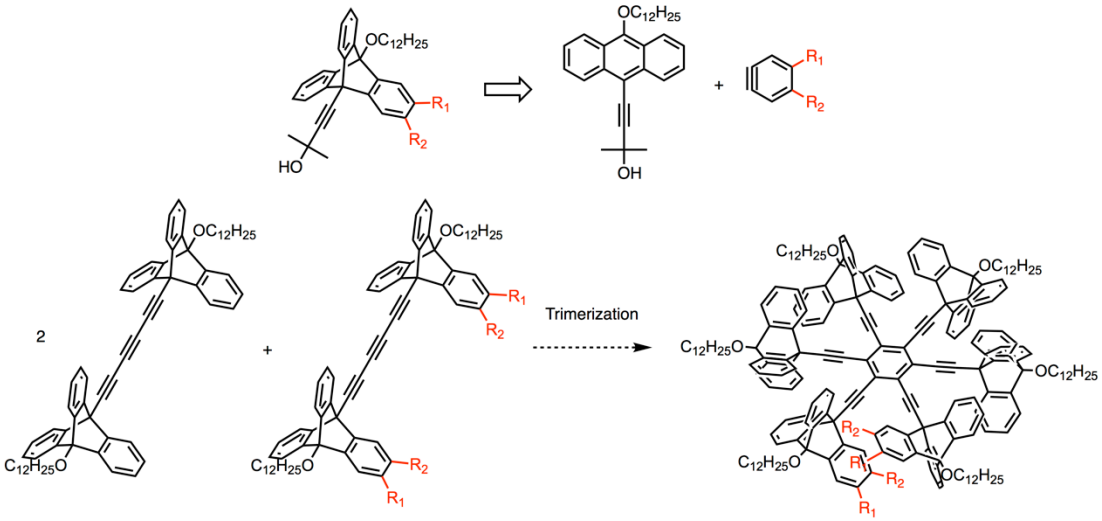

Evaluation of the gear slippage motion is possible by estimating the exchange rate between the *dl* and *meso* isomers of the obtained molecule. Comparing these values with the data described in **Section 2-4**, the effect of the bulky RuCp* complex as an inhibitor of rotational motion would give more information about the dynamics of molecular gearing in this system.

By expanding triptycene blades, the frequency of the gear slippage would be suppressed and more efficient motion transmission system could be realized. Trimethyl triptycene system might improve the gearing efficiency.

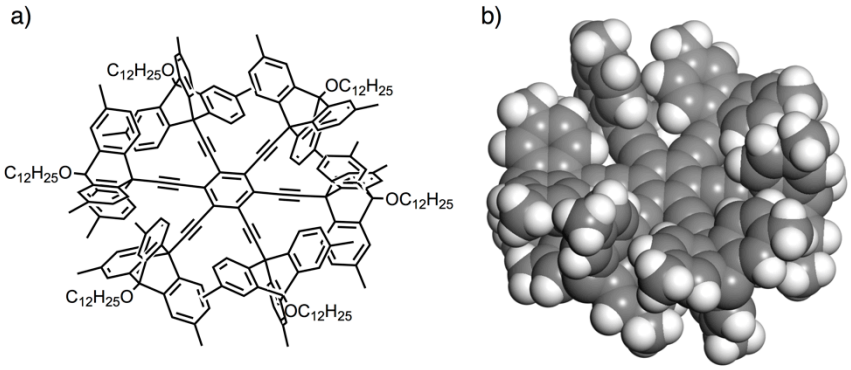

Figure 3-2-2. Expanded gearing system. a) Chemical structure. b) MM structure. Side chains are omitted for clarity.

Introducing nitrogen atoms to the molecule would add new function such as clutch system.

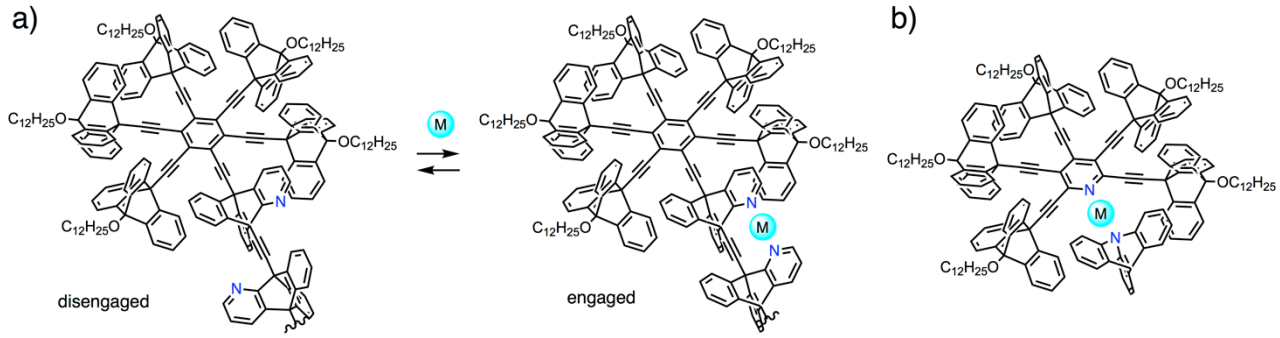

Figure 3-2-3. Examples of molecular clutch systems controlled by metal ion.

Solid-state NMR spectroscopy, gas-phase analysis, direct-observation by STM *etc*. will also provide other new insights.

Finally, an interdisciplinary field concerned with artificial molecular machines has only just begun and in an early stage of development of basic mechanical elements as mentioned in **Chapter 1**. Therefore, the realization of molecular machines comparable to biomolecules is still a long way off. Integration and assembly of each basic unit are essential for the construction of advanced artificial molecular machines. Construction of a system that can induce motions specific to external stimuli is the next key challenge.

I would like to conclude this research in the hope that molecular machine elements reported here will give useful insight into constructing sophisticated molecular machines in future, and become a mediator or hub responsible for mutual transmission of information between various machine elements.

A List of Publication

[Publication related to the thesis]

1. “A Circularly Arranged Sextuple Triptycene Gear Molecule”

Hitoshi Ube, Ryo Yamada, Jun-ichi Ishida, Hiroyasu Sato, Motoo Shiro, Mitsuhiko Shionoya

J. *Am*. *Chem*. *Soc*. **2017**, *139*, 16470–16473.

Acknowledgement

This research was supported by many people.

Professor Dr. Mitsuhiko Shionoya (The University of Tokyo) gave me a very interesting theme of molecular gearing system when I started my research career, which captivated me at first sight. Since then, he enthusiastically and patiently supervised me, and discussion with him was really fruitful time. I would like to express my deepest appreciation to him.

I am grateful to Assistant Professor Dr. Hitoshi Ube (The University of Tokyo) for giving me a lot of advice and time for discussion throughout my research.

I appreciate Associate Professor Dr. Shohei Tashiro (The University of Tokyo) and Assistant Professor Dr. Yusuke Takezawa (The University of Tokyo) to give me useful suggestions in doing research.

I would like to thank all the members of Shionoya laboratory for his or her support and advice. In particular, active discussion with Dr. Kazuma Sanada, Mr. Yoshihiro Yasuda and Mr. Atsushi Kawaguchi was really helpful. Also, Mr. Junichi Ishida left a lot of knowledge and results as a prior research. Without that knowledge, I think the synthesis in this research could not be completed.

I appreciate Dr. Hiroyasu Sato (Rigaku Corporation) and Dr. Motoo Shiro (Rigaku Corporation) for X-ray structural analysis for the gear molecule.

I would also like to express my gratitude to Advanced Leading Graduate Course for Photon Science (ALPS) program for their financial support, including the support for study abroad. I am thankful to Professor Nicolas Giuseppone (Université de Strasbourg, CNRS) for giving me an opportunity to study in his laboratory and discuss with him.

It was a great honor for me to be engaged in this research. Thank you very much.